Title
An Integrated Physical/link-access Layer Model Of Packet Radio Architectures

Author
Polydoros, Andreas

Publication Date
1994

CALIFORNIA PATH PROGRAM
INSTITUTE OF TRANSPORTATION STUDIES
UNIVERSITY OF CALIFORNIA, BERKELEY

An Integrated Physical/Link-Access Layer Model of Packet Radio Architectures

Andreas Polydoros

Communication Sciences Institute
University of Southern California

California PATH Research Report
UCB-ITS-PRR-94-20

This work was performed as part of the California PATH Program of the University of California, in cooperation with the State of California Business, Transportation, and Housing Agency, Department of Transportation; and the United States Department of Transportation, Federal Highway Administration.

October 1994

ISSN 1055-1425

An Integrated Physical/Link-Access layer Model of Packet Radio Architectures

An Integrated Physical/Link-Access layer Model of Packet Radio Architectures[1]

Prof. Andreas Polydoros
Principal Investigator

Communication Sciences Institute
Department of Electrical Engineering-Systems
University of Southern California
Los Angeles, CA 90089-2565

Contributors

Achilleas Anastasopoulos
Te-Kai Liu
Prokopios Panagiotou
Chung-ming Sun

[1]This work was performed as part of the California PATH Program of the University of California, in cooperation with the State of California Business, Transportation, and Housing Agency, Department of Transportation; and the United States Department of Transportation, Federal Highway Administration.

Working Group/AP, CSI/USC

Prokopios Panagiotou, Ed.

Acknowledgments

The Principal Investigator wishes to thank deeply the contributors Achilleas Anastasopoulos, Te-Kai Liu, Prokopios Panagiotou and Chung-ming Sun for a job done with great competence, dedication and professionalism.

An Integrated Physical/Link-Access layer Model of Packet Radio Architectures

Prof. Andreas Polydoros
Principal Investigator

April 1994

Abstract

The present annual report is in response to the contractual requirements of the Memorandum Of Understanding MOU#97, provided to the University of Southern California (USC) by the Partners for Advanced Transit and Highways (PATH) administered at the University of California, Berkeley, covering the first year of an approved two-year effort. The goal of this effort is to devise and analyze an integrated Physical/Link-Access Layer Model of Packet Radio Architectures, with application to the PATH/IVHS (Intelligent Vehicle Highway Systems) communication sub-system design between vehicles and infrastructure, as well as between vehicles on the move. The present report contributes to a generic conceptual model for system evaluation which can be used for quantification of the interaction between network layers. The research tasks that have been performed for achieving the project objectives include collection of data requirements for Advanced Traffic Management and Information Systems (ATMIS), Advanced Vehicle Control Systems (AVCS) as well as for an integrated ATMIS/AVCS system, definition of communication system requirements (user's integrated data traffic, attributes of the integrated system), analysis and performance evaluation of multiple access schemes for vehicle-to-roadway and vehicle-to-vehicle communications, identification of multiple access protocols that can accomodate the communication needs of the integrated ATMIS/AVCS data traffic, and a complete performance analysis of an asynchronous multi-cell Direct-Sequence Code Division Multiple-Access (DS/CDMA) microcellular system for both uplink (vehicle to base station) and downlink (base station to vehicle) communications.

Keywords: Data Communication, Intelligent Vehicle Highway Systems, Link Layer, Mobile Communication Systems, Radio

Executive Summary

The present annual report is in response to the contractual requirements of the Memorandum Of Understanding MOU#97, provided to the University of Southern California (USC) by the Partners for Advanced Transit and Highways (PATH) administered at the University of California, Berkeley, covering the first year of an approved two-year effort.

The scope of the contract is to devise and analyze an integrated Physical/Link-Access Layer Model of Packet Radio Architectures, with application to the PATH/IVHS communication sub-system design between vehicles and infrastructure, as well as between vehicles on the move. The detailed project objectives are:

- Address communication sub-system architectures for ATMIS and AVCS (including, possibly an integrated system) based on short-range packet radio designs.
- Identify, analyze and perform trade-off studies for a variety of design options.
- Perform original research and propose novel design alternatives.
- Build a generic analytical model for system evaluation which quantifies the interaction between network layers.
- Reach recommendations/conclusions for optimized systems.

In order to study and quantify the interaction between the Physical and the Link-Access layers of a packet radio system that can accomodate the communication needs of the integrated ATMIS/AVCS services, we have devised a generic conceptual model. The model

includes two modules for the performance evaluation of the two layers and identifies the effects of design options, vehicular traffic, physical environment, information flow and communication system requirements on the evaluation procedure. The generic model reveals the strong interconnection between the Physical and the Link-Access layers of this particular packet radio system. Therefore, in order to optimize the overall system, we must jointly optimize the two layers, rather than design, analyze, and optimize each layer independently from the other.

During the first year of this effort we determined the data volume for an integrated ATMIS/AVCS system. The integration of ATMIS and AVCS services promises to improve the traffic flow in existing freeways and surface streets and at the same time increase substantially the transportation safety and capacity of the freeways. Knowledge of data requirements is necessary for the determination of the communication requirements of the integrated system and furthermore for the estimation of spectrum needs and evaluation of the applicability of candidate communication technologies.

The design of an efficient multiple access protocol that can accomodate the heterogeneous data traffic of an integrated ATMIS/AVCS system has proven to be a very difficult and challenging task. The performance of well-known multiple access protocols was evaluated in each of the three communication links (vehicle-to-vehicle, vehicle to base station, and base station to vehicle) of a single cell, assumming that the spatial distribution of vehicles in the cell is uniform. Careful analysis of the simulation results shows that a single protocol cannot perform satisfactorily in every link. It is therefore, necessary to focus our efforts on the design and evaluation of new protocols. Towards this goal, we have identified two feasible multiple access protocols and discussed their design parameters.

A great part of this report addresses the performance of an asynchronous multi-cell Direct-Sequence Code Division Multiple-Access (DS/CDMA) microcellular system for both uplink (vehicle to base station) and downlink (base station to vehicle) communications. For the uplink, we have calculated the bit error rate, the outage probability, and the packet success rate for two modulation schemes (BPSK and DPSK), under the assumption of Rician/Nakagami fading and log-normal shadowing in the presence of adjacent-cell interference.

For the downlink, we have calculated the bit error rate and the outage probability. We have also identified a performance measure that allows us to investigate the effect of the macro-selection diversity on the suppression of adjacent-cell interference, and we studied the composite log-normal Rician distribution.

Contents

List of Figures

List of Tables

Chapter 1

Introduction

IVHS (Intelligent Vehicle Highway Systems) is a joint effort of public, private and academic sectors to develop and deploy solutions that can alleviate the existing transportation problems. IVHS will incorporate communication, control, and transportation technologies in order to improve the traffic flow and safety in existing freeways and surface streets. Efficient use of the existing transportation facilities and energy resources promises to reduce the current levels of congestion, thus improving the air quality and protecting the environment. The objectives of our efforts here at CSI (Communication Sciences Institute) are to identify, analyze and evaluate communication architectures for two IVHS applications, namely ATMIS and AVCS (including an integrated system).

Our study has focused on the analysis and interaction between modules of a conceptual Communication System Design Diagram devised at CSI, and described in detail in chapter 2. This diagram can serve as a general analytical tool for the design and evaluation of a Packet Radio Communication System for IVHS applications. Since the proposed design procedure is general, it can be also used as a design and evaluation tool for every Packet Radio System. The external and internal inputs, the evaluation modules and their interactions, as well as the design options imposed by economical and technological constraints are thoroughly discussed in this chapter.

In chapter 3, we discuss the data traffic in an integrated ATMIS/AVCS system. First, we

Chapter 2

Interaction of Conceptual Modules in PR-IVHS

2.1 Introduction

Our goal is to design and evaluate a packet radio (PR) communication sytem for IVHS applications. Although this system will be used for IVHS applications and services, the design procedure is general and can be used as an analytical tool for every packet radio communication system.

In order to design and optimize such a system we need a clear view of all the factors that affect its performance. We must also develop a deep understanding of the way the several layers are interacting with each other. In this model, we have to recognize, describe and classify all the external inputs, the models used to describe the physical world and the performance evaluation modules.

The difficulty in the analysis of a packet radio system as opposed to other communication networks, like optical fiber networks, is that the several layers cannot be designed and optimized independently from each other. Optimization of the overall system requires the joint optimization of the several layers.

The rest of the chapter is organized as follows. Section 2.2 presents a general viewpoint

of the design procedure. The design options and constraints are discussed in section 2.3. A detailed presentation of the communication system analysis and assessment diagram follows, together with the conclusions of this chapter.

2.2 General diagram

The design procedure for a PR-IVHS system is illustrated in figure 2.1. Initially, we choose a collection of design options, constrained by existing regulations and technology. The design options together with some external parameters are fed to the analysis and assesment box, where adequate performance measures are generated. After analyzing these measures, we can either stop the procedure, if the measures meet our specifications for the system performance, or reiterate it by selecting new design options. It may be the case that we cannot meet the requirements, no matter what our design options are. In this case, we have to relax the imposed constraints, or consider new technologies, that lead to a system design that meets our specifications.

2.3 Design Options and Constraints

In this section, we briefly discuss some of the options and constraints that the designer of a communication system for PR-IVHS faces, namely spectrum considerations, area of coverage, connectivity, and technology availability.

2.3.1 Spectrum Considerations

Spectrum considerations include the operating frequency, the number of assigned channels, the available bandwidth for each channel and the expected information rate of a channel. In order to establish the spectrum needs for IVHS applications, we must determine their communication requirements, which in turn requires knowledge of application and services requirements.

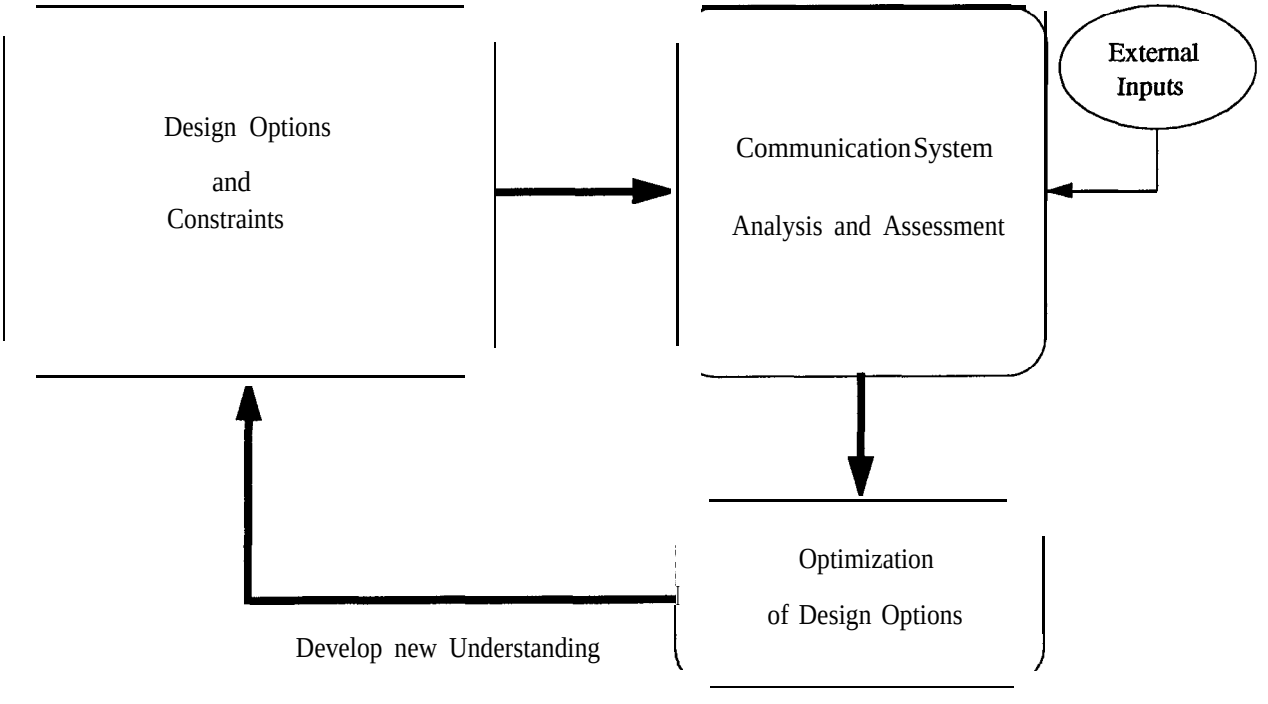

Figure 2.1: General Diagram

At the present time, the IVHS community is trying to develop a good understanding of IVHS applications and services. However, the scarcity of the radio frequency spectrum and the competition for spectrum from Personal Communication Systems (PCS) have forced the IVHS industry to try to assess spectrum needs before application requirements are fully known. It is certain that most of the IVHS applications will require allocation of dedicated bandwidth. Nevertheless, it is unknown if the allocated spectrum will be enough for all the envisioned application and services. Therefore, the most crucial applications should use the assigned spectrum and wherever possible, applications should share currently available spectrum with an existing service (TRB 1993b).

2.3.2 Area of Coverage

The unique channel characteristics of the freeway environment, which have been thoroughly analyzed in (Polydoros et al. 1993), correspond to the fading characteristics of a microcell environment. Microcellular systems operate at low power levels (few tens of mW) and the cell size varies from 0.2 to 1 km. The cell size is one of the most important design parameters, since it determines the number of users in the geographical area of coverage and the interference from other users in adjacent cells.

In order to provide mobile radio coverage to a large number of users, sharing a fixed communication resource (bandwidth), dynamic allocation of the resource is needed. The problem of efficiently utilizing a given bandwidth is addressed in detail in chapter 4.

2.3.3 Connectivity

Communication links can be classified according to the connectivity of the information source and the destination, as follows:

- One Way (simplex connection): Data are transmitted only in one direction; never in the reverse direction.

- Two Way On Demand (half-duplex connection): Data are transmitted in either direction but not simultaneously.

- Two Way In/Out (full-duplex connection): Data are transmitted in either direction simultaneously. In the last two cases, the transmitter functions also as a receiver (a transceiver) and vice versa.

Most of the transactions in PR-IVHS are Two Way On Demand, i.e. a vehicle sends a request for information, and the base station (or another vehicle) responds sending a message which contains the requested information (point-to-point communications). There are also cases where the base station or a vehicle addresses a message to all vehicles, or to a number of vehicles (point-to-multipoint communications).

2.3.4 Technology Availability

IVHS applications have different communication requirements regarding packet size, frequency of transactions, reliability, delay, etc. Apparently, a single technology cannot meet the diverse communication needs of all IVHS applications. Existing technologies should be identified and evaluated regarding their applicability to particular applications. Unmet communication needs have to be accommodated by new technologies.

2.4 Analysis and assessment diagram

As we discussed earlier, the general diagram forms a loop of the required steps, needed for designing and optimizing the packet radio system under consideration. Here we are focusing on the analysis and assessment box, which is shown in greater detail in figure 2.2. In this figure, we can identify three kinds of items, namely the external inputs, the internal inputs and the evaluation modules. The following subsections present a brief description of the several modules and their interconnection.

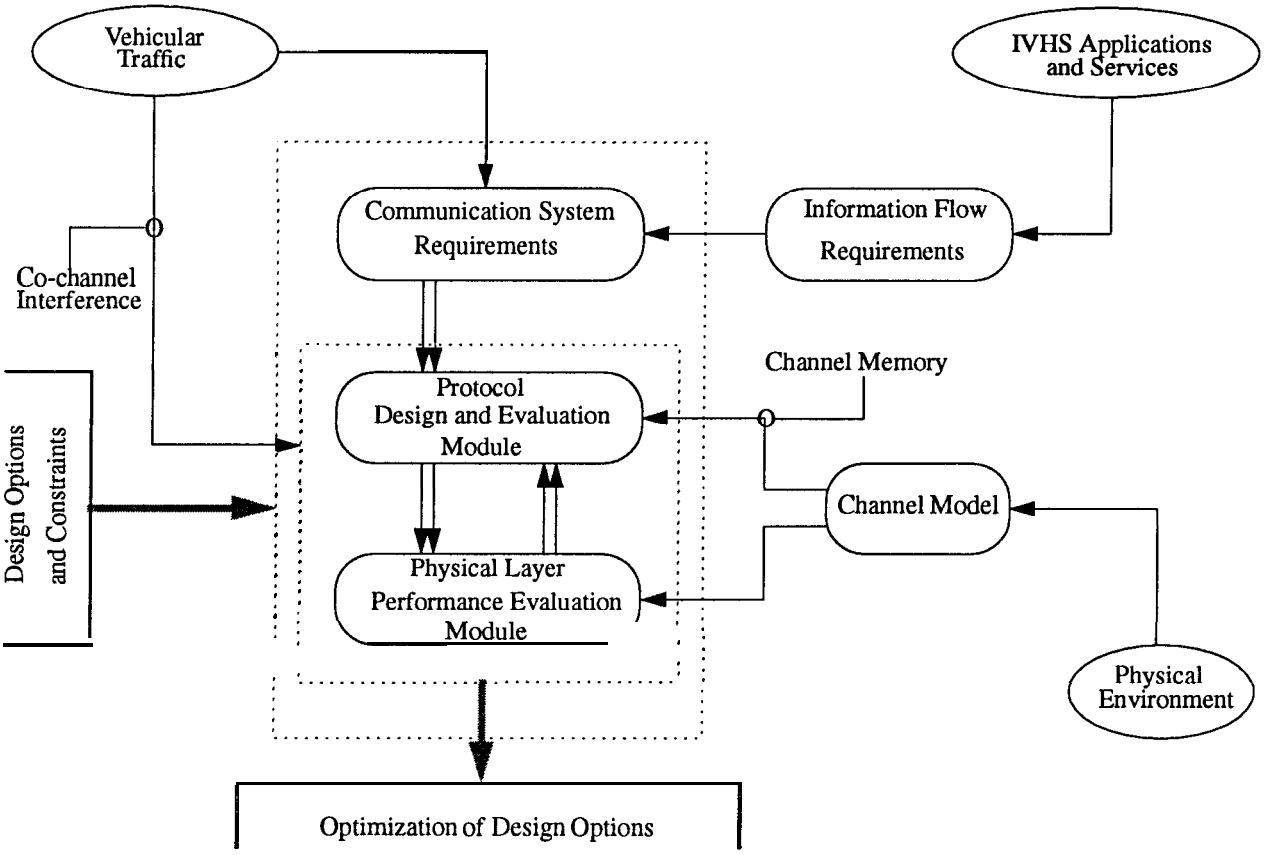

Figure 2.2: Analysis and assessment diagram

2.4.1 External Inputs

As the first group of inputs to our system we consider the services that this packet radio system must be able to provide to the users. There will be six applications and more than twenty services at the final stage of the IVHS deployment; each one having different demands regarding delay and reliability. For example, ATMIS is not a real-time application. Thus, depending on each service, the delay must be minimized from the customer standpoint. On the other hand, AVCS is a real-time application, where the acceptable delay is very short and the loss of information must be very small for safety reasons.

Although we consider only two of these applications, namely ATMIS and AVCS, they incorporate most, if not all, of the crucial design aspects of the overall project. It must be understood that this design problem we face is not an unconstrained one, but we have to seek a solution based on, or limited by, certain constraints on the architecture and the technology availability. It is highly probable that the final decisions will be based on economical, rather than technical considerations.

As we move from the more abstract to the more realistic input groups, we identify the next input which is vehicular traffic. The envisioned automated freeway system will consist of both automated (AUT) and driver-controlled traffic (DCT) lanes. It is obvious that the traffic load on the freeways, or on the surface streets, is translated to a number of customers that want to use the services provided by the system. On the other hand, the communication subsystem has to be flexible, in order to accomodate heavy traffic within the promised quality. As a first approach to the analysis of this problem, we consider different traffic scenarios (light, heavy, congested) and optimize the system under these conditions. One can suggest that vehicular traffic is the most important output of AVCS, since its ultimate goal is to improve the traffic flow in a freeway. This will lead to a lot of difficulties in the optimization of the overall system, since both the communication subsystem and the vehicle control subsystem will interact. Although this approach seems to be the correct one, it is needless in reality, since the impact of the data traffic on vehicular traffic is not very significant. On the other hand, vehicular traffic is the main factor that determines the data

traffic generated in the channel. Hence, we are justified in classifying it as an external input.

Moving even closer to the real world, we see that a crucial factor for the design, and hence the performance, of the system is the physical environment in which the system is going to operate. This includes the freeways and the surface streets. The freeway environment has unique channel characteristics. Thus, an adequate propagation model has to be found in order to sufficiently describe both the long and short term effects of this channel on the transmitted signal. The model used for this channel has to take into account several important characteristics of the channel, like propagation loss, multipath fading, shadowing, fading duration and delay spread. A great deal of research (Harley 1989), (Rustako et al. 1991), (Xia et al. 1992) has been conducted in the area of channel modelling and a widely accepted general model, or simplifications of it, is used to carry out the physical layer performance evaluation of several systems. We have to note at this point that the lack of measurements is, for the time being, an obstacle to the effort of channel modelling, since the justification of the models is based only on theoretical arguments.

2.4.2 Communication System Requirements

Information must flow to and from several entities of the system, in order to accomodate the communication needs of the applications. It is necessary to identify the different communication links and also to pose a certain structure (i.e., frame, packet) on this information, so that the communication system can efficiently move it from its source to its destination.

There are three basic communication links examined, namely the vehicle to base station link, which consists of ATMIS requests and AVCS control information, the base station to vehicle link, consisting of ATMIS information and AVCS control information, and the vehicle-to-vehicle link, with AVCS control information.

Regarding the structure of the information, we have to specify the number of bits required to represent each piece of information. In addition, we have to account for the bits that contain no information, like coding and synchronization bits, but have to be added to insure

an acceptable level of reliability. Of course, the selection of such a crucial parameter for the overall performance of the system is not arbitrary. It is a result coming from the lower layer performance and evaluation modules. However, it does not significantly change the communication requirements. The most important output of this module is the total data rate needed for all these applications to coexist and the requirements to be met.

2.4.3 Protocol Design and Evaluation Module

The design and evaluation of an efficient protocol is probably the most difficult task. Several multiple access protocols have to be considered for each communication link. The most challenging task is to design and evaluate a protocol that can be used for both vehicle to base station and vehicle-to-vehicle communications.

As we have already mentioned, the data traffic and the communication requirements of PR-IVHS are heterogeneous. In ATMIS, the data traffic is non-periodic and the the required throughput is high. On the other hand, AVCS is a real-time application, generating periodic data traffic and having strict demands on reliability. Great effort is taken in order to provide integrated solutions for all the services, which is always a very attractive feature for every communication system.

The measures used to evaluate the performance of the protocol layer are the throughput-delay for the vehicle to base station link, and the deadline failure probability for the vehicle-to-vehicle link. All these measures are analyzed in greater detail in chapters 4 and 5.

2.4.4 Physical Layer Performance Evaluation Module

The physical layer performance affects the overall system performance in the most direct way. Because of this reason, a general analytical tool that handles a wide range of options is needed. Although a thorough discussion on this module is presented in chapter 7, we mention here the several parameters that this tool takes into account. Both Spread Spectrum and narrowband systems can be analyzed in combination with various coherent and noncoherent

modulation schemes. Other features like coding, diversity (micro, macro) and power control strategies are also included in this tool.

The most important outputs of this module are the bit error probability, the packet success rate, and the outage probability, which are calculated in chapter 7, for an asynchronous multi-cell Direct-Sequence Code Division Multiple-Access (DS/CDMA) microcellular system.

2.4.5 Interaction of conceptual modules

As we have already mentioned, the concept of layering in this packet radio system is not so clear. In contrast with other traditional communication networks, where we can design, analyze and optimize each layer independently from the other, in this system such an approach fails.

We can see from figure 2.2 that there is a strong interaction between the physical and the protocol layer. In order to evaluate the performance of the protocol layer, the packet error probability as a function of several parameters is needed. On the other hand, a completely different physical layer performance may be the result of a different multiple access protocol.

Moreover, the channel model does not affect only the physical layer performance, but also the performance of the protocol layer through the channel memory. Indeed, the selection of the error control strategy is mainly determined by the channel memory. Finally, vehicular traffic is translated to users that want access to the shared communication channel. The generated co-channel interference greatly degrades the physical layer performance.

2.5 Conclusions

In this chapter, we presented a general procedure for designing a packet radio system, like the one needed to support IVHS applications. We also presented a list of the design options and constraints related to ATMIS and AVCS services. The ***communication system***

analysis and assessment diagram was the subject of an extended discussion, since it reveals new issues regarding this packet radio system, the most important of them being the strong interconnection between the physical and the protocol layers.

Chapter 3

Integrated ATMIS/AVCS Data Traffic

3.1 Introduction

As mentioned in chapter 2, a good understanding of IVHS application and communication requirements is needed before the establishment of spectrum needs and the evaluation of current technologies' suitability to support these applications. In this chapter, we examine the communication requirements of two IVHS applications, namely ATMIS and AVCS.

Section 3.2 presents the services that ATMIS and AVCS promise to offer to drivers. Section 3.3 describes the vehicular traffic in an envisioned automated freeway. The communication needs of an integrated ATMIS/AVCS system are discussed in section 3.4. The information flow requirements and the communication system requirements are analyzed in sections 3.5 and 3.6 respectively.

3.2 IVHS Applications and Services

There are six major applications of IVHS (Klein et al. 1993) :

1. Advanced Traffic Management Systems (ATMS)

2. Advanced Traveler Information Systems (ATIS)

3. Advanced Vehicle Control Systems (AVCS)

4. Advanced Public Transportation Systems (APTS)

5. Advanced Rural Transportation Systems (ARTS)

6. Commercial Vehicle Operations (CVO)

The following subsections present the combined services offered by ATMS and ATIS, and the features of AVCS.

3.2.1 Advanced Traffic Management and Information Systems (ATMIS)

ATMIS combines the services offered by ATMS and ATIS. The integration of these two applications promises to improve the traffic flow by detecting accidents and bottlenecks, and provide drivers with valuable guidance information (Jurgen 1991).

In ATMS, the traffic conditions are monitored by a surveillance system and the collected data are processed in a traffic management center (TMC). These data are used to inform drivers about traffic conditions, accidents, and alternative routes. ATMS services make possible the real-time adjustment of traffic control systems, which in conjuction with variable message signs for driver advice can reduce delays, expected travel time and accidents, thus optimizing the traffic flow on freeways and surface streets.

In ATIS, communication between vehicles and base stations provides the drivers with information about traffic conditions and information about services such as hotels, gas stations, restaurants etc. In-vehicle display units provide electronic maps, route selection, and real-time route guidance. In addition to trip-related information, ATIS services offer electronic vehicle identification for toll debting, safety advisory and warning messages, “Mayday” signaling and capabilities for immediate response in emergencies.

3.2.2 Advanced Vehicle Control Systems (AVCS)

AVCS technologies have the potential to increase substantially the transportation safety and capacity of the freeways, and to provide drivers with electronic equipment capable of performing driving functions. AVCS will combine current and future technologies (intelligent cruise control, vision enhancement systems, collision warning and avoidance systems, lane departure warning systems, automatic braking systems) to provide full vehicle and highway automation.

The first partially automated vehicles will be equipped with sensors and detection radars, making them capable of obstacle detection and avoidance. Later, the development of lateral (steering) and longitudinal (speed and spacing) control systems will enable platooning of vehicles and automatic lane-changing maneuvers. The full automatic steering of the vehicles will be the last step towards a completely automated vehicle control system, which will virtually eliminate the human driving functions and help to reduce accidents and increase traffic flow (Jurgen 1991).

3.3 Vehicular Traffic

In this section, we present the organization of traffic in an envisioned automated freeway. An automated freeway system incorporates roadway and roadside facilities, and specially equipped vehicles which operate under fully automatic lateral and longitudinal control. The automation of human driving functions will eliminate human errors, thereby reducing accidents and congestion. Furthermore, the air quality will improve, since the emissions caused by the current levels of congestion will be diminished because of a smoother traffic flow.

The ultimate goals of freeway automation are to maximize the traffic flow, increase the capacity of the existing freeways and reduce the number of accidents. Simulation results have shown that these goals can be achieved by organizing the vehicles in platoons (Varaiya 1991). According to a glossary of AVCS terminology (Shladover 1993a), platoon is defined

as “a group of vehicles operating under closely-coupled vehicle follower longitudinal control. The close coupling is achieved by communication among the member vehicles of information about vehicle movements and potential anomalies. Platooning can not be achieved with autonomous vehicles or point-follower longitudinal control.”

The first vehicle of a platoon is called the platoon leader and all the other vehicles are called followers. Any automated vehicle which is not member of a platoon is called a free agent. A free agent can be defined as a platoon of size one. It has been found (Varaiya 1991) that the optimum size of a platoon is 15-20 vehicles. The distance between vehicles within a platoon can be as small as 1 meter, whereas each platoon must keep a safe distance of approximately 64 meters from the preceding one (Linnartz 1993). We must note here, that the actual distance between vehicles or between platoons is a function of the constant speed that the vehicles must maintain and obviously of the feedback loop control technology.

Figure 3.1 shows the automated (AUT) and the driver-controlled traffic (DCT) lanes in a section of a freeway. In the driver-controlled traffic lanes, there are unequipped, partially automated (equipped for ATMIS services only) and fully automated vehicles (free agents), whereas in the automated lanes, only fully equipped vehicles are allowed. The envisioned trip scenario for a fully automated vehicle is as follows. Upon entrance in the freeway, the driver of the vehicle communicates with a base station and specifies a destination. The base station determines the optimum route that the vehicle has to follow (i.e., it assigns the vehicle to a lane and specifies the section of the freeway where it has to move to another lane, so that it can timely leave the freeway) and transmits the information to the vehicle. The vehicle is still under manual control in the non-automated lanes and the driver is responsible for moving the vehicle into the first automated lane. Once in an automated lane, the automatic control system is responsible for the steering and speed control of the vehicle.

3.3.1 Traffic Scenarios

The road traffic varies according to the time of the day (e.g., morning rush hours). For this reason, we consider three traffic scenarios, namely light, heavy and congested road

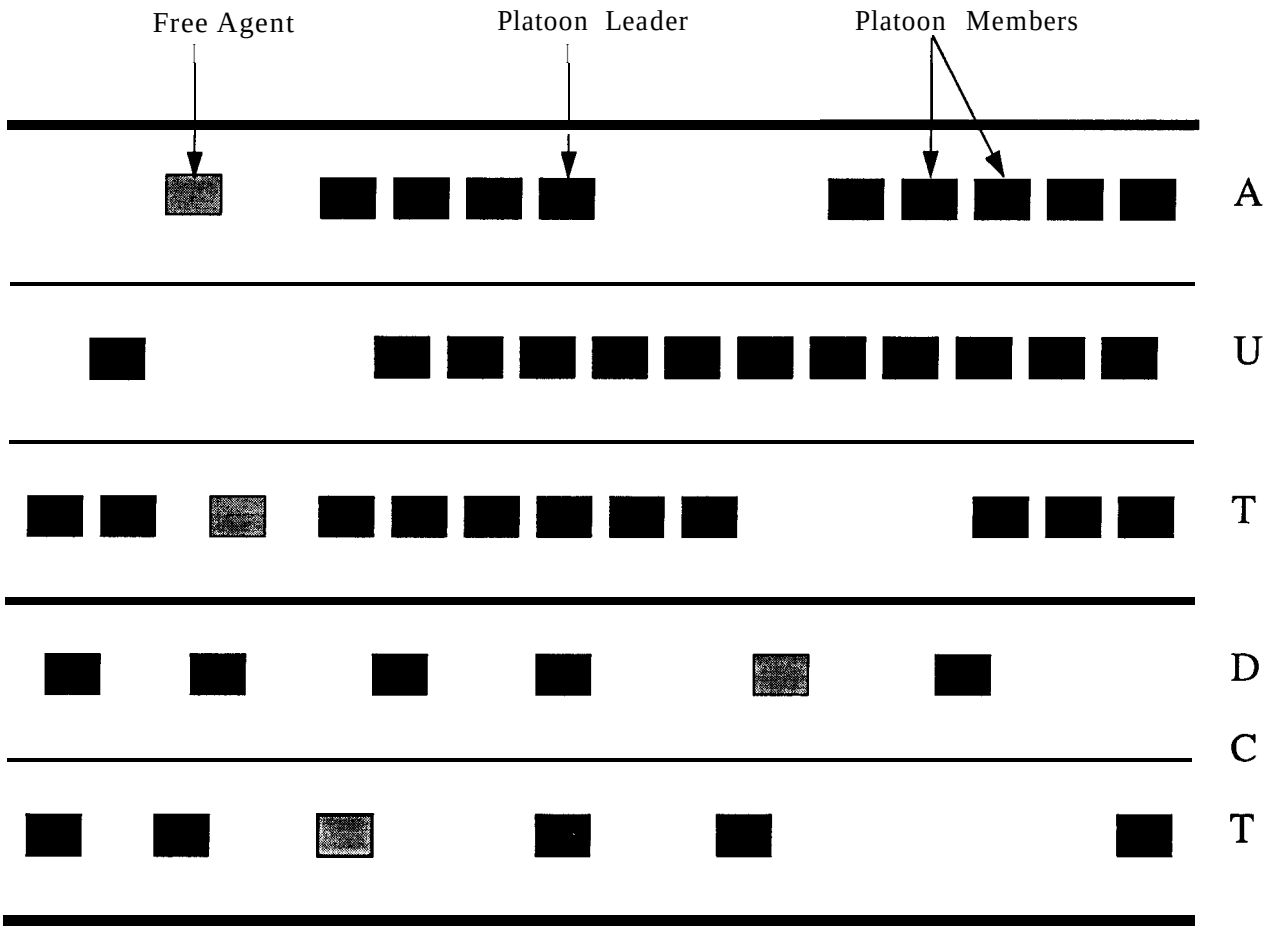

Figure 3.1: Automated and Driver-Controlled Traffic Freeway Lanes

traffic, in order to estimate the number of users in a cell. For the non-automated lanes, we use the California rule which dictates that the distance between vehicles is approximately a vehicle length (5 meters) for every 16 km.p.h. (10 m.p.h.) (Ioannou 1993). For the automated lanes, we assume that the distance between platoon members is 1 meter, the distance between platoons is 65 meters, and that light, heavy, and congested road traffic implies 10, 15, and 20 vehicles per platoon respectively.

The number of vehicles per kilometer per lane for the three scenarios is:

- Light Road Traffic (96 km.p.h. $\simeq$ 60 m.p.h.)
  - Automated Lanes: 80 vehicles/km/lane
  - Non-automated Lanes: 28 vehicles/km/lane
- Heavy Road Traffic (64 km.p.h. $\simeq$ 40 m.p.h.)
  - Automated Lanes: 165 vehicles/km/lane
  - Non-automated Lanes: 40 vehicles/km/lane
- Congested Road Traffic (32 km.p.h. $\simeq$ 20 m.p.h.)
  - Automated Lanes: 160 vehicles/km/lane
  - Non-automated Lanes: 66 vehicles/km/lane

3.4 Communication Needs

The leader and the members of a platoon must be in constant communication in order to maintain the desired spacing. The leader broadcasts its velocity and acceleration to all platoon members. In addition, each vehicle (except for the last one) transmits its own velocity and acceleration to the following one. The messages that have to be exchanged are time critical and need to be updated every 50msec to provide accuracy, safety and

smooth response to abrupt accelerations (Streisand 1992). The platoon leader can keep a safe headway from the preceding platoon by using its radar.

The following discussion implies that lane-changing maneuvers require communication between vehicles. Whenever a properly equipped vehicle enters an automated lane it becomes a free agent. It then communicates with the leader of the platoon ahead, requesting permission to join it. In response to this request, the leader gives the free agent permission to join the platoon, an ID number (i.e., its position in the platoon) and the target velocity and acceleration. If the platoon size is optimum, the platoon leader denies the permission. Furthermore, the free agent must inform the leader of the platoon behind, of its presence and provide location and speed information. Otherwise, the platoon leader-sensing a vehicle in a distance less than the headway-will slow down.

The platoon members can only execute lane-keeping maneuvers. When a platoon member wants to execute a lane-changing maneuver, it must first become a free agent. In this case a flurry of messages has to be exchanged between vehicles. The platoon member requests from the leader to split the platoon. Then, the leader asks the vehicles following and ahead of this member to change their speed (decelerate and accelerate respectively), transmitting the member's position in the platoon and the new target velocity and acceleration. The vehicle that requested the splitting of the platoon maintains its initial speed. After the vehicle's maneuver, the platoon leader must reassemble the platoon, asking the vehicles that decelerated to accelerate.

When the vehicle becomes a free agent and before it moves to an adjacent lane, it requests permission to join a platoon in that lane. A platoon leader gives permission to the free agent only if it is ahead of it and the platoon size is less than the optimum. When it moves, the free agent informs the other platoon leaders of the adjacent lane about its intention, transmitting its new velocity and acceleration.

The previous discussion clearly shows that lane-changing maneuvers require the exhange of a flurry of messages between vehicles. These messages are not critical, but the traffic will snarl up if failure to act within l-2 seconds occurs (Hitchcock 1993). If the lane-changing ma-

neuvers are handled by the base station, the vehicle that wants either to enter an automated lane or to move to another one, communicates directly with the base station. Then, the base station communicates with platoon leaders and other vehicles, so that the maneuvers can be executed in the most efficient way.

So far, we have discussed the communication needs for the various vehicle maneuvers in automated lanes, involving communication between vehicles. In addition to vehicle-to-vehicle communications there is also the need for communication between vehicles and base stations. The platoon leaders periodically send a message containing platoon status information to the base station. The base station periodically transmits to the platoon leaders the target velocity and acceleration, which optimizes the traffic flow to the platoon leaders. Furthermore, ATMIS equipped vehicles in both types of lanes (we assume that platoon members can also use ATMIS services) request information from the base station. These vehicles are also transmitting information about their status and their velocity, so that the base station can use them as a traffic probe. Finally, the base station sends messages containing traveler information and advisory in response to the requests for information from ATMIS users. The next section shows how these communication needs are translated into number of bits per message.

3.5 Information Flow Requirements

In this section, we try to assess the data requirements associated with the various communication needs. We first discuss the determination of a vehicle's location on the road. Then, we examine the message format and we discuss the various fields. Finally, we present the information flow requirements of the integrated ATMIS/AVCS system.

3.5.1 Determination of a vehicle's location on the road

Knowledge of a vehicle's location on the road is very important for the deployment of many IVHS applications. The location of a vehicle can be determined either by a central

control center or by the vehicle itself. Communication approaches for the determination of the location by a central control center include (TRB 1993a):

1. Triangulation by cellular or other ground stations
2. Triangulation by satellite receivers
3. In-pavement or roadside location beacons that detect passing vehicles at well-defined locations.

If the location is determined by the vehicle itself, potential approaches include:

1. Triangulation to cellular or other land-based transmitters of known location (e.g., Loran)
2. Triangulation to satellite receivers (e.g., GPS)
3. Recognition of location signals transmitted from in-pavement or roadside beacons which the vehicle passes.

In order to evaluate the above approaches, we must examine the accuracy and reliability they offer, the number of vehicles that can be handled simultaneously, the performance in different environments and the cost for infrastructure and in-vehicle equipment.

In a freeway environment, location information can be provided to the vehicles by magnetic strips mounted in the roadway. Such strips and the associated sensors have already been used as a reference system for an automated lateral control system test (Chang et al. 1993) and they have received considerable attention during the last year (Shladover 1993b). The vehicles can use them to obtain information about the freeway's direction and the lane number. In addition, a reference marker resets the vehicle's odometer at the beginning of a freeway's section, so that the vehicle can have knowledge of its actual location in that specific section.

Preamble	Source ID	Destination ID	Type of message	Data	Error Detecting/ Correcting Code

Figure 3.2: Message Format

3.5.2 Message Format

The message format is shown in figure 3.2. It consists of the following fields:

- PREAMBLE. The bits in the preamble are used for synchronization of the receiver to each incoming message. The preamble usually consists of 16 bits (Streisand 1992).
- SOURCE ID. This field contains information about the ID (address) and the location of the sender. Several addressing formats that have been proposed in the IVHS literature include vehicle-based addressing, platoon-based addressing, road-based addressing, and selective broadcast addressing (Sachs 1993). A permanent ID (such as the vehicle's serial number or license plate) for every properly equipped vehicle requires a large number of bits (e.g., 48 bits for the license plate (Sachs 1993)). This scheme results in waste of bandwidth, since a vehicle's ID must be unique only in one section of the freeway, due to the short range nature of communications (Hitchcock 1993). If magnetic strips are used for location information, the SOURCE ID field consists of 1 bit for the freeway's direction (North-South or East-West), 3 bits for the lane number (up to 8 automated lanes per direction), 5 bits for the position in the platoon (up to 32 vehicles in a platoon) and 10 bits for the actual position on the road (assuming that there is a reference marker every 1 kilometer), providing an accuracy of ± 0.5 meters. When the source of information is a base station, approximately 16 bits are neeeded for a unique base station ID (Streisand 1992).
- DESTINATION ID. This field contains the location of the message's recipient. It consists of 1 bit for the freeway's direction, 3 bits for the lane number and 5 bits for the position in the platoon, if the message is sent to a vehicle. In many cases this field

can be empty, since a vehicle, or a base station, can determine if it is the recipient of the message from the SOURCE ID and the TYPE OF MESSAGE fields.

- TYPE OF MESSAGE. This field consists of 8 bits describing the message type, such as "control information" or "request to join the platoon". With 8 bits we can have up to 256 unique messages.

- DATA FIELD. This field contains information, such as the velocity and the acceleration of the sender, the target velocity and acceleration that the recipient of the message has to follow, an ID number, electronic maps, etc. Velocity and acceleration require 8 bits each, giving an accuracy of $\pm 0.5 km/h$. Electronic maps and other information require a large number of bits.

- ERROR DETECTING/CORRECTING FIELD. This field consists of redundant bits for detection and/or correction of transmission errors. Error detection requires at least 16 bits (Linnartz 1993). Error control strategies are discussed in more detail in section 6.2.

The information flow requirements are summarized in Table 3.1. We notice that the messages from a vehicle to the base station for both ATMIS and AVCS are short (64 - 100 bits/message), since they contain only control information (velocity and acceleration), or simple requests for information which can be determined by the TYPE OF MESSAGE field. For the same reason, vehicle-to-vehicle and base station to vehicle transactions for AVCS, also require short messages. Base station to vehicle transactions for ATMIS require the transmission of long messages (e.g., digitized maps) which can be broken up into several packets, each containing, say 512 bits.

	Vehicle to BS	BS to Vehicle	Vehicle-to-Vehicle	
			Intra-platoon	Inter-platoon
ATMIS	Info requests Traffic probe (short messages)	Traveler info & advisory (long messages)	—	
AVCS	Platoon status information Requests for lane changes (short messages)	Target velocity & acceleration Handling of lane changes (short messages)	Lane keeping maneuvers Lane changing maneuvers (short messages)	Lane changing maneuvers (short messages)

Table 3.1: Information Flow Requirements

3.6 Communication System Requirements

At the present time, the exact values of the necessary parameters for calculation of the communication system requirements are not completely known. Thus, instead of providing numbers that may be non-realistic, we only identify the parameters that we need to know in order to calculate the communication requirements (i.e., the data rate) for the various communication links in PR-IVHS.

- Vehicle-to-vehicle (Intra-platoon)
  - cell size
  - number of automated lanes
  - number of vehicles per platoon
  - number of bits per message
  - repetition rate
  - number of lane changes per kilometer per second
  - number of exchanged messages per lane change
  - number of bits per message
- Vehicle-to-vehicle (Inter-platoon)
  - number of lane changes per kilometer per second

- number of exchanged messages per lane change
- number of bits per message

- Vehicle to base station
  - number of platoon per cell
  - repetition rate for platoon status information
  - number of bits per message
  - number of lane changes per kilometer per second
  - number of exchanged messages per lane change
  - number of bits per message
  - number of ATMIS users per cell
  - frequency of ATMIS transactions
  - number of bits per message

- Base station to vehicle
  - number of platoon per cell
  - repetition rate for control information
  - number of bits per message
  - number of lane changes per kilometer per second
  - number of exchanged messages per lane change
  - number of bits per message
  - number of ATMIS users per cell
  - frequency of the various ATMIS transactions
  - number of bits per message

3.7 Conclusions

In this chapter, we examined the data traffic in an integrated ATMIS/AVCS system. We presented the services that the two applications will provide to the drivers in the future, and we described the vehicular traffic in an envisioned automated freeway system. Then, we discussed the communication needs of the integrated ATMIS/AVCS services. The information flow requirements were presented in section 3.5, where we analyzed the various fields of a message giving some tentative number of bits and we suggested a possible way for determination of a vehicle's location on the road, based on magnetic strips mounted on the roadway. Finally, we identified the necessary parameters for calculation of the communication system requirements. Once the values of these parameters are known, the communication requirements can be evaluated.

Chapter 4

Multiple Access Schemes for PR-IVHS

4.1 Introduction

In IVHS, vehicles communicate with base stations and other vehicles using a shared radio channel. One of the key problems in designing a communication system for IVHS is the coordination of the channel accessing, so that the bandwidth can be efficiently utilized.

Many multiple access schemes have been proposed in the literature (Abramson 1993), for allocation of portions of a given bandwidth to a large number of users. Depending on the communication needs of a specific application, different multiple access schemes have different performance. In IVHS, there are three communication links, namely the vehicle-to-vehicle link, the vehicle to base station link, and the base station to vehicle link. The performance analysis of several multiple access schemes in each of the three links can provide us with a better insight about the suitability of these schemes for PR-IVHS communications.

This chapter is organized as follows. In section 4.2, we identify the features and the communication needs for each of the three communication links. In section 4.3, we examine three classes of multiple access schemes, namely fixed assignment schemes, random access schemes, and reservation schemes. The feasibility of each class of multiple access schemes for the three communication links of PR-IVHS is examined in section 4.4.

4.2 Communication Links

In this section, we study the communication needs for each communication link, namely the vehicle-to-vehicle link (peer link), the vehicle to base station link (uplink), and the base station to vehicle link (downlink).

4.2.1 Vehicle-to-Vehicle Communication Link

Communication between vehicles can be further divided into two types; intra-platoon and inter-platoon communications.

Intra-platoon Communications

Intra-platoon communications refer to vehicle-to-vehicle communications within a platoon. The nature of communications is short range and periodic, with sporadic transmission of requests and acknowledgements between platoon leaders and platoon members.

In particular, the leader of each platoon broadcasts the target velocity and acceleration to all platoon members periodically. In addition, every platoon member (except for the last one) transmits its velocity and acceleration to the following vehicle periodically (20 times per second) (Sachs 1992).

If the lane-changing maneuvers require communication between vehicles, whenever a vehicle wants to leave its platoon, it requests permission from the platoon leader. Then, the platoon leader broadcasts a platoon-split command, so that the platoon member can become a free agent. After the lane-changing maneuver, the platoon leader must remerge the platoon.

Inter-platoon Communications

Inter-platoon communications refer to communications between platoon leaders as well as between platoon leaders and free agents (platoons of size one). This kind of communication is required if the lane-changing maneuvers are not handled by the base stations. A lane-changing maneuver is initiated whenever a free agent wants to join a platoon, or when a platoon member wants to leave its platoon. The communication needs for these maneuvers have been discussed in section 3.4.

4.2.2 Vehicle to Base Station Link

Uplink communications include random requests and periodic messages containing vehicle-status information. The packets containing requests from vehicles arrive at a base station in a random fashion. In addition, the platoon leaders transmit their status information to a base station periodically, so that the traffic management center can use them as a traffic probe in order to optimize the traffic flow in the freeway.

4.2.3 Base Station to Vehicle Link

In the downlink, a base station transmits messages containing the information requested by the vehicles as well as messages containing control information (velocity and acceleration) for optimization of the traffic flow. If different subchannels are allocated to different base stations by means of FDM (Frequency Division Multiplexing), TDM (Time Division Multiplexing, or CDM (Code Division Multiplexing) there will be no contention in the downlink (i.e., no multiple access problem).

4.3 Multiple Access Schemes

In PR-IVHS, vehicles communicate with base stations and other vehicles via a shared radio channel. Due to the scarcity of the radio frequency spectrum, efficient utilization of the shared bandwidth is required. In order to efficiently share the channel with other users, a vehicle has to follow certain rules whenever it transmits a message. Otherwise, vehicle transmissions may interfere with each other and the performance of the system would degrade.

A multiple access scheme, also known as multiple access protocol, is a set of rules that specify how users (vehicles) should access the shared radio channel. Multiple access schemes can be classified into three main classes, namely fixed assignment schemes, random access schemes, and reservation schemes. Each of these three classes has its advantages and disadvantages depending on the user requirements. We will discuss these classes in the following subsections.

4.3.1 Fixed Assignment Schemes

These schemes are the traditional method for multi-user communications. The radio channel is divided into several subchannels, one for each user. These subchannels are separated in such a way that transmissions in one subchannel do not interfere with simultaneous transmissions in another subchannel. Fixed assignment schemes include frequency division multiplexing (FDM), time division multiplexing (TDM), and code division multiplexing (CDM).

These schemes can offer high throughput when the source requirements are known and the data traffic is heavy. Otherwise, when the data traffic is bursty these schemes are wasteful. For example, a subchannel may be lightly loaded, but other subchannels with heavy load cannot share their load with this subchannel, due to the characteristics of fixed assignment schemes. Thus, these schemes can waste channel time, leading to inefficient utilization of bandwidth.

4.3.2 Random Access Schemes

In these schemes, the channel is shared by the users in a statistical multiplexing fashion. Whenever a user wants to transmit a packet, it can use the whole channel for the transmission. If the channel load is not heavy, the packet transmission time, using these schemes, is always shorter than the time required in fixed assignment schemes.

Random access schemes include ALOHA (Abramson 1970), Slotted-ALOHA (Roberts 1975), (Zhang 1992), Framed-ALOHA (Okayed et al. 1978), (Schulte 1983), (Westerlies et al. 1989), CSMA (Carrier Sense Multiple Access) (Kleinrock et al. 1975), (Tobagi 1982), BTMA (Busy Tone Multiple Access) (Tobagi et al. 1975), ICMA (Idle-signal Casting Multiple Access) (Chua 1992), and CDRA (Code Division Random Access) (Polydoros 1987), (Pronios 1990).

ALOHA

When an ALOHA scheme is used, the users can transmit messages at any time. If more than one user transmits at the same time, a collision occurs. If a collision occurs, the messages will be destroyed and the users involved in the collision have to retransmit them after waiting a random period of time. Figure 4.1 illustrates the channel sharing, for the ALOHA scheme. This scheme is very simple, but the maximum channel capacity is low (0.18 or $1/2e$). Furthermore, whenever the channel load exceeds the maximum channel capacity, the messages suffer infinite delay. This is called the instability problem of ALOHA.

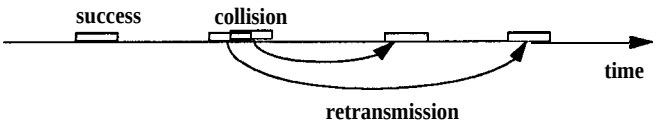

Figure 4.1: The ALOHA scheme.

Slotted-ALOHA

In Slotted-ALOHA (S-ALOHA), the time is divided into time slots of the same length. The length of a time slot is equal to the transmission time of a packet plus some guard time to compensate for the propagation delay. Thus, a packet can be only transmitted at the beginning of each slot (see figure 4.2). Confining the packet transmission within a slot, reduces the collision probability compared to ALOHA and increases the maximum channel capacity to 0.36 (or $1/e$).

Although S-ALOHA improves the maximum channel capacity, the instability problem still remains. Two approaches are used to solve this problem; collision resolution and dynamic transmission probability. Collision resolution algorithms include the tree algorithms (Capetanakis 1979) and the splitting algorithms (Mosely 1985). Algorithms that can adjust the transmission probability or the length of the random delays include the binary exponential backoff algorithm (Metcalfe 1976) and the pseudo-Bayesian algorithm (Rivest 1987).

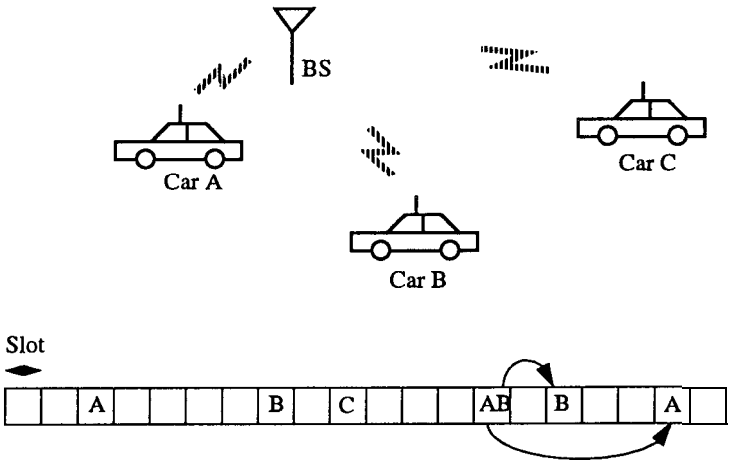

Figure 4.2: The Slotted-ALOHA scheme.

Framed-ALOHA

The channel time is slotted, and a number of slots is designated as a frame (see figure 4.3 for the frame structure). A user can transmit only one packet per frame, regardless of the frame length. The frame structure is useful when the users transmit packets periodically, provided that the period equals the frame length.

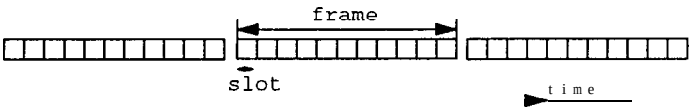

Figure 4.3: The structure of the Framed-ALOHA scheme.

CSMA (Carrier Sense Multiple Access)

In the CSMA scheme, the user senses the channel activity before it proceeds with packet transmission. If the channel is idle, the user starts the transmission of a packet. On the other hand, if the channel is busy (i.e., another user is transmitting a packet), it will reschedule the packet transmission after waiting a random period of time and sensing the channel activity. Collisions may still occur if more than one users sense that the channel is idle, simultaneously. In other words, collisions occur due to the non-zero propagation delay or the sensing overhead. When collisions occur, all packets are retransmitted after a random period of time.

This scheme works better when the ratio of the propagation delay to packet transmission time is small. Then, the channel capacity of CSMA can be close to one. However, the CSMA scheme suffers from the hidden terminal problem (see figure 4.4). The problem is solved by using the BTMA scheme, which is presented in the next section.

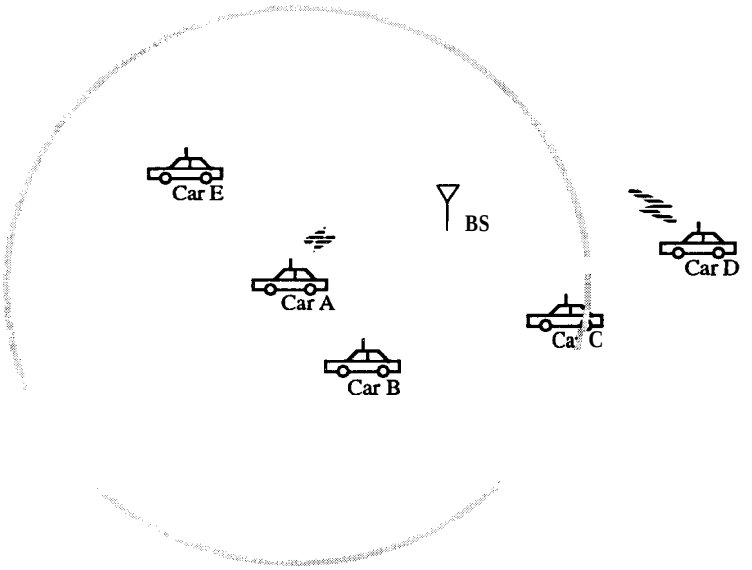

Figure 4.4: The hidden terminal problem in the CSMA scheme.

BTMA (Busy Tone Multiple Access)

BTMA is a variation of CSMA. In the context of a multihop packet radio network, users who are two hops away from each other may not be able to detect simultaneous transmissions by carrier sensing. This is known as the hidden terminal problem. In order to solve this problem, the receiver (BS in figure 4.5) broadcasts a busy tone while it is receiving a packet. The users, detecting the busy tone, will refrain from transmission and collisions will be avoided. In figure 4.5, vehicle D, after detecting a busy tone, will not interfere with the transmission of vehicle A.

ICMA (Idle-signal Casting Multiple Access)

ICMA is a variation of BTMA. It is used in a centralized one-hop star network where a number of users want to send messages to the base station. The ICMA scheme works as follows. The base station keeps broadcasting an idle signal while it is not receiving a message. Upon detection of an idle signal, the user can transmit a message to the base station. When

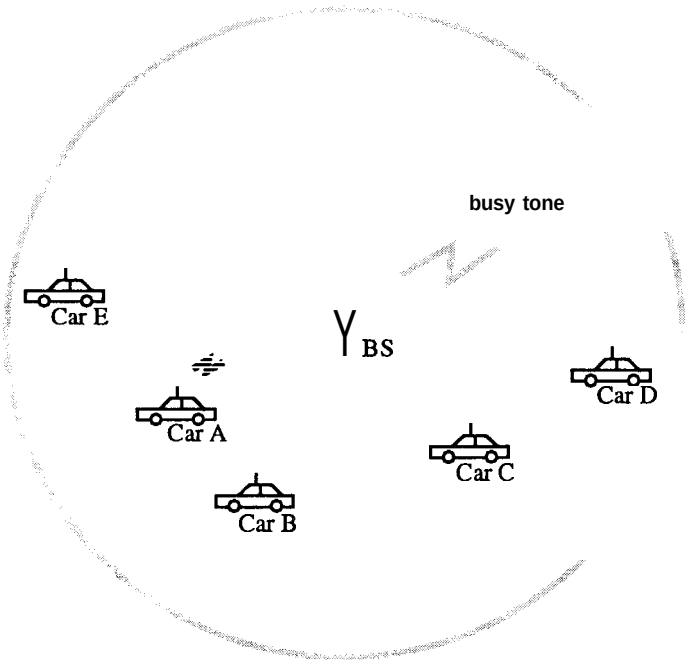

Figure 4.5: The BTMA scheme.

the base station is receiving a message it turns off the idle signal and thus, no users interfere with the on-going transmission.

ICMA outperforms BTMA when the channel is fading and signals cannot be detected. In particular, when the lost signal is a busy tone (in BTMA), the user may initiate a transmission that will interfere with the on-going transmission to the base station, whereas if the lost signal is an idle signal (in ICMA), the user can avoid packet collisions and suffer only some extra delay.

CDRA (Code Division Random Access)

This scheme uses spread spectrum techniques, so that simultaneous collision-free transmissions can be possible. In CDRA, a packet is spread by a pseudo orthogonal code sequence before its transmission. If the spreading codes are properly assigned, packets that

are simultaneously transmitted can be received successfully with high probability.

4.3.3 Reservation Schemes

In reservation schemes, a user makes a reservation before it transmits its message. The reservation schemes are similar to the fixed assignment schemes, but the subchannels are dynamically assigned to the users via the reservation process.

The control of systems employing reservation schemes can be either central or distributed. Reservation schemes with central control include PRMA (Packet Reservation Multiple Access) (Goodman et al. 1989) and D-TDMA (Dynamic Time Division Multiple Access) (Wilson et al. 1993). Schemes with distributed control include R-ALOHA (Reservation ALOHA) (Crowther 1973), CSAP (Concurrent Slot Assignment Protocol) (Mann 1988), DCAP (Decentralized Channel Access Protocol) (Zhu et al. 1991), AC/ID (Access Control with Interference Detection) (Hubner et al. 1991) and R-BTMA (Reservation Busy Tone Multiple Access) (Tabbane 1992).

R-ALOHA

R-ALOHA was first used in satellite communications, where a number of earth stations communicate with each other via a satellite which functions as a transponder. The channel is split into two subchannels; the uplink and the downlink. The transponder transmits whatever it receives from the uplink to the downlink.

This protocol works as follows. In the uplink, the time is structured in frames similar to those of Framed-ALOHA. Any user who wants to transmit a packet will randomly choose a slot which was not used in the previous frame. If the transmission is successful, the corresponding slot in the next frame will be reserved for this user. When the user finishes the transmission of all of its packets, the slot will be free for contention again.

This scheme can provide high throughput, if users transmit packets periodically. Fi-

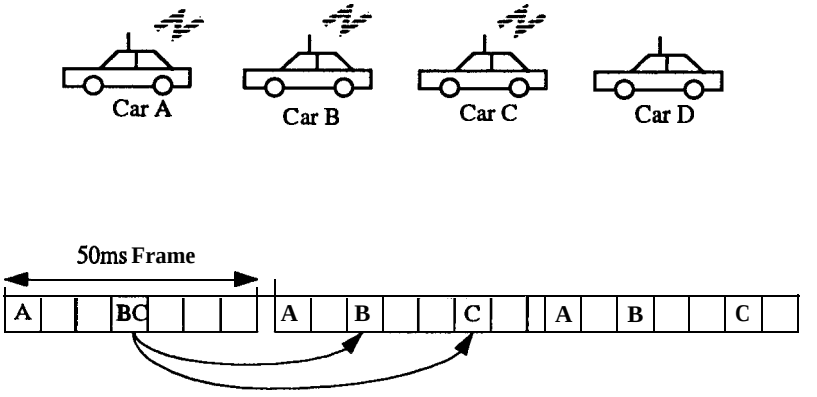

Figure 4.6: The R-ALOHA scheme.

gure 4.6 shows an example of an R-ALOHA scheme which can be used for intra-platoon communications.

PRMA (Packet Reservation Multiple Access)

PRMA is a variation of R-ALOHA and is used in terrestrial packet radio communication systems, where a number of local stations want to communicate with a central base station. Local stations use the uplink for transmission of packets to the central station, whereas the central station uses the downlink to acknowledge the received messages from the local stations.

CSAP (Concurrent Slot Assignment Protocol)

CSAP is a distributed (no base station) reservation-based vehicle-to-vehicle communication protocol. In vehicle-to-vehicle communications, a vehicle broadcasts its status (e.g., velocity, acceleration, etc.) to its neighboring cars periodically. Figure 4.7 shows the frame structure in the CSAP scheme. As in R-ALOHA, the time is slotted and structured in frames

containing a fixed number of slots (e.g., N). In each slot, there is an extra N-bit header that records the status of every slot in a frame as seen by the transmitter. The vehicles monitor (using special hardware) the status of every slot, continuously. The kth bit is set to 0 if the kth slot is sensed to be empty or a collision has occured; it is set to 1 if the packet in the kth slot is received correctly. By exchanging the channel status seen by each vehicle, a vehicle can select a slot to transmit its packet once per frame.

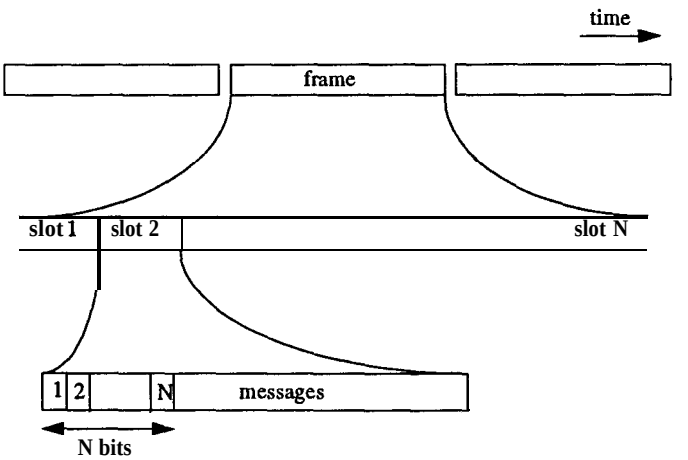

Figure 4.7: The frame structure in the CSAP scheme.

DCAP (Decentralized Channel Access Protocol)

DCAP is also a distributed vehicle-to-vehicle communication protocol. The difference from CSAP is the way that the N-bit header is handled. To be more specific, the kth bit will be set to 0 if the corresponding kth slot is detected to be empty, whereas it will be set to 1 if the corresponding slot is used (success or collision). Moreover, DCAP requires special hardware for detection of interference outside the transmission region in order to avoid packet collision.

AC/ID (Access Control with Interference Detection)

AC/ID is another vehicle-to-vehicle communication protocol, which combines the reservation mechanism of R-ALOHA and the carrier sensing technique. The time axis is structured into TDMA frames, which are similar to those of R-ALOHA. A station is assumed to be able to transmit a packet in one slot with two options. It can either use the whole slot to transmit the whole packet, or it can use some portion of a slot to measure the channel quality (e.g., SNR) and the rest of the slot to transmit a shorten packet. A station that has reserved a slot can use option 1 to transmit whole packets, but it can occasionally use option 2 to detect the possible interference in the slot which is reserved for it. If it detects interference, it will access another free slot. In order to know which slots are free for access, a station needs to measure the channel quality for all slots all the time and store the results in its local bitmap for future reference. By randomly using option 2 to detect the on-going interference, AC/ID is capable of collision detection. Figure 4.8 illustrates how this scheme works.

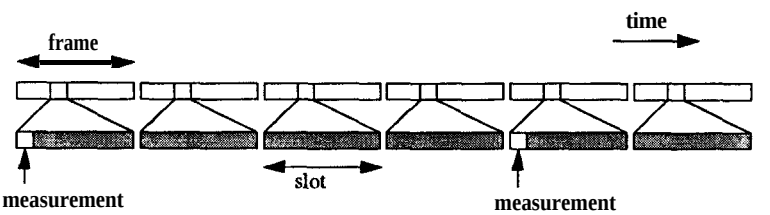

Figure 4.8: The AC/ID scheme.

R-BTMA (Reservation Busy Tone Multiple Access)

R-BTMA is also a vehicle-to-vehicle communication protocol, which combines implicit reservation as in R-ALOHA and a busy tone mechanism as in BTMA. In R-BTMA, there are two slotted channels (see figure 4.9); the one is called data channel (DC) and the other is called busy tone channel (BTC). The detection of a busy tone in BTC indicates that the corresponding data slot is being used by another vehicle. When a vehicle successfully

receives a packet in a slot, it transmits a busy tone at the corresponding slot in the BTC. Therefore, by listening to the BTC, a vehicle can find the status of the corresponding slots in the data channel. If no busy tone is detected in a slot, the corresponding data slot is either in an idle state or in a collision state. If a busy tone is detected, the corresponding data slot is being reserved and the potential user will refrain from transmitting in this slot.

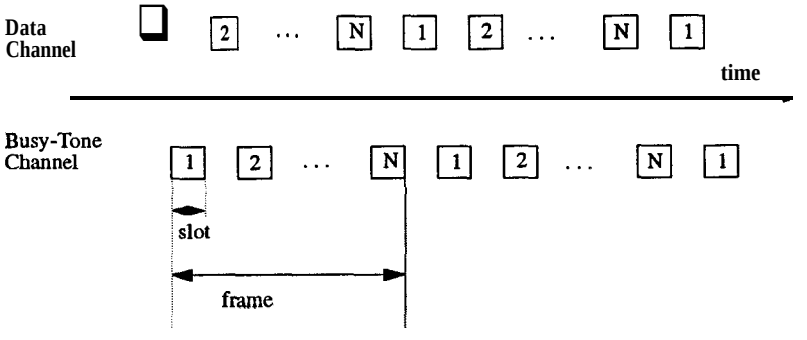

Figure 4.9: The R-BTMA scheme.

D-TDMA (Dynamic Time Division Multiple Access)

D-TDMA is used in centralized one-hop radio networks, where a number of local stations want to communicate with the central station. There are two orthogonal channels; one is called uplink and the other is called downlink. The uplink is a slotted channel, where some slots are designated as reservation slots and some slots are the data slots (see figure 4.10). In order to transmit data packets to the central station, a local station sends a reservation packet to the central station. When the central station receives the reservation packet, it informs the local station when it should transmit the data packets. If the central station does not receive the reservation packet (due to collision or channel noise), the local station will time out and retransmit a reservation packet. There are two types of services supported by D-TDMA; periodic services such as voice and non-periodic services such as data. For voice service, the central station allocates a slot in the TDMA frame periodically, until the local station finishes its transmission. For data service, the central station allocates a number

of data slots requested by the local station for transmission of its data packets. Although the reservation packets for both types of services are transmitted in the reservation slots, using a random access scheme like S-ALOHA, the retransmission mechanisms are different. For data service, if the reservation packet is not successfully received by the central station, the local station will time out and retransmit it after a random period of time, whereas for voice service, the local station will retry in the next frame, because voice service requires short delay. If a local station that needs voice service cannot get the acknowledgment for a pre-determined number of frames, it will block the call instead of overflowing the reservation channel.

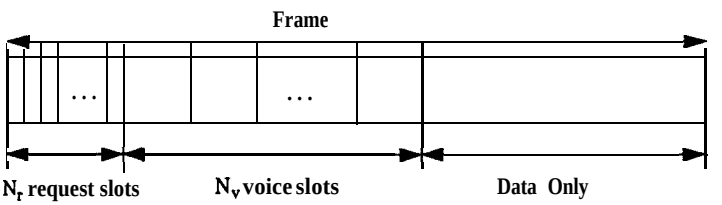

Figure 4.10: The frame structure of the D-TDMA scheme.

4.4 Multiple Access Options for PR-IVHS

In this section, we discuss the feasibility of each type of multiple access schemes, based on the communication need of the three communication links. In the uplink (vehicle to base station), vehicles transmit requests for information randomly and status reports periodically. It is obvious that fixed assignment schemes are not compatible with this kind of data traffic, because it is very inefficient to allocate one subchannel for each of the vehicles in the freeway. Random access and reservation schemes are the possible options. Although, reservation schemes are very efficient for periodic data traffic, random access schemes may be able to accommodate both types of data traffic, if the period of the periodic status reports is not short enough to justify the extra complexity of reservation.

In the downlink, due to the large and steady information flow from the base station to

vehicles, fixed assignment schemes like TDM or FDM are the best candidates. Distributed reservation schemes such as R- ALOHA are also possible, but the complexity will be increased because neighboring base stations need to coordinate the channel accessing with each other.

For the vehicle-to-vehicle link, hybrid and random access schemes are more efficient than other schemes for intra-platoon and inter-platoon communications respectively. In the case of intra-platoon communications, periodic vehicle status reports and random requests for lane-changing maneuvers are the two primary considerations. Because of the totally different nature of the two types of data traffic, the hybrid schemes that combine the merits of random access and reservation are the most promising options. For example, a TDMA frame structure with some slots dedicated to non-periodic request packets (using S-ALOHA) and some slots dedicated to periodic status packets (using R-ALOHA) is one possible hybrid scheme. This hybrid scheme will be examined in detail in chapter 5. In inter-platoon communications, requests for lane-changing maneuvers occur randomly and infrequently. Thus, random access schemes are the most suitable options for this type of communication. Fixed assignment schemes are too inefficient for vehicle-to-vehicle communications.

4.5 Conclusions

In this chapter, we studied three classes of multiple access schemes for the three communication links in PR-IVHS. We compared the advantages and the disadvantages of each class and we concluded that the choice of the most suitable schemes for PR-IVHS depends strongly on the communication needs of each link. The next chapter presents the quantitative performance analysis of some typical multiple access schemes chosen among the feasible schemes presented here.

Chapter 5

Performance Evaluation of Multiple Access Schemes for PR-IVHS

5.1 Introduction

In chapter 4, we discussed the relation between multiple access schemes and the communication needs of each of the three communication links. We saw that a multiple access scheme can be suitable for one communication link but not for another, because of the different communication needs of each link. In order to select the most suitable multiple access scheme for a specific communication link, quantitative analysis is required. In this chapter, we will analyze and evaluate the performance of some typical multiple access schemes for PR-IVHS. The performance analysis allows us to compare different schemes (protocols) and construct new integrated protocols that may be more suitable for PR-IVHS.

There are mainly two types of communications in PR-IVHS, namely periodic and non-periodic communications. Their common characteristic is the small packet size (see chapter 3 for the packet format). This makes slotted random access schemes especially appealing for non-periodic communications. The major difference between the two types is the different delay constraints. In particular, the periodic type requires short delay and high reliability, whereas the non-periodic type does not have stringent delay constraints. Thus, the criteria (performance measures) used to evaluate the protocol performance are different. The

measures for the performance evaluation of protocols are presented in section 5.2.

In order to make the analysis mathematically tractable, we make the following assumptions for all the protocols under consideration:

- The performance of the protocols is evaluated for a single cell, assuming that the spatial distribution of vehicles in the cell is uniform. The number of vehicles in a region of a certain area is a function of the vehicular traffic density only

- In vehicle to base station communications, a vehicle sends requests to base stations randomly, via the uplink (long range, multipoint to point communications)

- In inter-platoon communications, a vehicle communicates with the leader of its platoon or with other platoon leaders randomly, via the inter-platoon link (medium range, point-to-point communications)

- In intra-platoon communications, a vehicle transmits its status to its follower periodically, via the intra-platoon link (short range, point-to-point communications)

- We assume that the three links (i.e., uplink, inter-platoon link, and intra-platoon link) use orthogonal communication subchannels (TDM or FDM), so that they do not interfere with each another.

The performance of Slotted-ALOHA, Framed-ALOHA, and Spread Spectrum S-ALOHA is analyzed in sections 5.3, 5.4, and 5.5, respectively. In particular, we examine how these protocols perform in each of the three communication links (for a single cell). In section 5.6, we present and discuss the design parameters of two protocols for the integrated ATMIS/AVCS data traffic, where all the communication links in a single cell share the same time-frequency domain.

5.2 Performance Measures

One of the measures used for the performance evaluation of a protocol is the throughput of a node (base station or vehicle), which is the average number of packets per second that are successfully received by the node. A good protocol should provide as large a throughput as possible. The packet delay is the time elapsed from the generation of the packet at the transmitter to the successful reception at the receiver. A good protocol should provide as small a packet delay as possible.

Some real-time applications (e.g., AVCS) may require that the packet delay be less than a specified time interval, which is called the deadline period. A packet that is delayed for more than the deadline period will become useless, even if it is received correctly later. The deadline failure probability (DFP) is the probability that the delay of a real-time packet is longer than the deadline period.

Therefore, we have two different performance measures for different applications. For non-real-time communications, it is desirable to have high throughput. On the other hand, it is more important to have small DFP for real-time communications. In the following performance analysis, we use the throughput as the performance measure for vehicle to base station and inter-platoon communications, and the DFP as the performance measure for intra-platoon communications.

5.3 S-ALOHA

This protocol has been introduced in chapter 4. The performance of S-ALOHA in a radio environment depends strongly on the channel model. Although the maximum throughput of S-ALOHA is 0.36 (or $1/2e$), the capture effect can improve its performance (Roberts 1975). In a terrestrial radio environment, signals from transmitters at different locations arrive at the receiver with different power levels due to the propagation loss. It is therefore, possible for the receiver to successfully "capture" the strongest signal, although it suffers interference

from other transmissions. The packets that survive collision can increase the maximum throughput of S-ALOHA.

Usually, the packet that is captured by the receiver corresponds to either the first signal to arrive or the strongest signal. Different capture criteria will lead to different capture probabilities. In our analysis, we parametrize the capture probability as a known function.

5.3.1 Vehicle to Base Station Link

The throughput S at a base station is given by (Polydoros 1987):

$$S = \sum_{k=1}^{\infty} P_s(k) f(k) \tag{5.1}$$

where $f(k)$ is the probability that ***k*** vehicles transmit in a slot, and $P_s(k)$ (the conditional capture probability) is the probability that one of them will be captured by the receiver at the base station given that ***k*** vehicles transmit in a slot. The number of transmissions per slot is usually assumed to be a Poisson random variable with mean G. That is,

$$\mathbf{f(k)} = \frac{e^{-G} G^k}{k!} \tag{5.2}$$

$P_s(k)$ is closely related to the spatial distribution of vehicular traffic, the channel characteristics, the propagation attenuation of the signal, etc. It is the key parameter for the computation of the throughput. Many efforts have been made to find the conditional capture probability using several assumptions (Linnartz 1992), (Zhang 1992), (Goodman 1987).

5.3.2 Inter-platoon Link

This scenario is very similar to the vehicle to base station communications, except that the inter-platoon communications are point-to-point. Here we are looking at a particular receiver, which is called the tagged receiver. The tagged receiver is trying to receive a packet, which suffers from other inter-platoon data traffic interference. The data traffic is assumed to be Poisson distributed with mean G. The probability that the tagged receiver

will successfully receive a packet is given by

$$P_s = \sum_{k=0}^{\infty} P_s(k) f(k) \tag{5.3}$$

where ***f(k)*** is the probability that ***k*** interfering vehicles transmit in a slot, and $P_s(k)$ (the conditional capture probability) is the probability that a packet will be captured by the tagged receiver, given that ***k*** interfering vehicles transmit in a slot. Suppose that the number of transmissions per slot is assumed to be a Poisson random variable of mean G. That is,

$$f(k) = \frac{e^{-G} G^k}{k!} \tag{5.4}$$

Then, the throughput is simply the product

$$S = G * P_s \tag{5.5}$$

5.3.3 Intra-platoon Link

Assuming that the control system of an automated vehicle requires that a status packet from the preceding vehicle in the platoon should be successfully received at least once within a deadline period, we can find the DFP for two cases.

In the first case, the deadline period has the same starting time for every vehicle. When its deadline period starts, a vehicle transmits in a slot with probability p, until it successfully transmits its status packet or until the next deadline period starts. We assume that a vehicle transmitting in a slot will succeed, if there are no other simultaneous transmissions in its neighborhood, which is called the vulnerable circle. Assuming that the distribution of vehicles in the freeway is uniform, the number of vehicles in the vulnerable circle is a constant for all vehicles. In our analytical model, we assume that there are M vehicles located within the vulnerable circle of each other and there are no other sources of interference.

The number of vehicles that have not made any successful transmission in the current deadline period, which is called the backlog size, constitutes a Markov chain with state space 0 , 1, 2 ,..., M. When the deadline period starts, the backlog size is ***M.*** The backlog size decreases gradually with time. When the current deadline period ends, the value of the

backlog size (over ***M)*** is the DFP. Figure 5.1 shows a plot of the DFP as a function of ***F*** (the number of slots in a deadline period) for $M=50$. As expected, the DFP decreases as F increases. This figure also shows that the optimal transmission probability p, which minimizes the DFP, depends on ***F.***

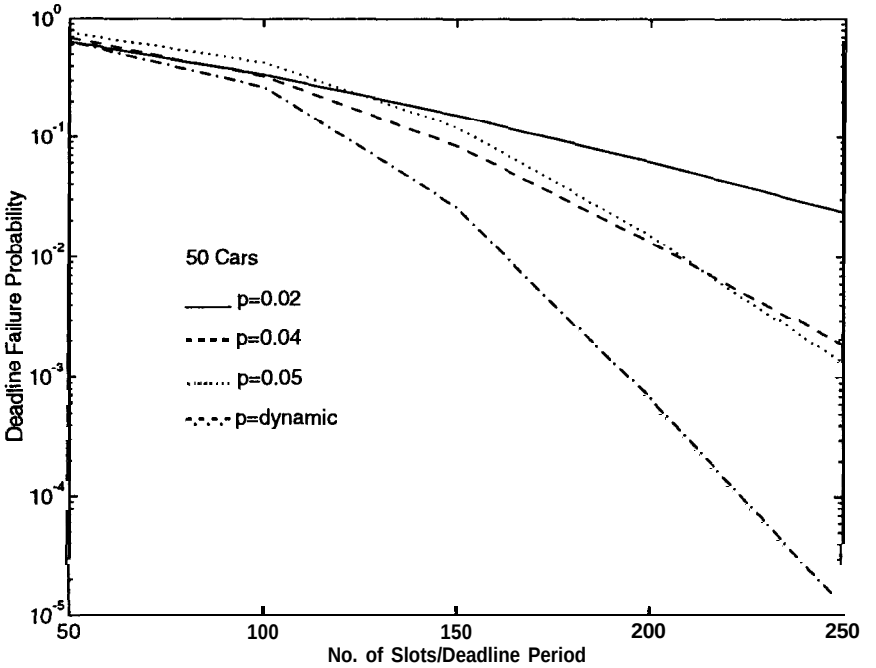

Figure 5.1: DFP for S-ALOHA (synchronous deadline period).

In the second case, every vehicle chooses randomly the starting time of its deadline period. When its deadline period starts, the vehicle transmits in a slot with probability ***p,*** until it successfully transmits its status packet or until its next deadline period starts. Figure 5.2 shows a plot of the DFP as a function of ***F,*** for the asynchronous deadline period case. Similarly to the first case, the optimal transmission probability depends on ***F.***

5.4 Framed-ALOHA

For the Framed-ALOHA scheme, we assume that ***L*** slots constitute a frame. Every vehicle is allowed to transmit only one packet per frame. Any vehicle which wants to transmit a

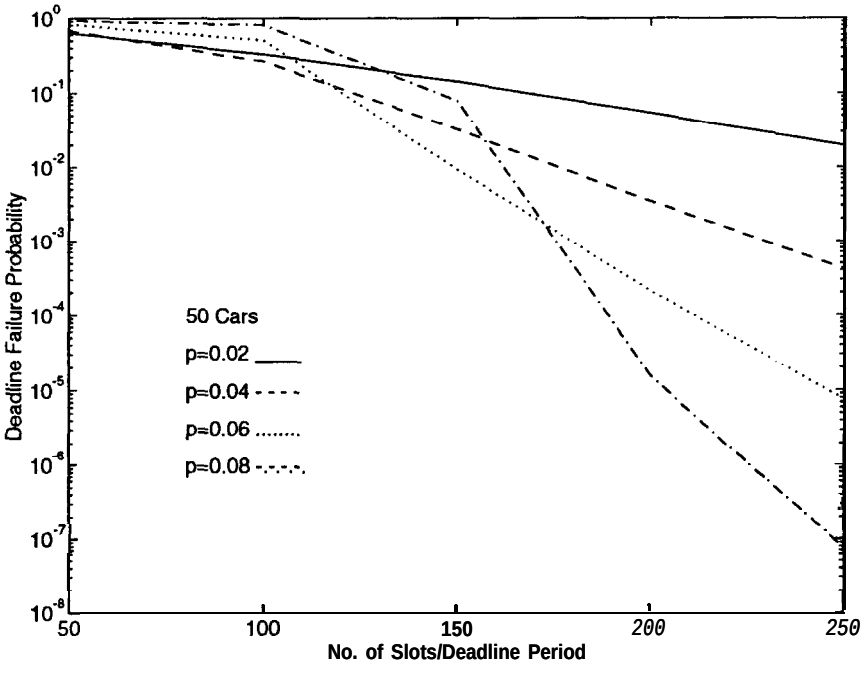

Figure 5.2: DFP for S-ALOHA (asynchronous deadline period).

packet will randomly choose one slot in the next frame. If the transmission is not successful, the packet will be retransmitted after a random period of time.

5.4.1 Vehicle to Base Station Link

The performance measure of interest for this link is the throughput at the base station. The general expression for the throughput S is given by

$$S = \frac{1}{L}\sum_{k=1}^{\infty} E[\text{No. of successful packets} \mid k \text{ active packets in a frame}] f(k) \qquad (5.6)$$

where ***f(k)*** is the probability that ***k*** vehicles transmit in a frame. Note that S is measured in packets per slot. Assuming that the number of packets transmitted in a frame is a Poisson random variable with mean G, the throughput is given by

$$S = \frac{1}{L}\sum_{k=1}^{\infty} E[\text{No. of successful packets} \mid k \text{ active packets in a frame}] \frac{e^{-G}G^k}{k!} \qquad (5.7)$$

The key parameter for the evaluation of the throughput is the expected number of successfully transmitted packets given that ***k*** packets are transmitted in a frame. If we assume that two

simultaneous transmissions will result in a collision at the base station (in the worst case), then

$$E[\text{No.ofsuccessfulpackets}|\ \text{kactivepacketsinaframe}] = k(1-1/L)^{k-1} \tag{5.8}$$

5.4.2 Inter-platoon Link

We assume there are M vehicles in the vulnerable circle of the tagged receiver. We further assume that the aggregate number of transmissions in the circle per frame has the distribution f(k) with mean G. The probability that the tagged receiver will successfully receive a packet that is destined to it is

$$P_s = \sum_{k=1}^{M}(1-\frac{1}{L})^{k-1} f(k) \tag{5.9}$$

The throughput (packets/slot) per vehicle can be computed as

$$\frac{GP_s}{ML} \tag{5.10}$$

5.4.3 Intra-platoon Link

We assume that every vehicle is required to successfully transmit its status packet to its follower at least once in every deadline period. Furthermore, we assume that a deadline period consists of F frames, and the deadline period of every vehicle has the same starting time. When the deadline period starts, every vehicle selects a slot in a frame randomly and transmits its packets until it succeeds or until the end of the deadline period. The DFP is just the probability that a vehicle does not succeed in any of the frames. We denote X_i as the backlog size after frame i. It is obvious that X_i, i = 1,. . . , F, is a Markov chain. The DFP can then be computed by the expected backlog size (over M), after frame F.

5.5 Spread Spectrum S-ALOHA (SS/S-ALOHA)

In SS/S-ALOHA, the channel time is slotted and the slot duration is equal to the packet transmission time. A receiver can successfully receive a packet if the specified capture criterion is satisfied.

5.5.1 Vehicle to Base Station Link

The performance measure of interest for this link is the throughput at the base station. The general expression for the throughput S is given by

$$S = \sum_{k=1}^{\infty} E[\text{No. of successful packets} \mid k \text{ active packets}] f(k) \tag{5.11}$$

where ***f(k)*** is the probability that ***k*** vehicles will transmit in a slot. We assume that the number of transmitted packets in a slot is a Poisson random variable with mean G. Then, the throughput S is given by

$$S = \sum_{k=1}^{\infty} E[\text{No. of successful packets} \mid k \text{ active packets}] \frac{e^{-G} G^k}{k!} \tag{5.12}$$

The key parameter for the evaluation of the throughput is the expected number of successfully received packets given that ***k*** packets are transmitted in a slot. This number depends on the channel characteristics, the spreading ratio, the code rate (if an error correction code is used), the power control scheme, and the spatial distribution of the vehicular traffic. We assume that the key parameter has the geometric distribution given below

$$E[\text{No. of successful packets} \mid k \text{ active packets}] = k u^{k-1}, \; 0 < u < 1 \tag{5.13}$$

The above assumption together with the Poisson assumption leads to the following relation

$$S = G e^{-(1-u)G} \tag{5.14}$$

The maximum throughput G/e is obtained when

$$G = \frac{1}{1-u} \tag{5.15}$$

Figure 5.3 illustrates a plot of S versus G for different values of u.

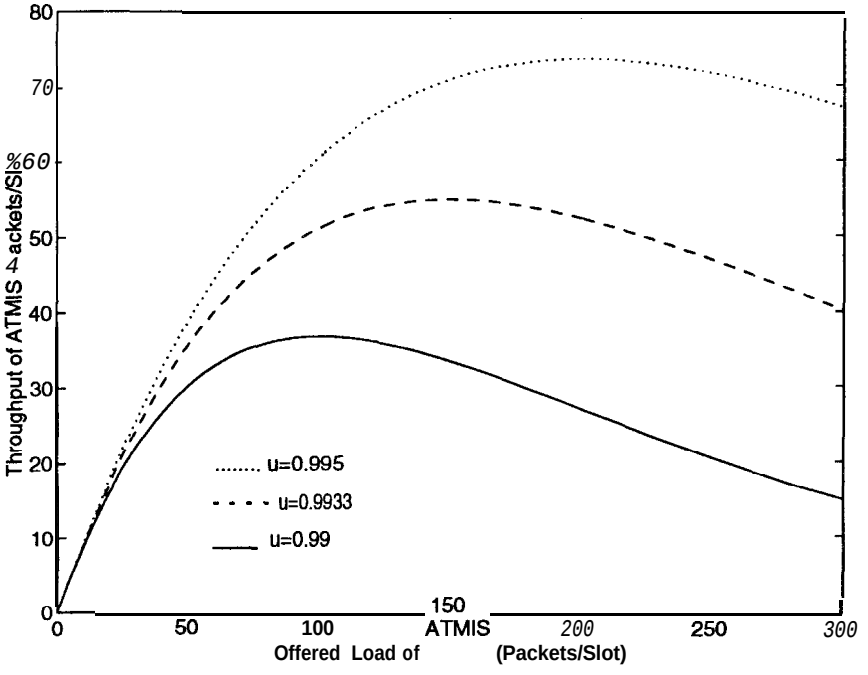

Figure 5.3: Uplink throughput for the SS/S-ALOHA scheme.

5.5.2 Inter-platoon Link

In order to evaluate the throughput for this link, we can use the same reasoning as in the S-ALOHA case for inter-platoon communications. The success probability for a particular pair of transmitter and receiver is given by

$$P_s = \sum_{k=1}^{\infty} P_s(k) f(k) \tag{5.16}$$

If the mean number of active transmissions per slot is G, the throughput is given by the product

$$S = G * P_s \tag{5.17}$$

5.5.3 Intra-platoon Link

We assume that the vehicles in the freeway are uniformly distributed and they simultaneously transmit periodic status packets to their followers within the deadline period. Then,

the DFP is exactly the same as the packet error probability, which depends on the SNR, the spreading ratio, and the channel characteristics.

5.6 Integrated Protocols

In this section, we present the design parameters for two protocols that can accommodate the communication needs of the integrated ATMIS/AVCS data traffic. The first of the presented protocols is a non-spreading scheme, called SR-ALOHA, which combines the features of S-ALOHA and R-ALOHA. The second protocol is a SS/S-ALOHA scheme.

5.6.1 SR-ALOHA

Taking into account the periodic data traffic of intra-platoon communications and the non-periodic data traffic of inter-platoon and vehicle to base station communications, the channel time in SR-ALOHA is structured into TDMA frames shown in figure 5.4.

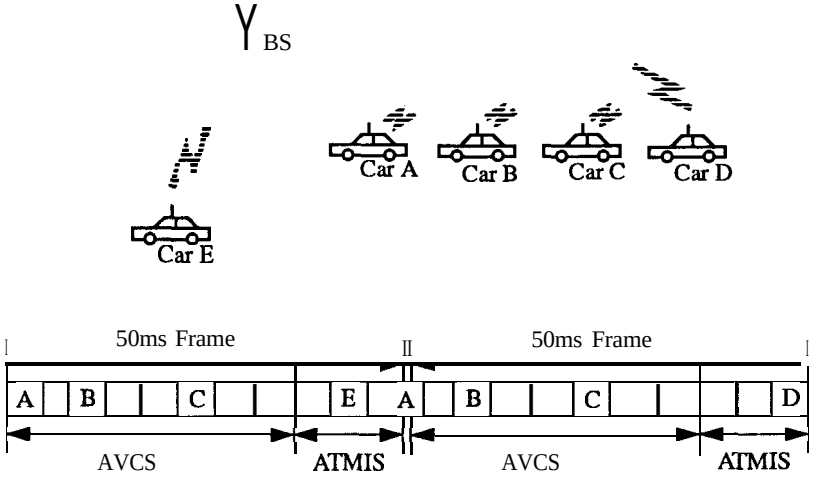

Figure 5.4: The frame structure of SR-ALOHA.

A number of slots in the frame is allocated to periodic data traffic (AVCS) and the slots are accessed by R-ALOHA. In other words, once a vehicle successfully transmits its status

packet to its follower in a slot, it will keep using the corresponding slot in the following frames. If an error occurs, the vehicle will switch to another slot which is detected as idle. In the steady state, every vehicle will have a slot in a frame to transmit its status packet. In addition to the slots allocated to periodic data traffic, some slots are reserved for non-periodic data traffic (ATMIS) and are accessed by S-ALOHA.

The proper allocation of slots for periodic and non-periodic data traffic in order to achieve sufficiently low DFP for periodic (intra-platoon) communications as well as high throughput for non-periodic (inter-platoon and vehicle to base station) communications is a trade-off study, which will be the focus of our efforts in the second year of this project.

5.6.2 SS/S-ALOHA

Spreading techniques can make simultaneous collision-free transmissions possible. Therefore, it is obvious that the SS/S-ALOHA protocol can be a very good candidate for the integrated data traffic. The key parameter is the determination of the optimal spreading ratio. Although a higher spreading ratio implies higher number of simultaneous transmissions, the packet transmission time (delay) will increase as the spreading ratio increases. The optimal spreading ratio should maximize the throughput and maintain the DFP below a specified threshold.

Figure 5.5 illustrates how the spreading ratio affects the performance of the protocol. We assume that the deadline period for periodic packets is 50 msec (see chapter 3). Given the bandwith and the spreading ratio, the number of slots in 50 msec can be determined. Using more slots in 50 msec (lower spreading ratio), we have more options for accomodating the integrated data traffic. For example, if there are two slots in 50 msec we can assign one slot for periodic data traffic and the other slot for non-periodic data traffic. This trade-off analysis for the optimal spreading ratio will be our future work.

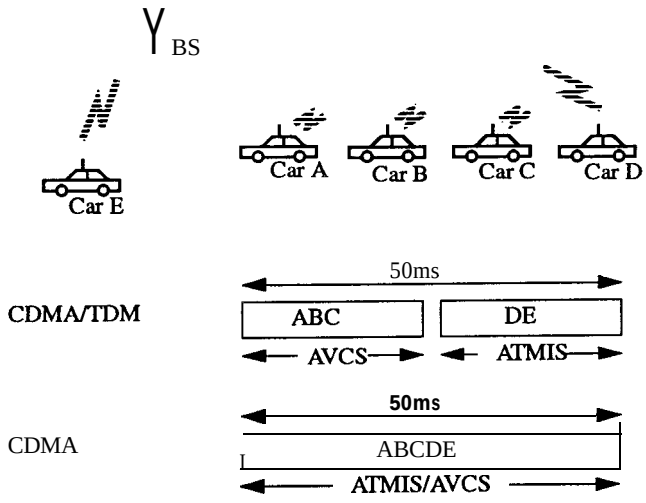

Figure 5.5: Spreading ratios for SS/S-ALOHA.

5.7 Conclusions

In this chapter, we analyzed the performance of three multiple access protocols in each of the three communication links, for a single cell. Two different performance measures are used for the performance evaluation of the protocols. The throughput is used for non-real-time communications, whereas the deadline failure probability is used for real-time communications (e.g., intra-platoon communications).

The throughput depends on two parameters; the conditional capture probability and the distribution of the number of active transmissions. The conditional capture probability, which depends on the capture criterion and the modulation scheme, is a parametric distribution which is evaluated in the physical layer. The number of active transmissions is assumed to be Poisson distributed, since it is very difficult to find the actual distribution analytically. For SS/S-ALOHA, assuming that the conditional capture probability follows a geometric distribution, we find that the maximum throughput is the offered load divided by e.

The deadline failure probability depends on the transmission probability p and the number of slots F in a deadline period for S-ALOHA (or the number of frames in a deadline period for Framed-ALOHA). For S-ALOHA, it is interesting to find that there exists no p

that can minimize the DFP. The DFP is also a function of F (depending on the bandwidth). For SS/S-ALOHA, the DFP depends strongly on the spreading ratio.

Since our goal is to find a single protocol that can accommodate all the communication needs of the integrated ATMIS/AVCS data traffic, we presented two integrated protocols, namely SR-ALOHA and SS/S-ALOHA. The most important design parameter for SR-ALOHA (a hybrid scheme of S-ALOHA and R-ALOHA) is the ratio of the number of slots for periodic data traffic to the number of slots for random data traffic, whereas the most important design parameter for SS/S-ALOHA is the spreading ratio. The optimal design parameters should be able to maximize the throughput for random data traffic and maintain the DFP below a certain threshold at the same time. The optimization of these design parameters will be the focus of our future efforts.

Chapter 6

Modulation, Coding, and Spreading Techniques for PR-IVHS

6.1 Digital Modulation Techniques

Digital modulation is the process by which digital symbols are transformed into waveforms that are compatible with the characteristics of the channel (Sklar 1988). Without modulation, it is rather difficult to transmit the baseband (low frequency) signals by radio. This section presents a description of basic modulation techniques for use in digital radio communication systems. We also discuss the criteria for selection of appropriate modulation techniques for digital cellular systems and we suggest some candidates that may be suitable for PR-IVHS communications.

6.1.1 Basic Digital Modulation Techniques

There are three basic digital modulation techniques: phase shift keying (PSK), frequency shift keying (FSK), and amplitude shift keying (ASK). Besides these schemes, hybrid schemes (e.g., quadrature amplitude modulation – &AM) have also received considerable attention, because they offer efficient utilization of bandwidth.

Phase Shift Keying

The general analytic expression for PSK modulation is

$$s_i(t) = \sqrt{2P}\cos(2\pi f_c t + \theta_i) \qquad 0 \le t \le T; \quad i = 1, \ldots, M \tag{6.1}$$

For binary PSK (BPSK), the value of θ_i is either 0" or 180". Precise phase reference is required in order to implement coherent detection. In practice, the receiver uses a carrier synchronization loop to extract the phase of the received signal. The synchronization loop exhibits an M-fold phase ambiguity and the receiver suffers a performance degradation. In order to resolve phase ambiguities, we can employ a modified form of BPSK which is called differential PSK (DPSK). In this scheme, the binary data are conveyed via transition in carrier phase (e.g., no transition may correspond to zero and a 180" transition may correspond to one). This is called differential encoding and it can resolve phase ambiguities generated by performing a nonlinear operation (e.g., phase-locked-loop) on the received waveform to extract the reference phase. The receiver, instead of attempting to extract a coherent phase reference it uses the signal from the previous symbol interval as a reference for the current symbol interval. However, DPSK can work only when the phase variations between two successive symbols is small. Moreover, the bit error rate (BER) performance of DPSK is worse than that of coherent BPSK (Proakis 1989).

Besides binary PSK, quaternary PSK (QPSK) is also used in digital radio systems because it offers higher channel efficiency. Channel efficiency is a measure of the performance of modulation schemes regarding their efficient utilization of bandwidth and is usually given in bits/sec/Hz. For QPSK, two data bits are encoded into one of four possible carrier phases, spaced 90" apart. This scheme conveys two bits of information during each symbol, and its ideal channel efficiency is 2 bits/sec/Hz, which is twice the efficiency of BPSK. As in the binary case, the data can be differentially encoded and differentially detected. This scheme is denoted by DQPSK. In recent years, a modified version of QPSK, called offset-QPSK (OQPSK) or staggered QPSK (SQPSK) has come into use. This scheme offers more rapid spectral roll-off and thus produces less interference to adjacent channels than conventional QPSK. The reason is that the abrupt phase shift of OQPSK is at the most 90°, which is

only half of the phase shift of QPSK.

Frequency Shift Keying

The general analytic expression for FSK modulation is

$$s;(t) = \sqrt{2P}\cos(2\pi f_i t + \theta) \qquad 0 \le t \le T; \quad i = 1, \ldots, M \tag{6.2}$$

where the frequency term, f_i, can take M possible values. The simplest form of FSK modulation is the binary FSK **(BFSK)** where two frequencies separated by Δf Hz are used. In FSK schemes, it is common to specify the frequency spacing in terms of the modulation index h, which is defined as

$$h = \Delta f \cdot T \tag{6.3}$$

Orthogonal signaling is usually employed in FSK schemes, so that each tone (sinusoids) in the signal set does not interfere with any of the other tones. In order for the signal set to be orthogonal, h must be larger than $1/2$ and 1 for coherent and noncoherent detection of **BFSK,** respectively (Sklar 1988).

Continuous-Phase FSK (CP-FSK) (Garrison 1975), which is a form of FSK, has received considerable attention because it can avoid the abrupt phase changes at the bit transition instants encountered in the other FSK implementations. Thus, CP-FSK has the advantage of rapid spectral roll-off and it produces less interference to adjacent channels.

Another FSK variation that has received considerable interest is minimum-shift-keying (MSK). MSK is a special case of CP-FSK where $h = 1/2$ and coherent detection is used. MSK can be also intepreted as a special case of OQPSK with sinusoidal pulse weighting (Pasupathy 1979). This scheme possesses constant envelope which allows the use of power-efficient nonlinear amplifiers. This is very beneficial for high-power transmissions. Furthermore, since MSK is a variation of FSK, we can employ noncoherent detection (e.g., by means of a discriminator). Gaussian MSK (GMSK), which has been used in the GSM mobile cellular system (Cox 1992), is a modified form of MSK where Gaussian low-pass filtering is used for

premodulation (Murota 1981).

Amplitude Shift Keying

The general expression of the transmitted signal for ASK modulation is

$$s_i(t) = \sqrt{2P_i}\cos(2\pi f_c t + \theta) \qquad 0 \le t \le T; \quad i = 1, \ldots, M \tag{6.4}$$

where the amplitude term, $\sqrt{2P_i}$ can take M discrete values. For binary ASK signaling (also called On-Off Keying – OOK) the two amplitude states are $\sqrt{2P}$ and zero. OOK was one of the earliest forms of digital modulation used in radio telegraph at the beginning of the century. Simple ASK is no longer widely used in modern digital communication systems.

Amplitude Phase Keying

For the combination of ASK and PSK, which is called Amplitude Phase Keying (APK), the general analytic expression is

$$s_i(t) = \sqrt{2P_i}\cos(2\pi f_c t + \theta_i) \qquad 0 \le t \le T; \quad i = 1, \ldots, M \tag{6.5}$$

which illustrates the indexing of both the signal amplitude term and the phase term. The resulting signals can be arranged in a signal amplitude and phase signal space. Figure 6.1 shows an example of the signal space locations of the possible transmitted signals for 16-ary APK. When the set of M symbols in the phase-amplitude space have a rectangular constellation, the scheme is referred as QAM (Sklar 1988).

As with any digital cellular systems, there are several criteria which must be considered in the selection of a modulation scheme for PR-IVHS. The most important criteria are

- **Out-of-Band Attenuation:** One of the spectral characteristics of a modulation scheme is the out-of-band attenuation, which is defined as the attenuation of the signal's power spectrum at a specific frequency separation from the center frequency of

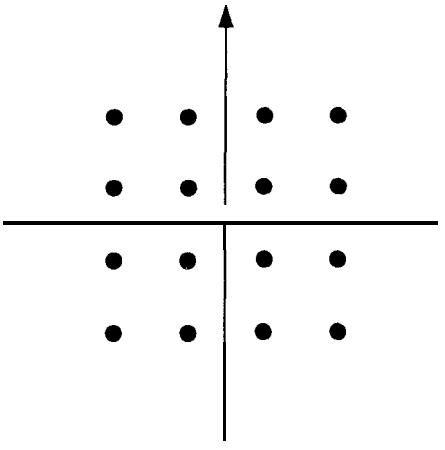

Figure 6.1: Signal Constellation of 16-ary QAM

the carrier. The larger the attenuation, the smaller the interference generated by the signal to adjacent channels. Therefore, the frequency separation between two successive channels can be reduced. In general, for frequencies far away from the center frequency (i.e., $(f - f_c)T >> 1$), the spectrum of ASK and PSK signals falls off as f^{-2}, whereas that of CP-FSK signals fall off as f^{-4}.

- **Spectrum Efficiency versus Co-channel and Adjacent channel Interference:** In conventional digital radio communication systems, the main measure of efficiency is the channel efficiency which is concerned with maximizing the information rate for a given bandwidth. However, due to the frequency reuse factor in cellular systems, spectrum efficiency, which is concerned with maximizing the number of channels in a cell, receives considerable interest (Lee 1989), (Gejji 1992). The spectrum efficiency of several modulation schemes in lineal microcells have been studied in (Webb 1992), assuming a Rayleigh fading channel and an operating frequency of 1.8 GHz. The simulation results indicate that for low BER ($< 5 \boxtimes 10^{-2}$), 4-ary PSK provides the best performance, whereas for high BER, particularly when the signal-to-noise ratio is high, 32-ary and 64-ary star QAM seem more appropriate.

- **Cost and Complexity:** It is rather difficult to evaluate the cost of a modulation scheme without knowledge of the specific system requirements. Nevertheless, the modulation schemes that we have mentioned can be classified according to their inherent complexity; the results are shown in figure 6.2 (Oetting 1979).

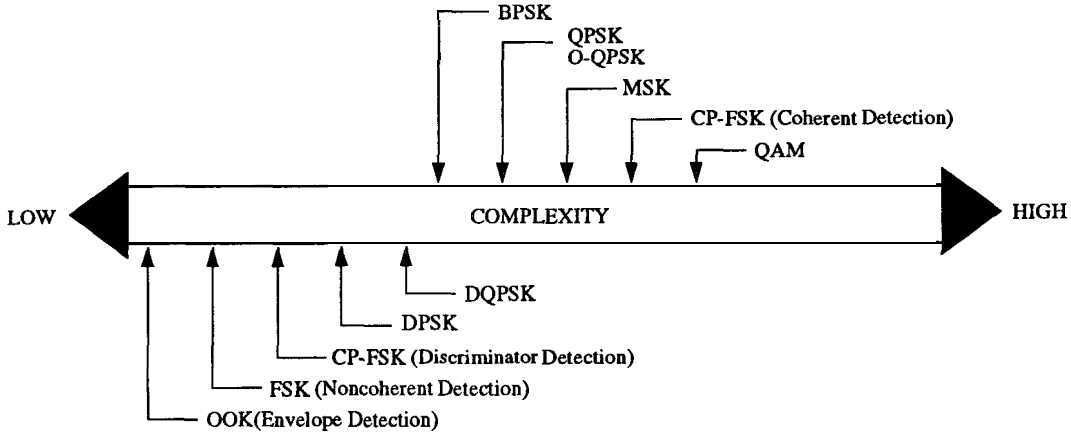

Figure 6.2: Relative Complexity of Modulation Schemes

- **BER Requirement:** Low BER performance (approximately 10^{-4} (Polydoros et al. 1993)) ***is*** required for IVHS applications.

Taking into account the above criteria, binary and quaternary modulation schemes may be the best choices for IVHS applications, because they are simple to implement and can resist co-channel interference. Of course, further analysis, based on the specific system and operational requirements of PR-IVHS, is required in order to select the most appropriate modulation method.

6.2 Error Control Strategies

Digital signals transmitted over a physical channel are subject to channel impairments, such as noise, fading, and interference from other signals. The received signal contains digital symbols with errors that tend to degrade the performance of the communication system.

If each transmitted symbol is affected independently of the other symbols, errors occur randomly in the received data sequence. In radio channels however, the channel effects are not independent from symbol to symbol and errors occur in bursts due to signal fading caused by multipath. One of the major concerns in the design of a communication system is the control of these errors, so that reliable reproduction of the transmitted data can be

obtained. One method of error control in data transmission is coding. The key idea of coding is to add redundant bits in the transmitted data sequence, in order to combat the noisy and fading characteristics of the physical channel.

In the following subsection we discuss the coding gain. Subsequent subsections present the two strategies for controlling transmission errors, namely the forward-error correction (FEC) strategy and the automatic-repeat-request (ARQ) strategy. We also discuss the basic properties of error control codes (both block and convolutional) and we present some well-known codes. Finally, we examine which of the above strategies is appropriate for error control in PR-IVHS.

6.2.1 Coding Gain

Figure 6.3 (Sklar 1988) illustrates the bit error performance of uncoded and coded BPSK over an AWGN. We notice that coded BPSK performs better than the uncoded $(1,1)$ after a threshold is exceeded (5.5 dB in this case). Before this threshold, coded BPSK performs worse than the uncoded case, because the redundant bits result in reduced energy per bit. The reduction in energy per coded bit is compensated by the performance improvement, after the threshold (Sklar 1988).

The reduction in the required energy-to-noise ratio, to achieve a specified error performance, of an error-correcting coded system over an uncoded one with the same modulation is defined as the coding gain (Sklar 1988). The use of an error-control code reduces the probability of bit error in the receiver, or reduces the required energy-to-noise ratio to achieve a specified probability of bit error. The price that we pay is a reduction of the data rate, or if we want to maintain a constant data rate, an expansion of the required bandwidth (Lin 1983).

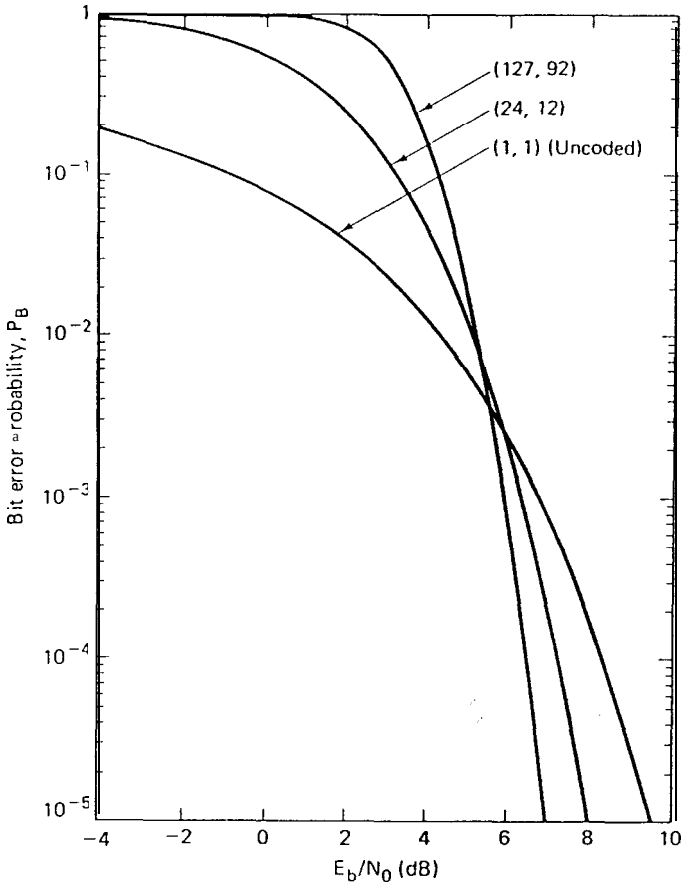

Figure 6.3: Bit error performance of uncoded and coded BPSK

6.2.2 Forward-Error Correction (FEC)

In a system employing FEC, we use a code with good error-correcting capability. If the decoder detects the presence of errors in the received data sequence, it attempts to determine their exact locations and then corrects them. If the decoder fails to determine the exact locations of errors, the received message will be decoded incorrectly. Coded systems that employ FEC, are advantageous for one-way communication links and for channels with high bit error rate. The disadvantages of these systems are the complexity of the decoding equipment and the large amount of redundancy required for error correction.

6.2.3 Automatic-Repeat-Request (ARQ)

In an ARQ system, the code is used only for error detection. If no errors are detected by the decoder, the receiver sends an acknowledgment (ACK) to the transmitter, indicating that the data have been received correctly. Otherwise, it notifies the transmitter, sending a negative acknowledgment (NAK), and waits for retransmission of the message. Incorrect decoding occurs when the receiver fails to detect the presence of errors. The probability of an undetected error can be made very small, using a proper linear code (Lin 1983). Figure 6.4 (Sklar 1988) illustrates three ARQ schemes.

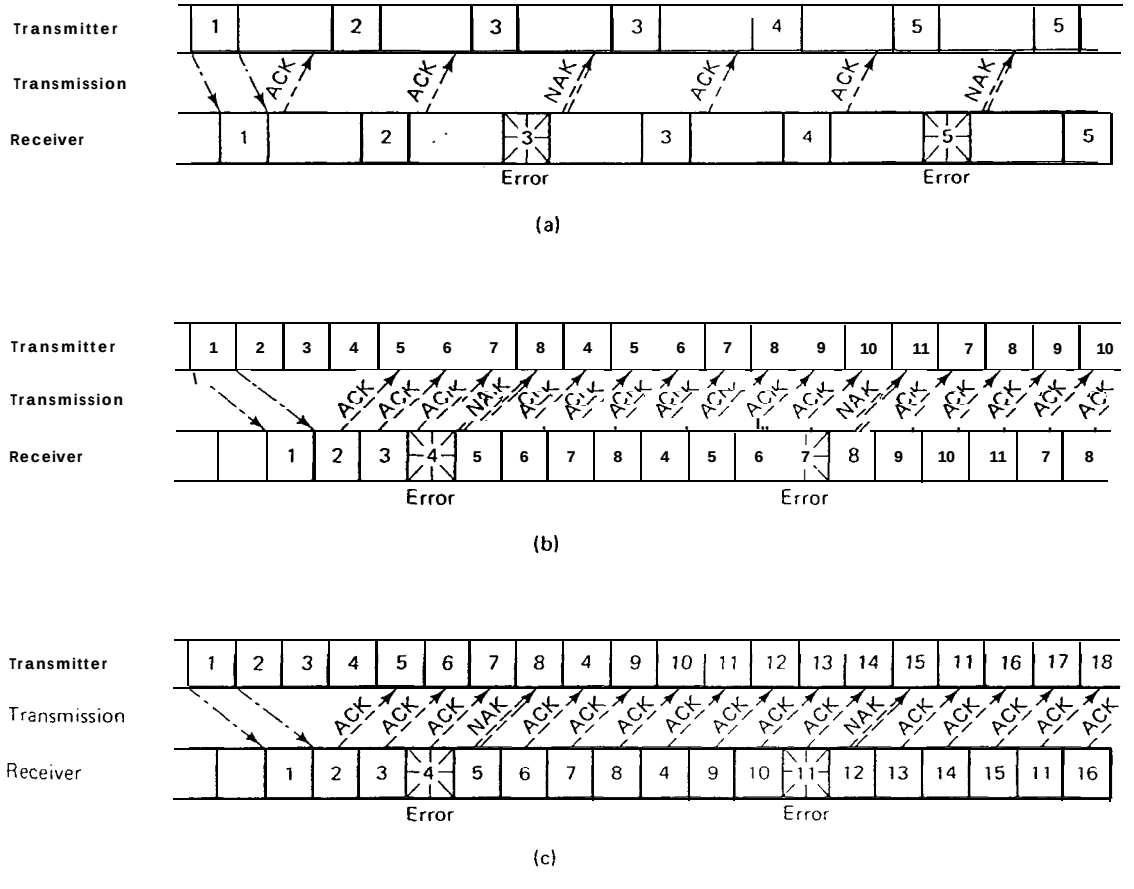

Figure 6.4: ARQ schemes. (a) Stop-and-wait (b) Go-back-N (c) Selective-repeat

Stop-and-wait ARQ (figure 6.4(a)) requires a half-duplex connection. After the transmission of a message, the transmitter waits for an ACK or a NAK from the receiver before it proceeds with the next message. If it receives an ACK (i.e., no errors have been detected),

it sends the next message. If a NAK is received, it retransmits the message. In some cases (e.g., a deep fading), the above procedure may be repeated many times before the message is correctly received.

Go-back-N ARQ (figure 6.4(b)) is a continuous ARQ scheme. The transmitter sends messages and receives acknowledgments continuously. When it receives a NAK, it backs up to the message in error and resends all the messages, starting with the erroneously received message. In this scheme, a number is assigned to every message and to every acknowledgment, so that the transmitter knows which message is associated with which acknowledgment.

Selective-repeat ARQ (figure 6.4(c)) is another continuous ARQ scheme. The difference in this case is that the transmitter resends only the corrupted message. Then, instead of resending all the subsequent correctly received messages, it continues where it had left off. Continuous ARQ schemes require a full-duplex connection.

The stop-and-wait scheme is used in half-duplex communication links and in systems where the transmission time is longer than the time required to receive an acknowledgment. Continuous ARQ schemes are more efficient than stop-and-wait but they are also more expensive. Finally, selective-repeat ARQ is more efficient than the Go-back-N ARQ but requires more logic and buffering.

The major advantages of ARQ schemes over FEC are the simpler decoding equipment and the small amount of redundancy required for error detection. On the other hand, the requirement for a reverse link and the low system throughput, when the channel bit error rate is high, are the disadvantages of ARQ.

6.2.4 Linear Block Codes

The encoder for a block code tranforms a sequence of k message symbols into a block of n ($n > k$) symbols, which is called a code word. A binary block code is constructed with symbols from the binary field (0 or 1). At the output of the encoder there are 2” different

code words, corresponding to the 2^k different messages. Linear block codes are described by the notation (n, ***k,*** d_{min}), where d_{min} is the minimum distance between code words (i.e, the minimum number of places where the code words differ) (Kumar 1991).

The minimum distance determines the error-detection and the error-correction capability of the code. A block code with minimum distance d_{min} is capable of detecting $d_{min} - 1$ errors and correcting $t = \lfloor (d_{min} - 1)/2 \rfloor$ errors* (Lin 1983). The ratio R = ***k/n*** is called the code rate. Note that $R \leq 1$ and that in a binary code the data rate is reduced by a factor of R. Thus, in order to maintain a constant data rate, the coded system requires a bandwidth expansion by a factor of l/R.

6.2.5 Convolutional Codes

A convolutional code is described by the notation ***(n, k, m).*** Here, n does not define a code word block length as in block codes. The important characteristic of convolutional codes is that the encoder has a memory order of ***m*** (i.e., the n encoder outputs at a given time, depend on the ***k*** inputs and on ***m*** previous input blocks). Usually, ***k*** and n are small integers and redundancy is added by increasing the memory order ***m.*** In order to achieve low probabilities of error, the memory ***m*** must be made large (Lin 1983). The code rate of a convolutional code is R = ***k/n.*** When the information sequence has finite length kL, the code word has length ***n(L*** + ***m)*** and the code rate is $R = kL/n(L +$ ***m).*** Then, the convolutional and the block code rates are approximately equal when ***L >> m.***

6.2.6 Well-known Codes

The following list presents some of the most important block codes that are being widely used in digital communications (Bhargava 1983):

- **Bose-Chaudhuri-Hocquenghem (BCH) Codes**: They are the best constructive codes for channels that affect each transmitted symbol independently from the others.

[1] $\lfloor (d_{min} - 1)/2 \rfloor$ denotes the largest integer no greater than $(d_{min} - 1)/2$.

These codes belong to the general class of cyclic codes and they have the following parameters:

- Code length: $n = 2^m - 1, \quad m = 3, 4, 5, \ldots$
- Number of information symbols: $k \geq n - mt$
- Minimum distance: $d \geq 2t + 1$

- **Reed Solomon Codes:** Each symbol is comprised of mbits. The parameters of these codes are:
  - Code length: $n = 2^m - 1$ symbols $= m \cdot (2^m - 1)$ bits
  - Number of parity symbols: $(n - k) = 2t$ symbols $= m \cdot 2t$ bits
  - Minimum distance: $d = 2t + 1$ symbols

- **Golay Code:** It is a perfect code (Kumar 1991) with parameters (23, 12, 7). It is widely used as a (24, 12, 8) code by adding an extra parity bit which is a parity check over the other 23 bits. This code does not generalize to other combinations of n and k.

- **Hamming Codes:** They are also perfect codes and they belong to the general class of cyclic codes. Their parameters are:
  - Code length: $n = 2^m - 1$
  - Number of parity symbols: $k = m$
  - Minimum distance: $d = 3$

- **Maximum-Length Codes (Simplex Codes):** These codes are related to maximal-length sequences which are used in spread spectrum communications and for closed-loop TDMA synchronization. Their parameters are:
  - Code length: $n = 2^m - 1$
  - Number of parity symbols: $k = m$
  - Minimum distance: $d = 2^m - 1$

- **Quadratic Residue Codes:** They are cyclic codes with minimum distances typically comparable to those of BCH codes of comparable lengths. Their parameters are:
  - Code length: n = p (p is a prime number of the form $8m \pm 1$)
  - Number of information symbols: $k = (p + 1)/2$
  - Minimum distance: $d > \sqrt{n}$

6.2.7 Error Control for PR-IVHS

The suitability of an error-control strategy for PR-IVHS depends on the communication needs of each link. In the vehicle-to-vehicle link, messages are transmitted every 50 msec and thus, there is no need for retransmissions when an error is detected. However, these messages are safety critical and must be received correctly or at least errors must be detected, so that the receiver can discard a corrupted message. Therefore, the FEC strategy seems more appropriate for this communication link.

The messages exchanged in the other two communication links are not safety or time critical. Therefore, ARQ schemes can be employed in these links. We must point out however, that the choice of the most appropriate ARQ scheme depends on the delay requirements of the system.

6.3 Spread Spectrum Techniques

The discussion of modulation techniques in section 6.1 has been concerned with issues like the efficiency of these techniques regarding the utilization of signal energy and bandwidth. In most communication systems, these are the most important concerns. There are situations however, (and PR-IVHS is certainly one of them) where it is necessary for the system to resist intentional or unintentional interference, to operate with a low energy spectral density for low detectability and low crosstalk, to provide multiple-access capability without tight external control, or to make it difficult for unauthorized receivers to observe the message,

providing this way message privacy (Cook 1983). In such situations, it may be appropriate to sacrifice the efficiency aspects of the system in order to enhance the above-mentioned features (Scholtz 1982). Spread-spectrum (SS) techniques offer a very attractive way to accomplish these objectives.

6.3.1 Classification of Spread Spectrum Modulation Techniques

Spread-spectrum refers to signaling schemes which are based on some kind of coding and where the transmitted signal (modulated carrier) is made to occupy a bandwidth many times larger than that of the unspread (message) signal (Cooper 1986). This by itself however, is not sufficient, because there are other modulation methods that also spread the spectrum of a signal. For example FM or PCM modulated signals may have bandwidths that are much greater than the message bandwidth. A second criterion has to be met in order for a system to qualify as a SS system. The transmision bandwith must be determined by some function that is independent of the message and it is known to the receiver.

There are a lot of ways of classifying the SS techniques. One way is by modulation. The most common modulation techniques employed are the following:

- Direct-Sequence
- Frequency-Hopping
- Time-Hopping
- Chirp
- Hybrid Methods

In the following, a brief description of the most common schemes is presented.

Direct-Sequence (DS)

A DS/SS signal is an already modulated signal which is amplitude (or equivalently phase) modulated by a very high rate NRZ (Nonreturn-to-zero) binary stream of digits (Taub 1986). Thus, if the original signal $s(t)$ is a BPSK signal

$$s(t) = \sqrt{2P_s}d(t)\cos(2\pi f_c t) \tag{6.6}$$

where $d(t)$ is the binary message sequence of ± 1 every T_b seconds, the DS/SS signal is

$$u(t) = g(t)s(t) = \sqrt{2P_s}g(t)d(t)\cos(2\pi f_c t) \tag{6.7}$$

where $g(t)$ is a pseudo-random noise (PN) binary sequence having the values ± 1, and these values are switched in a pseudorandom manner every T_c seconds (the chip time). Therefore, DS/SS achieves spectrum spreading by modulating the original signal with a signal that has wider bandwidth than the data bandwidth.

Frequency-Hopping (FH)

FH/SS modulation utilizes the large spectrum provided for SS systems by periodically changing the carrier frequency of the transmitted signal. The carrier frequency of the original signal is kept constant within the hop interval T_h, but it changes every $T_h = 1/f_h$ seconds (Taub 1986). In the most common case, starting with a BFSK signal

$$s(t) = \sqrt{2P_s}\cos(2\pi f_c t + d(t)\Omega + \theta) \tag{6.8}$$

where $d(t)$ is again the binary message sequence of ± 1 every T_b seconds, we end with a FH modulated signal, by varying the carrier frequency, so that

$$u(t) = \sqrt{2P_s}\cos(2\pi f_i t + d(t)\Omega + \theta) \tag{6.9}$$

The frequency, chosen each T_h seconds, is selected in a pseudo-random manner from a specified set of frequencies.

Time-Hopping (TH)

The TH/SS system is the counterpart of the FH/SS system in the time domain. In a TH/SS system, the time axis is divided into frames of duration T_f and each frame is subdivided into M time slots. In each frame, only one slot, chosen in a pseudo-random manner between the M slots, is used for transmission of a burst of k bits. Since the slot duration is T_f/M and the bit duration for a binary modulation is $T_f/(Mk)$, the bandwidth occupied by this SS system is in the order of Mk/T_f. This bandwidth is used to transmit T_f/k bits /sec, so that an expansion factor of approximately M is achieved.

Hybrid Methods

In addition to the afore-mentioned forms of SS modulation, there are some hybrid combinations which offer certain advantages over, or at least extend the usefulness of, the previous techniques (Dixon 1976). By combining one or more of the previous techniques, we can have a system with features that cannot be obtained by using a single modulation method. In this way, we can have the advantages of one method, while avoiding its drawbacks. An interesting thing is that implementation complexity is not necessarily increased. Many different hybrid combinations are possible. Some of them are:

- DS/FH
- DS/TH
- FH/TH
- DS/FH/TH

6.3.2 Comparison of Spread Spectrum Techniques

As we have discused earlier, there are a lot of ways to implement a spread spectrum system. Each way requires (Pickholtz 1991):

- signal spreading by means of a code
- synchronization between transmitters and receivers
- care to insure that some of the signals do not overwhelm the others
- source and channel coding to optimize performance and total throughput.

We have already discussed the most common ways to accomplish the first one. We begin with a narrowband message signal, and after the spreading proccess, we transmit a wideband signal. As we have mentioned in the definition of a spread spectrum system, the spreading is achieved in a way that is independent of the message. This second criterion is of great importance, since it suggests that we cannot analyze the performance of a spread spectrum system, using arguments based on the concept of bandwidth expansion factor. Indeed, although the bandwidth expansion is very large, it cannot combat white noise (as in FM), because this expansion is achieved by a signal that is independent of the message (Cooper 1986).

Although spread spectrum systems cannot combat white noise, they are being employed in order to overcome problems that have much more detrimental effects on the communication system performance than white noise (especially in environments like the one of PR-IVHS). In general, personal wireless and cellular communications must deal with a variety of interference forms, primarily "the four multiples" (Viterbi 1991): multiple-user access, multiple cell-cites, multipath and multiple media.

Regarding the second requirement, we have to mention an important characteristic of spread spectrum systems that has a serious impact on the design and implementation of the spread spectrum transmission protocols in a packet radio network. Spread spectrum transmission protocols are the rules that dictate the selection of the spreading sequence to be used in the transmission of a particular packet. The selection can be based on the identity of the transmitter, the identity of the intented receiver, or several other factors. Spreading code protocols are divided into the following three broad categories (Pursley 1987):

- **Common code**

  It is the simplest transmission protocol to implement. A common spreading sequence is used for all transmissions. Discrimination between two or more incoming packets is made on the basis of the time of arrival of the packets and the time offsets among the received versions of the sequences. This protocol is simple but has not good capture properties, since collisions can occur not only between packets destined to the same receiver but also between packets destined to different receivers.

- **Receiver-oriented codes**

  For this protocol, each receiver is assigned a distinct spreading sequence and all transmissions to the receiver must use this sequence. The performance of such a protocol depends on the timing mechanism for generating the sequence and on the time offsets between different packets transmitted to the same receiver. When two or more packets, using the same phase of the same spreading sequence, arrive at the receiver at nearly the same time, there will be insufficient time separation between the two sequences to permit the receiver to distinguish between them. As a result, a collision occurs with the same effect as in narrow-band systems, i.e., loss of data. An important difference in spread spectrum systems however, is the possibility that two packets collide, yet, at the same time a third packet is succesfully received (by using a different spreading sequence). Thus, in spread spectrum systems the error mechanism that Ieads to collisions is different from the random errors that might occur when multiple packets are transmitted simultaneously, perhaps to different receivers, using different sequences or time offsets of the same sequence.

- **Transmitter-oriented codes**

  In this case, each transmitter is assigned a distinct code for transmissions, so that packets transmitted by different users will be on different spreading sequences, and they will not collide even if the transmissions begin at exactly the same time. There will be, of course, random errors due to the mutual interference between the two transmissions. This scheme has better capture properties than the receiver-oriented case, but puts considerable burden on the receiver to search over the whole code space

of all the transmitters within range, in anticipation of a transmission.

Common spreading codes are appropriate for broadcast-type of applications because all radios are "tuned" to the same code at all times. Transmitter-oriented codes are also suitable for broadcasting but receiver-oriented are not appropriate for this type of communications, because a separate transmission is needed for each receiver.

As far as the third requirement is concerned, we have to note that in a packet radio environment, strong signals at the receiver can swamp out the effects of weaker signals. So the receiver will receive significant interference from a signal transmitted by a nearby interferer and may not receive succesfully the signal transmitted by the desired transmitter that is either distant, or is subject to severe shadowing or fading at that time. This is the so called "near-far" problem (Taub 1986), and is of great importance in our PR-IVHS applications.

Although extended research is required in order to determine the performance of the spread spectrum systems in the PR-IVHS environment, we can list some of the advantages and disadvantages of the three most common spread spectrum techniques, namely the DS, FH and TH (Cooper 1986).

- DS systems

  Advantages

  - Best noise and antijam performance
  - Most difficult to detect
  - Best discrimination against multipath

  Disadvantages

  - Require wide-band channel with little phase distortion
  - Long acquisition time
  - Fast code generator needed

- Near-far problem

- **FH systems**

  Advantages

  - Greatest amount of spreading
  - Can be programmed to avoid portions of the spectrum
  - Relatively short acquisition time
  - Less affected by near-far problem

  Disadvantages

  - Complex frequency synthesizer
  - Error correction needed

- **TH systems**

  Advantages

  - High bandwidth efficiency
  - Simpler implementation than FH
  - Useful when transmitter is average-power limited but not peak-power limited
  - Near-far problem avoided

  Disadvantages

  - Long aquisition time
  - Error correction needed

As a final note, we have to mention that the limitations of spread spectrum systems are mostly due to technology and therefore, can be overcome (Schilling 1991). The limitation in DS/SS systems is the ability to spread the spectrum using a very high chip rate. Today, the maximum chip rate attainable using CMOS is 70 Mchips/sec. However, commercially available GaAs FET devices can operate at 2 Gchips/sec. The limitation in FH/SS systems

is the ability of a frequency synthesizer to change frequencies without generating spurious signals. The Numerically Controlled Oscilators (NCOs) can generate such a signal, but only on hop rates up to 1 Mhop/sec and over a 20 MHz bandwidth. However, necessity is the mother of invention, and wide bandwidth NCOs are on the horizon.

Chapter 7

Performance Analysis of Multi-cell Direct-Sequence Systems in Microcells

7.1 Introduction

In this chapter, we will study the performance of an asynchronous multi-cell Direct-Sequence Code Division Multiple-Access (DS/CDMA) microcellular system for IVHS applications. This work extends our previous research (Polydoros et al. 1993) in the following aspects.

1. **Multi-Cell Systems:** In this analysis, we extend the system model from single-cell to multi-cell and evaluate the bit error rate (BER), the outage probability, and the packet success rate for BPSK and DPSK modulation schemes in the presence of other-cell interference. In addition to the shadowed Rician channel, we also study the system performance in a Nakagami fading channel. These two fading models are of great interest in microcellular systems.

2. **A New Analytical Model:** We have established a new analytical model which can take into account the user's spatial distribution, the arbitrary chip waveform, the power control function, and the macro-selection diversity. The effect of using the

macro-selection diversity to reduce the Multiple-Access Interference (MAI) from other cells is also investigated.

3. **Base Station to Vehicle (Downlink) Communications:** In addition to vehicle to base station (uplink) communications, we also evaluate the downlink performance of DS/CDMA microcellular systems which has not received sufficient attention in the literature.

The remainder of this chapter is organized as follows. In section 7.2, we describe the analytical model and evaluate the uplink performance of an asynchronous multi-cell DS/CDMA system with shadowed Rician/Nakagami fading. The downlink performance is studied in section 7.3. Conclusions and future work are given in section 7.4.

7.2 Uplink Performance Analysis

7.2.1 System Model

The models of the radio channel, the transmitter, and the receiver are established in this section. The commonly adopted lineal microcellular layout for dense urban streets and highways is shown in figure 7.1. The service area is segmented into sections and every section is called a cell. We assume that the base station (BS) is at the center of the cell and the distance between two BS' is D. The BS can distinguish the users by assigning a different spreading code to each one of them. The frequency band is reused in each cell. We further assume that the transmitters employ omni-directional antennas. Thus, any user in the system will suffer interference from users in the same cell as well as from users in other cells.

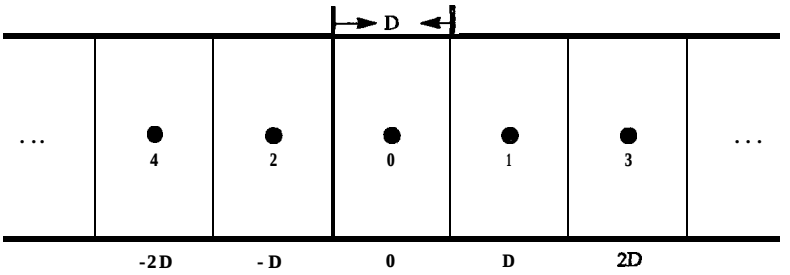

Figure 7.1: Lineal Microcellular Layout

Channel Model

The land mobile radio channel can be characterized statistically by three independent, multiplicative propagation mechanisms, namely multipath fading, shadowing, and UHF groundwave propagation (Lee 1986). Hence, the lowpass equivalent complex impulse response of the microcellular mobile radio channel, h(t), can be expressed as

$$h(t) = \sqrt{L_p(r) 10^{X/10}}\, \gamma\, e^{j\phi}\, \delta(t-\tau) \tag{7.1}$$

where $L_p(r)$ is the propagation loss due to the groundwave propagation, with r denoting the distance from the BS; $10^{X/10}$ represents the shadowing, with the zero-mean random variable X accounting for the fluctuations of the received power around the propagation loss; γ is the multipath fading; and ϕ, τ are the random phase and propagation delay, respectively, which are uniformly distributed over [0, 2π) and $[0,T)$, with T denoting the bit interval. The second moment of γ is normalized to be 1. In this model, the channel is assumed to be non-frequency selective for the following reasons. First, various studies have indicated that the delay spread of microcellular systems in an urban street environment is less than a few microseconds (Bultitude et al. 1989) and may be much less in a highway environment (Polydoros et al. 1993) Thus, the returned paths cannot be resolved, unless the system bandwidth is sufficiently large. Second, using this assumption may be interpreted as going after a worst-case analysis, since a frequency selective channel will not undergo the broad deep fades that the flat channel will (Milstein et al. 1992). Furthermore, the channel is also assumed to be slow fading relative to the bit interval, i.e., the amplitude of the received signal is constant over the whole bit interval. This kind of channel is called flat-flat channel (Biyari 1990), i.e., non-frequency selective and slow fading.

The commonly adopted propagation loss model in microcells is described by the law (Harley 1989)

$$L_p(r) = C_p\, r^{-a}\, (1 + r/g)^{-b} \tag{7.2}$$

where C_p is a constant, the exponent a is the basic propagation loss exponent for the short distance, whereas the exponent b accounts for the additional propagation loss exponent for the distance beyond the Fresnel break point g of the attenuation curve. The distance g is 100-300 meters (Xia et al. 1992), (Harley 1989).

Two common models of multipath fading used in microcells are the Rician and Nakagami models. The probability density function (pdf) of a Rician distributed random variable γ is (Proakis 1989)

$$f_\gamma(y) = \frac{y}{\sigma_s^2} \exp\left(-\frac{y^2+\alpha^2}{2\sigma_s^2}\right) I_0\left(\frac{\alpha y}{\sigma_s^2}\right) U(y) \tag{7.3}$$

where U(y) is a unit step function and $I_0(x)$ is the modified zero-order Bessel function. The Rician factor K is defined as the ratio of the power of the specular component to that of the Rayleigh scattered component, i.e., $K = \alpha^2/(2\sigma_s^2)$. Since $E(\gamma^2) = \alpha^2 + 2\sigma_s^2 = 1$, it is straightforward to find that $\alpha^2 = K/(K+1)$ and $\sigma_s^2 = 1/[2(K+1)]$, respectively. Hence, (7.3) can be rewritten as

$$f_\gamma(y) = 2(K+1)y \exp[-(K+1)y^2 - K]\; I_0\left[\sqrt{4K(K+1)}\, y\right] U(y) \tag{7.4}$$

If $K = 0$, $f_\gamma(y)$ becomes the pdf of a Rayleigh random variable. In addition to the Rician fading model, we are also interested in the Nakagami fading channel. The pdf of a Nakagami distribution is

$$f_\gamma(y) = \frac{2m^m y^{2m-1}}{\Gamma(m)} \exp(-my^2)\, U(y) \tag{7.5}$$

The Nakagami distribution will be discussed in detail in section 7.2.2.

The Transmitted Signal

Let $b_{kn}(t)$ be the data signal of the n^{th} user in cell k. For BPSK modulation, $b_{kn}(t)$ is the information sequence, whereas for DPSK modulation, $b_{kn}(t)$ is the differentially encoded

version of the n^{th} user's information sequence. The data signal $b_{kn}(t)$ can be expressed as

$$b_{kn}(t) = \sum_{j=-\infty}^{\infty} b_j^{(kn)} p(t - jT) \tag{7.6}$$

where $b_j^{(kn)}$ is the j^{th} data bit in the binary information sequence and p(t) is a rectangular pulse whose value equals unity in $0 \leq t \leq T$ and zero otherwise. The information sequence $b_j^{(kn)}$ is modeled as an i.i.d. sequence, taking on values ± 1 with equal probability.

The spreading waveform $a_{kn}(t)$ can be written as

$$a_{kn}(t) = \sum_{j=-\infty}^{\infty} a_j^{(kn)} \psi(t - jT_c) \tag{7.7}$$

where $a_j^{(kn)}$ is the jth chip of the n^{th} user's signature sequence and $\psi(t)$ represents a chip pulse with arbitrary shape. Note that $\psi(t) = 0$ except for $0 \leq t \leq T_c$, where T_c^{-1} is the chip rate of the DS/CDMA system. The chip pulse shape is normalized so that $\int_0^{T_c} \psi^2(t)dt = T_c$. We assume that each bit is encoded with η chips, i.e., $T = \eta T_c$, and that perfect alignment exists between bits and chips. The factor η is called the spreading ratio. In order to make the computations independent of the choice of the employed spreading sequences, we further assume that the spreading sequence code consists of a sequence of i.i.d. random variables taking on values ± 1 with the same probability. For an asynchronous DS/CDMA system, the random sequence code gives approximately the same analytical result as that of a non-randomly chosen code (Yung 1991), (Geraniotis et al. 1991).

In a DS/CDMA system, power control is required in order to combat the so called near-far effect (Turin 1984) as well as to mitigate the channel impairments. In this analysis, we assume that the power control can only compensate for the propagation loss and the shadowing, but not for the fast-varying multipath fading. We also investigate the effect of macro-selection diversity on reducing the multiple access interference (MAI). The macro-selection diversity is a technique in which the user is power controlled by the BS with the least attenuation. Therefore, its transmitted power will be proportional to this minimum attenuation and hence, it will produce the least interference to all other BS' (Viterbi et al. 1993). Suppose that the set of BS' that the mobile can select is limited to the N_c nearest.

Hence, the transmitted signal, $S_{kn}(t)$, of the n^{th} user in cell $\boldsymbol{k}$ can be expressed as

$$S_{kn}(t) = \sqrt{\frac{2P_0}{\max_{j\in\mathcal{S}_c}\left\{PL_{kn}^{(j)}\right\}}}\, a_{kn}(t)\, b_{kn}(t)\cos(2\pi f_c t + \theta_{kn}) \tag{7.8}$$

where f_c is the common carrier frequency, P_0 is the nominal power set by the receiver, θ_{kn} is the random phase of the modulator, $PL_{kn}^{(j)}$ represents the propagation loss and the shadowing encountered by the user n in cell $\boldsymbol{k}$ communicating with the BS j, and $\mathcal{S}_c$ is the set containing the user's N_c nearest BS's. Thus, $PL_{kn}^{(j)}$ can be expressed as

$$PL_{kn}^{(j)} = L_p\left[r_{kn}^{(j)}\right]\cdot 10^{X_{kn}^{(j)}/10} \tag{7.9}$$

where $r_{kn}^{(j)}$ is the distance between the user $\boldsymbol{kn}$ and the BS j and $10^{X_{kn}^{(j)}/10}$ represents the associate shadowing.

If the user in the system is power controlled by the nearest BS, i.e., $N_c = 1$, its transmitted signal becomes

$$S_{kn}(t) = \sqrt{\frac{2P_0}{PL_{kn}}}\, a_{kn}(t)\, b_{kn}(t)\cos(2\pi f_c t + \theta_{kn}) \tag{7.10}$$

The Received Signal

For the desired user $0i$ which is power controlled by the BS 0, the received signal can be expressed as

$$\begin{aligned} r_{0i}(t) = {} & \sqrt{2P_0}\gamma_{0i}a_{0i}(t-\tau_{0i})b_{0i}(t-\tau_{0i})\cos(2\pi f_c t + \Phi_{0i}) \\ & + \sum_{n=1,n\neq i}^{N_0}\sqrt{2P_0}\sqrt{\chi_{0n}}\gamma_{0n}a_{0n}(t-\tau_{0n})b_{0n}(t-\tau_{0n})\cos(2\pi f_c t + \Phi_{0n}) \\ & + \sum_{k=1}^{K}\sum_{n=1}^{N_k}\sqrt{2P_0}\sqrt{\chi_{kn}}\gamma_{kn}a_{kn}(t-\tau_{kn})b_{kn}(t-\tau_{kn})\cos(2\pi f_c t + \Phi_{kn}) \\ & + n(t) \end{aligned} \tag{7.11}$$

where N_k is the number of active users in cell $\boldsymbol{k}$, K is the number of interfering cells under consideration, τ_{kn} is the time delay, $\Phi_{kn} = \theta_{kn} - 2\pi f_c\tau_{kn} + \phi_{kn}$ is a random variable uniformly distributed over $[0, 2\pi)$, $n(t)$ is the AWGN with two-sided power spectral density $\mathcal{N}_0/2$, and

χ_{kn} is defined as

$$\chi_{kn} = \min_{j \in S_c} \left\{ \frac{PL_{kn}^{(0)}}{PL_{kn}^{(j)}} \right\} \quad ,1 \leq n \leq N_k; \;\; 0 \leq k \leq K \tag{7.12}$$

For $N_c = 1$, $\chi_{0n} = 1$ and $\chi_{kn} = PL_{kn}^{(0)}/PL_{kn}^{(k)}$, $k \neq 0$.

In this analysis, we assume that $\{\chi_{kn}\}, \{a_j^{(kn)}\}$, $\{b_j^{(kn)}\}, \{\tau_{kn}\}, \{\Phi_{kn}\}$, and $\{\gamma_{kn}\}$ are mutually independent and that the users are uniformly distributed in the cells.

7.2.2 Bit Error Rate Analysis

In this subsection, we will derive the BER for the multi-cell DS/CDMA system with Rician or Nakagami multipath fading and log-normal shadowing. We consider both the BPSK and DPSK modulation schemes.

BER Analysis in Rician Fading Channels

BER for BPSK

The receiver for a DS/CDMA system employing BPSK modulation is shown in figure 7.2. We assume that the receiver can perfectly track the phase and the time delay of the desired user. Since only the relative delays and phases are important, we can set $\tau_{0i} = \Phi_{0i} = 0$ without loss of generality.

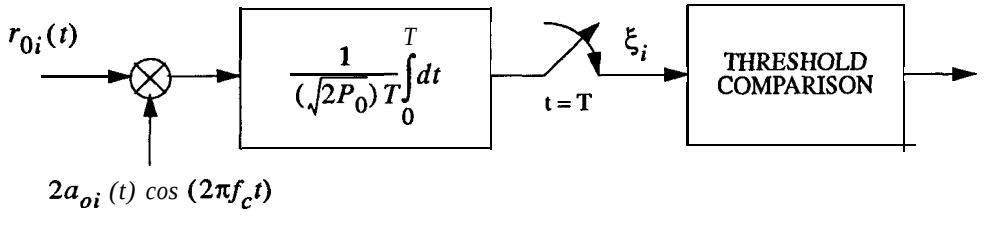

Figure 7.2: Receiver for a DS/CDMA system employing BPSK modulation

By utilizing the distributional analysis (Lehnert et al. 1987), the correlator output ξ_{0i}

can be written (see Appendix A) as follows

$$\begin{aligned}\xi_{0i} &= \gamma_{0i} + \sum_{n=1,n\neq i}^{N_0} \sqrt{\chi_{0n}}\gamma_{0n}\cos(\Phi_{0n})W_{0n} \\ &\quad + \sum_{k=1}^{K}\sum_{n=1}^{N_k} \sqrt{\chi_{kn}}\gamma_{kn}\cos(\Phi_{kn})W_{kn} + n^* \\ &= \gamma_{0i} + MAI + n^* \\ &= \gamma_{0i} + T \end{aligned} \tag{7.13}$$

where n^* is a zero-mean Gaussian random variable with variance $\mathcal{N}_0/(2P_0T) = \mathcal{N}_0/2E_b$ and E_b is the bit energy, T is the total interference which includes the multiple access interference, MAI, and the AWGN, n^*, and W_{kn} is given by

$$W_{kn} = \frac{1}{T}\left[P_{kn}R_\psi(S_{kn}) + Q_{kn}\hat{R}_\psi(S_{kn}) + X_{kn}f_\psi(S_{kn}) + Y_{kn}g_\psi(S_{kn}) \right] \tag{7.14}$$

where

$$\begin{aligned}\hat{R}_\psi(S) &= \int_S^{T_c} \psi(t)\psi(t-S)\,dt \\ R_\psi(S) &= \hat{R}_\psi(T_c - S) \\ f_\psi(S) &= \hat{R}_\psi(S) + R_\psi(S) \\ g_\psi(S) &= \hat{R}_\psi(S) - R_\psi(S) \end{aligned} \tag{7.15}$$

and the random variable S is uniformly distributed over [0, T_c). The random variables P_{kn} and Q_{kn} are taking the values ± 1 with equal probability. X_{kn} can be treated as the summation of A = $(\eta - 1)/2$ independent unbiased Bernoulli trials whose probability distribution function is given by

$$P_{X_{kn}}(j) = \binom{A}{\frac{j+A}{2}} 2^{-A} \quad , \quad j \in \{-A, -A+2, \ldots, A-2, A\} \tag{7.16}$$

Y_{kn} has the same distribution as X_{kn}. In addition, P_{kn}, Q_{kn}, X_{kn}, and Y_{kn} are conditionally mutually independent given the desired signature sequence (Lehnert et al. 1987).

Let us define the random vectors $\underline{\chi}, \underline{\gamma}, \underline{\Phi}$, and $\underline{S}$ as $(\sum_{k=0}^{K} N_k - 1)$-component vectors of the form $\underline{\chi} = (\chi_{0,1}, \ldots, \chi_{0,i-1}, \chi_{0,i+1}, \ldots, \chi_{K,N_K})$ and similarly for the rest. If all the signature sequences are completely random, the spreading ratio is sufficiently large, and the random

vectors $\underline{\chi}, \underline{\gamma}, \underline{\Phi}$, and $\underline{S}$ are fixed, MAI can be accurately modeled by a Gaussian random variable (Morrow et al. 1989), (Morrow et al. 1992). This is called the Improved Gaussian Approximation (IGA) method. Thus, T is also a conditional Gaussian random variable. We define the conditional variance Ψ of T as

$$\Psi = \mathbf{Var}(T \mid \underline{\chi}, \underline{\gamma}, \underline{\Phi}, \underline{S}) \tag{7.17}$$

Since the random variables P_{kn}, Q_{kn}, X_{kn}, and Y_{kn} are zero-mean and conditionally independent, the MAI from each interfering user is conditionally independent of the others. Furthermore, n^* is independent of the MAI terms. Using the fact that the variance of summations of independent random variables is equal to the summations of the variance of each random variable, Ψ is given by

$$\begin{aligned}\Psi &= \mathbf{Var}(n^*) + \mathbf{Var}\left[\sum_{n=1,n\neq i}^{N_0} \sqrt{\chi_{0n}}\gamma_{0n}\cos(\Phi_{0n})W_{0n} \mid \underline{\chi}, \underline{\gamma}, \underline{\Phi}, \underline{S}\right] \\ &\quad + \mathbf{Var}\left[\sum_{k=1}^{K}\sum_{n=1}^{N_k} \sqrt{\chi_{kn}}\gamma_{kn}\cos(\Phi_{kn})W_{kn} \mid \underline{\chi}, \underline{\gamma}, \underline{\Phi}, \underline{S}\right] \\ &= \frac{\mathcal{N}_0}{2E_b} + \sum_{n=1,n\neq i}^{N_0} \chi_{0n}\gamma_{0n}^2 Z_{0n} + \sum_{k=1}^{K}\sum_{n=1}^{N_k} \chi_{kn}\gamma_{kn}^2 Z_{kn}\end{aligned} \tag{7.18}$$

where Z_{ij} is

$$\begin{aligned}Z_{ij} &= \mathrm{Var}\left[\cos(\Phi_{ij})\, W_{ij} \mid \underline{\Phi}, \underline{S}\right] \\ &= \cos^2(\Phi_{ij})\, \mathrm{var}\left[W_{ij} \mid S_{ij}\right]\end{aligned} \tag{7.19}$$

The conditional variance for $W = W_{ij}$ can be computed as follows

$$\begin{aligned}\mathbf{Var}[W|S] = \frac{1}{T^2}\{&E\left[P^2 R_\psi^2(S)|S\right] + E\left[Q^2 \hat{R}_\psi^2(S)|S\right] \\ &+ E\left[X^2 f_\psi^2(S)|S\right] + E\left[Y^2 g_\psi^2(S)|S\right]\}\end{aligned} \tag{7.20}$$

Since P and Q take the values ± 1 with equal probability, their variance is 1. The variance of X can be found by expressing X as a sum of $(\eta-1)/2$ independent symmetric Bernoulli trials and noting that

$$E\left[X^2 f_\psi^2(S)|S\right] = \left(\frac{\eta-1}{2}\right) f_\psi^2(S) \tag{7.21}$$

For the same reason,

$$E\,[Y^2 g_\psi^2(S)|S] = \left(\frac{\eta - 1}{2}\right) g_\psi^2(S) \tag{7.22}$$

Using equations (7.15), (7.20) and (7.21), Z_{ij} can be simplified as follows

$$Z_{ij} \;=\; \cos^2(\Phi_{ij})\frac{\eta}{T^2}\left[R_\psi^2(S_{ij}) \;+\; \hat{R}_\psi^2(S_{ij})\right] . \tag{7.23}$$

Because T is a symmetrically distributed random variable, the conditional BER given $b_0^{(0i)}$ does not depend on the value of $b_0^{(0i)}$, so we take it to be 1. Thus, the conditional BER, $P_b(\Psi, \gamma_{0i})$, for BPSK is

$$P_b(\Psi, \gamma_{0i}) = P_r(\,\gamma_{0i} + T < 0 \;|\, b_0^{(0i)} = 1\,) \;=\; \mathrm{Q}\left[\frac{\gamma_{0i}}{\sqrt{\Psi}}\right] \tag{7.24}$$

where $\mathbf{Q}(x)$ is the complementary error function defined as $\frac{1}{\sqrt{2\pi}}\int_x^\infty \exp(-y^2/2)\,dy$.

Hence, the average BER of the user i who is power controlled by the BS 0 can be evaluated by

$$\begin{aligned} P_b \;&=\; E_{\Psi,\gamma_{0i}}[\,P_b(\Psi, \gamma_{0i})\,] \\ &= E_\Psi\{E_{\gamma_{0i}}[\,P_b(\Psi, \gamma_{0i}) \;|\; \Psi\,]\} \end{aligned} \tag{7.25}$$

Using equation (19) in (Lindsey 1964), the conditional probability of error can be written as

$$\begin{aligned} P_b(\Psi) \;&=\; E_{\gamma_{0i}}[\,P_b(\Psi, \gamma_{0i}) \mid \Psi\,] \\ &= \int_0^\infty \mathbf{Q}\left(\frac{y}{\sqrt{\Psi}}\right) 2(K+1)y\exp[-(K+1)y^2 - K]\, I_0\left[\sqrt{4K(K+1)}y\right] dy \\ &= \mathbf{Q}(u, w) \;-\; \frac{1}{2}\left(1 + \sqrt{\frac{d}{1+d}}\right)\exp\left(-\frac{u^2+w^2}{2}\right)\; I_0(uw) \\ &= \mathbf{Q}(u, w) \;-\; \frac{1}{2}\left(1 + \sqrt{\frac{d}{1+d}}\right)\exp\left[-\frac{K(1+2d)}{2(1+d)}\right] I_0\left[\frac{K}{2(1+d)}\right] \end{aligned} \tag{7.26}$$

where $\mathbf{Q}(u,$ w) is the Marcum Q-function (Marcum et al. 1960) defined by

$$\mathbf{Q}(u, w) = \int_w^\infty z\exp[-(z^2 + u^2)/2] I_0(uz)\,dz \tag{7.27}$$

and

$$d = \frac{1}{2(K+1)\Psi}$$

$$u = \sqrt{\frac{K\left[1+2d-2\sqrt{d(1+d)}\right]}{2(1+d)}}$$

$$w = \sqrt{\frac{K\left[1+2d+2\sqrt{d(1+d)}\right]}{2(1+d)}}$$

If we set $K = 0$, then

$$P_b(\Psi) = \frac{1}{2} - \frac{1}{2}\sqrt{\frac{(1/2\Psi)}{1+(1/2\Psi)}} \tag{7.28}$$

which is the BER for the BPSK signal in a Rayleigh fading channel with signal-to-noise ratio $1/2\Psi$ (Proakis 1989).

The average BER is then

$$P_b = E_\Psi[P_b(\Psi)] = \int_0^\infty P_b(\psi) f_\Psi(\psi)\, d\psi \tag{7.29}$$

In order to find the pdf of Ψ, we have to derive the pdf of the random variable $\chi_{kn}\gamma_{kn}^2 Z_{kn}$ and then, use the $(N_0 + \sum_{k=1}^{K} N_k - 2)$-fold convolution to derive the pdf of Ψ. This is really mathematically intractable. One practical way is to use the Monte Carlo Integration method (Kavehrad et al. 1987), (Press et al. 1989) to remove the conditioning on all random vectors. That is,

$$P_b = \lim_{M\to\infty} \frac{1}{M} \sum_{j=1}^{M} P_b(\Psi_j) \tag{7.30}$$

Another approximation method which has been commonly used, because of its simplicity, is the Standard Gaussian Approximation SGA method (Milstein et al. 1992), (Misser et al. 1992), where τ is assumed to be an unconditional zero-mean Gaussian random variable. This implies that τ can be completely described by its variance. Thus, the average BER computed by this method is

$$P_b^G = P_b[E(\Psi)] = P_b(\mu_\psi) \tag{7.31}$$

where μ_ψ is

$$\begin{aligned}\mu_\psi &= E(\Psi) \\ &= \frac{\mathcal{N}_0}{2E_b} + \sum_{n=1,n\neq i}^{N_0} E(\chi_{0n})E(\gamma_{0n}^2)E(Z_{0n}) + \sum_{k=1}^{K}\sum_{n=1}^{N_k} E(\chi_{kn})E(\gamma_{kn}^2)E(Z_{kn}) \\ &= \frac{\mathcal{N}_0}{2E_b} + \frac{m_\psi}{\eta}\left[\sum_{n=1,n\neq i}^{N_0} E(\chi_{0n}) + \sum_{k=1}^{K}\sum_{n=1}^{N_k} E(\chi_{kn})\right] \end{aligned} \tag{7.32}$$

in which $E(\gamma_{ij}^2)=1$ and $m_\psi = \frac{1}{T_c^2}E[\hat{R}_\psi^2(S)] = \frac{1}{T_c^2}E[R_\psi^2(S)]$. For a rectangular chip pulse shape, $m_\psi = 1/3$. For a half-sine chip pulse shape of the form $\psi(t) = \sqrt{2}\sin(\pi t/T_c)$, $m_\psi = (15 + 2\pi^2)/(12\pi^2)$. For a raised-cosine chip pulse shape of the form

$$\psi(t) = \sqrt{\frac{2}{3}}[1 - \cos(2\pi t/T_c)],$$

$m_\psi = 1/6 + 35/(48\pi^2)$ (Polydoros et al. 1993).

We can define M_χ as follows

$$M_\chi = \sum_{n=1,n\neq i}^{N_0} E(\chi_{0n}) + \sum_{k=1}^{K}\sum_{n=1}^{N_k} E(\chi_{kn}) \tag{7.33}$$

which can be interpreted as the average interference power from the interfering users without considering the effect of relative delays and phases between the desired user and the interfering users. M_χ is derived in Appendix B, where the expression is generalized for shadowing with arbitrary distribution.

For $N_c = 1$, the mobile user is power controlled by the nearest BS and, without considering the other-cell interference, M_χ equals $N_0 - 1$, which is just the average number of interfering users in the same cell. In order to account for the effect of other-cell interference, we assume that the number of active users N in each cell is the same and we define the relative other-cell interference (Viterbi et al. 1994), f_I, as follows

$$f_I = \frac{M_\chi - (N-1)}{N} \tag{7.34}$$

Therefore, μ_ψ in equation (7.32) can be rewritten as

$$\mu_\psi = \frac{\mathcal{N}_0}{2E_b} + \frac{m_\psi(N-1)}{\eta}\left[1 + \frac{N}{N-1}f_I\right] \tag{7.35}$$

Compared with that of a single-cell DS/CDMA system, the effective number of interfering users in a multi-cell system increases by a factor $\left[1 + \frac{N}{N-1} f_I\right]$ which will reduce the frequency reuse efficiency. In Tables 7.1 and 7.2, we calculate f_I as a function of σ for N_c=1, 2, and 3 when the break point g is 200 m, the cell length is 1 km, and the propagation exponent pair is $(a,b)=(1.5,1.0)$ and $(2.0,2.0)$, respectively. σ is the standard deviation (STD) of the shadowing in dB.

σ (dB)	N_c = 1	N_c = 2	N_c = 3
0	0.2896	0.2896	0.2896
2	0.3581	0.2995	0.2983
4	0.6765	0.3396	0.3348
6	1.9533	0.4759	0.3686
8	8.6198	0.9803	0.6411

Table 7.1: f_I as a function of σ for N_c=1, 2, and 3 with a= 1.5 and b= 1.0

σ (dB)	N_c = 1	N_c = 2	N_c = 3
0	0.1525	0.1525	0.1525
2	0.1886	0.1534	0.1534
4	0.3563	0.1580	0.1579
6	1.0288	0.1764	0.1730
8	4.5398	0.2514	0.2113

Table 7.2: f_I as a function of σ for N_c=1, 2, and 3 with a=2.0 and b=2.0

From these Tables, we observe that significant improvement in f_I is obtained by using N_c = 2 instead of N_c = 1, but only a small improvement is obtained when we go from N_c = 2 to N_c = 3. In figure 7.3, we plot f_I as a function of σ with the propagation exponents as parameters. It can be seen that the propagation exponents have a great impact on f_I.

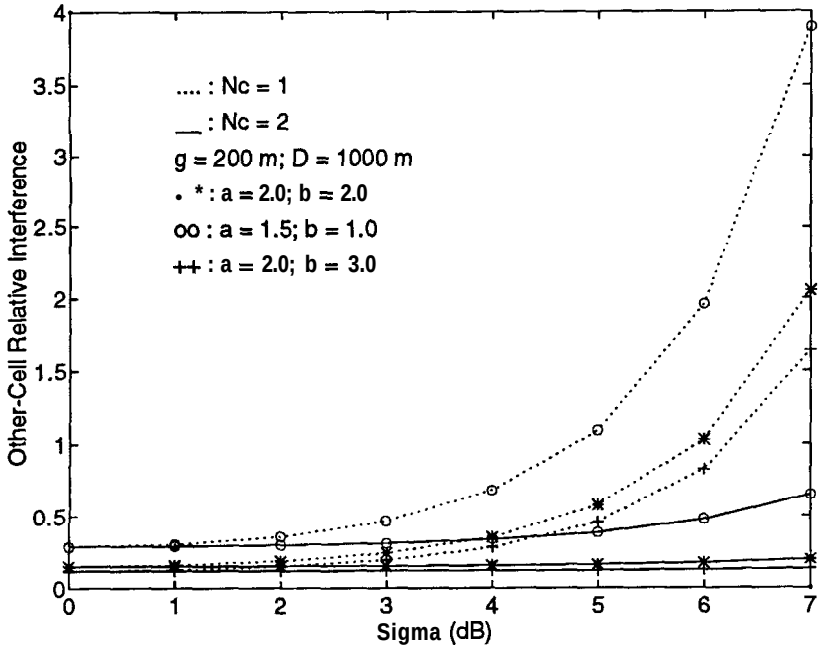

Figure 7.3: f_I versus σ for $N_c = 1$ and $N_c = 2$

BER for DPSK

For DPSK demodulation, a possible implementation of the differentially-coherent matched filter receiver for a DS/CDMA system is shown in Fig. 7.4 (Sklar 1988)

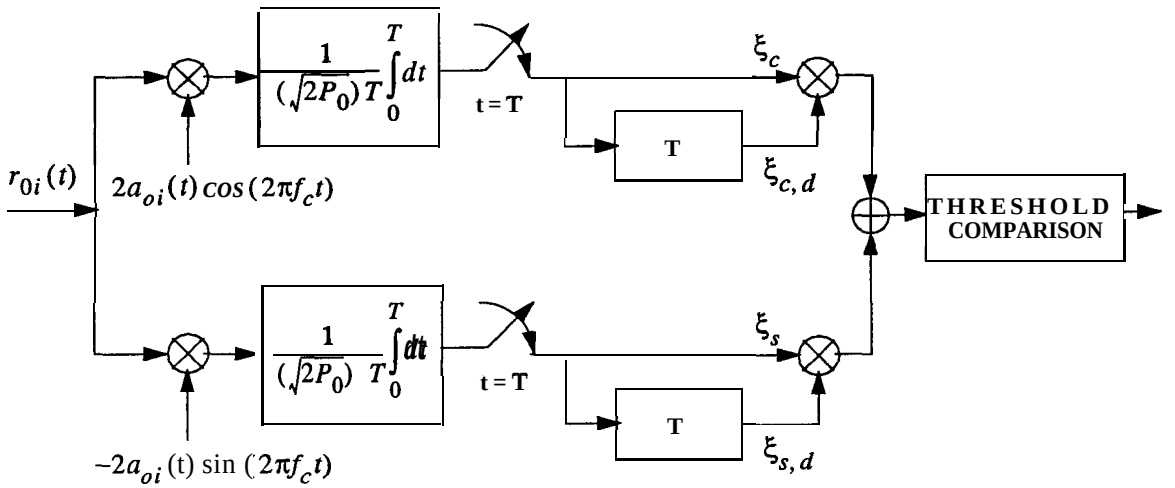

Figure 7.4: Receiver for a DS/CDMA system employing DPSK modulation

The demodulator has two branches; the first one matches the in-phase component and the second one matches the quadrature component. The output of the in-phase branch ξ_c is

$$\xi_c = \frac{1}{\sqrt{2P_0}T}\int_0^T r_{0i}(t)2a_{0i}(t)\cos(2\pi f_c t)\,dt \qquad (7.36)$$

The output of the quadrature branch ξ_s is given by the equation (7.36) with the $[\cos(\cdot)]$ term replaced by [- sin(.)]. The receiver forms the statistics $\xi_c\xi_{c,d}+\xi_s\xi_{s,d}$ and compares it with a zero threshold. For this kind of receiver, the conditional BER for the desired user using the IGA method is (Proakis 1989):

$$P_b(\Psi,\gamma_{0i}) = \frac{1}{2}\exp\left(-\frac{\gamma_{0i}^2}{2\Psi}\right) \qquad (7.37)$$

where γ_{0i} is the faded amplitude of the desired signal and Ψ is the conditional variance of the total interference.

Averaging over γ_{0i}, gives

$$P_b(\Psi) = E_{\gamma_{0i}}[\ P_b(\Psi,\gamma_{0i})\ ]$$

$$= \int_0^\infty \frac{1}{2}\exp(-\frac{y^2}{2\Psi})\frac{y}{\sigma_s^2}\exp\left(-\frac{y^2+\alpha^2}{2\sigma_s^2}\right) I_0\left(\frac{\alpha y}{\sigma_s^2}\right) dy$$

$$= \frac{\zeta}{2}\int_0^\infty z\exp\left(-\frac{z^2+\hat{\alpha}^2}{2}\right) I_0(\zeta\hat{\alpha}z)\, dz \qquad (7.38)$$

where $\zeta = \sqrt{\Psi/(\Psi+\sigma_s^2)}$ and $\hat{\alpha} = \alpha/\sigma_s = \sqrt{2K}$.

Let $\alpha_0 = \zeta\hat{\alpha}$. Then, the conditional BER, $P_b(\Psi)$, becomes

$$\begin{aligned} P_b(\Psi) &= \frac{\zeta^2}{2}\left\{\int_0^\infty z\exp\left(-\frac{z^2+\alpha_0^2}{2}\right) I_0(\alpha_0 z)\, dz\right\}\exp\left(\frac{\alpha_0^2-\hat{\alpha}^2}{2}\right) \\ &= \frac{\zeta^2}{2}\exp\left(\frac{\alpha_0^2-\hat{\alpha}^2}{2}\right) \\ &= \frac{\Psi}{2(\Psi+\sigma_s^2)}\exp\left(\frac{K\sigma_s^2}{\Psi+\sigma_s^2}\right) \\ &= \frac{\Psi}{2\Psi+1/(K+1)}\exp\left[-\frac{I\cdot}{2(K+1)\Psi+1}\right] \end{aligned} \qquad (7.39)$$

where $\sigma_s^2 = 1/[\,2(K+1)]$.

Note that if $K = 0$, (7.39) reduces to $1/2[1+1/(2\Psi)]$ which is the BER for DPSK signals in a Rayleigh fading channel with $E_b/\mathcal{N}_0 = 1/(2\Psi)$. On the other hand, if $K \to \infty$, (7.39) becomes $\frac{1}{2}\exp\left(-\frac{1}{2\Psi}\right)$, which is the BER for DPSK signals in an AWGN channel with $E_b/\mathcal{N}_0 = 1/(2\Psi)$. Meanwhile, the average BER calculated by the SGA method yields

$$\begin{aligned} P_b^G &= P_b(\mu_\psi) \\ &= \frac{\mu_\psi}{2\mu_\psi+1/(K+1)}\exp\left[-\frac{K}{2(K+1)\mu_\psi+1}\right] \end{aligned} \qquad (7.40)$$

which has the same form as (7.39), except that Ψ is replaced by μ_ψ.

BER Analysis in Nakagami Fading Channels

In this section, we will study the BER performance for DS systems in Nakagami-m multipath fading channels with log-normal shadowing. The Nakagami-m distribution is a central x-distribution with a nonintegral degree of freedom (where the degree of freedom is greater than or equal to 1), which was introduced by Nakagami (Nakagami 1960) as an approximation to two other distributions that he had previously employed, the Nakagami-n and

the Nakagami-q distributions. The Nakagami-n, which is also called the Rician distribution, is a noncentral x-distribution with two degrees of freedom. The amplitude of a complex Gaussian random variable whose real and imaginary components are uncorrelated and have nonzero mean and equal variance satisfies this distribution. If the real and imaginary parts of a complex Gaussian random variable are uncorrelated and have zero mean and unequal variance, the envelope of this variable will follow the Nakagami-q distribution.

The reasons why researchers are interested in the Nakagami-m (for convenience, we omit the symbol "-m" in the following discussion) distribution are the following. First, it has greater flexibility and accuracy in matching some experimental data than Rayleigh, log-normal, or Rician distributions (Adu-Dayya et al. 1991). Second, it offers features of analytical convenience in comparison to the Rician distribution. Therefore, the analytical expressions for the Nakagami model often possess greater mathematical simplicity than those for the Rician one. Third, the Nakagami distribution is a general distribution which has the Rayleigh and the one-sided Gaussian distributions as its special cases. Furthermore, it can be used to approximate the Rician distribution by a transformation shown below. A summary of the Nakagami distribution properties and a list of references on Nakagami fading can be found in (Nakagami 1960) and (Beaulieu 1991) respectively.

However, there are some limitations associated with the Nakagami fading model. First, it does not provide a clear intuitive picture of the fading mechanism (in contrast to the Rician model in which the received signal is the superposition of the specular and the scattered components). Moreover, the phase distribution, which is frequently of great importance in coherent communications, does not appear in the model. Finally, the goodness-of-fit tests used by ionospheric physicists to match measured scintillation data to a Nakagami distribution usually do not give a special weighting to the deep-fading tail of the distribution. That is, we may have a better fit near the median of the distribution than in the tail, although it is the tail behavior which is of greater significance to communication systems performance (Crepeau 1992).

The pdf of a normalized Nakagami distribution can be written as follows

$$f_{\gamma_{0i}}(y) = \frac{2m^m y^{2m-1}}{\Gamma(m)} \exp(-my^2) \quad U(y) \tag{7.41}$$

where $E(\gamma_{0i}^2) = 1$, the fade parameter m whose value should be no less than $1/2$ is defined as $1/\mathbf{Var}(\gamma_{0i}^2)$, and $\Gamma(x)$ is the gamma function (Abramowitz et al. 1964) which is defined as $\Gamma(x) = \int_0^\infty t^{x-1} \exp(-t)\, dt$. If $m = 1/2$, then γ_{0i} is a one-sided Gaussian random variable. If m = 1, then γ_{0i} follows a Rayleigh distribution. Furthermore, Nakagami (Shaft 1974) has shown that the Nakagami distribution and the Rician distribution are closely related by the factor

$$K = \frac{\sqrt{m^2 - m}}{m - \sqrt{m^2 - m}} = \sqrt{m-1}\,(\sqrt{m} + \sqrt{m-1}) \tag{7.42}$$

where K is the Rician factor. For large values of m, K can be approximated by $2(m - 1)$.

In figure 7.5 we show the value of K as a function of its relative m by applying (7.42). In figure 7.6, the comparison of the Nakagami with its related Rician distribution is illustrated. If m = 6, the corresponding Rician factor K is 10.20 dB; if m = 11, K will be 13.12 dB, using equation (7.42). We can find that these density function pairs fit well. Therefore, for analytical convenience, researchers intend to replace the Rician distribution by its relative Nakagami peer (Ho et al. 1993). In the following, we will examine the feasibility of this argument by comparing their BER performances instead of just comparing their pdf'.

As derived earlier, the conditional BER, $P_b(\Psi, \gamma_{0i})$, is equal to $Q(\gamma_{0i}/\sqrt{\Psi})$ for BPSK signals and is equal to $\frac{1}{2}\exp(-\gamma_{0i}^2/2\Psi)$ for DPSK signals, respectively.

Thus, the conditional BER, $P_b(\Psi)$, can be evaluated by

$$\begin{aligned} P_b(\Psi) &= E_{\gamma_{0i}}\,[\,P_b(\Psi, \gamma_{0i})\,] \\ &= \int_0^\infty P_b(\Psi, y) f_{\gamma_{0i}}(y)\, dy \end{aligned} \tag{7.43}$$

Wojnar (Wojnar 1986) has shown that the integration in equation (7.43) for BPSK and DPSK signals can be expressed as a single incomplete beta function (Abramowitz et al.1964)

$$P_b(\Psi) = \frac{1}{2}\left[\frac{m}{m+1/(2\Psi)}\right](m, b) \tag{7.44}$$

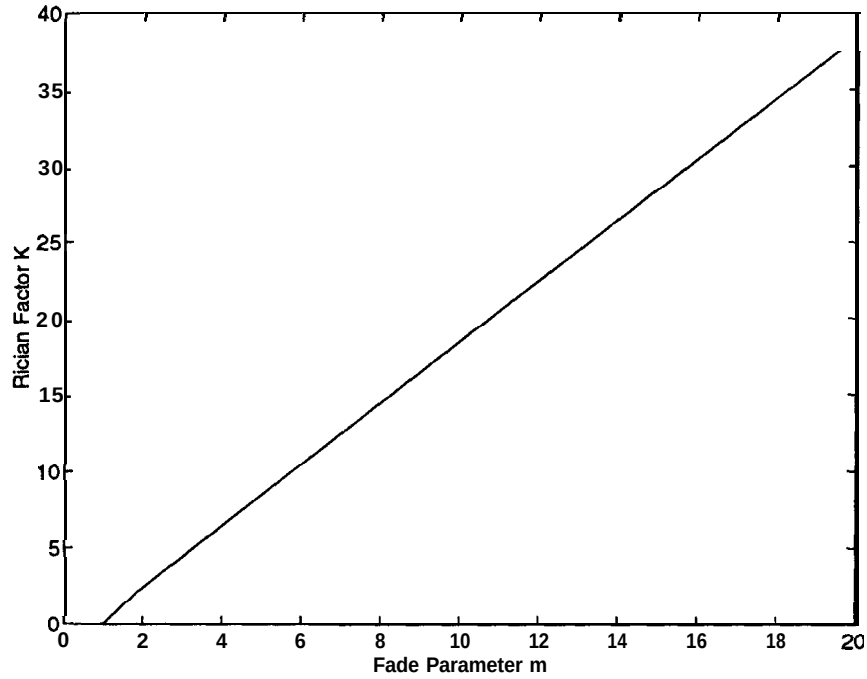

Figure 7.5: The Rician Factor K versus the Fade Parameter m

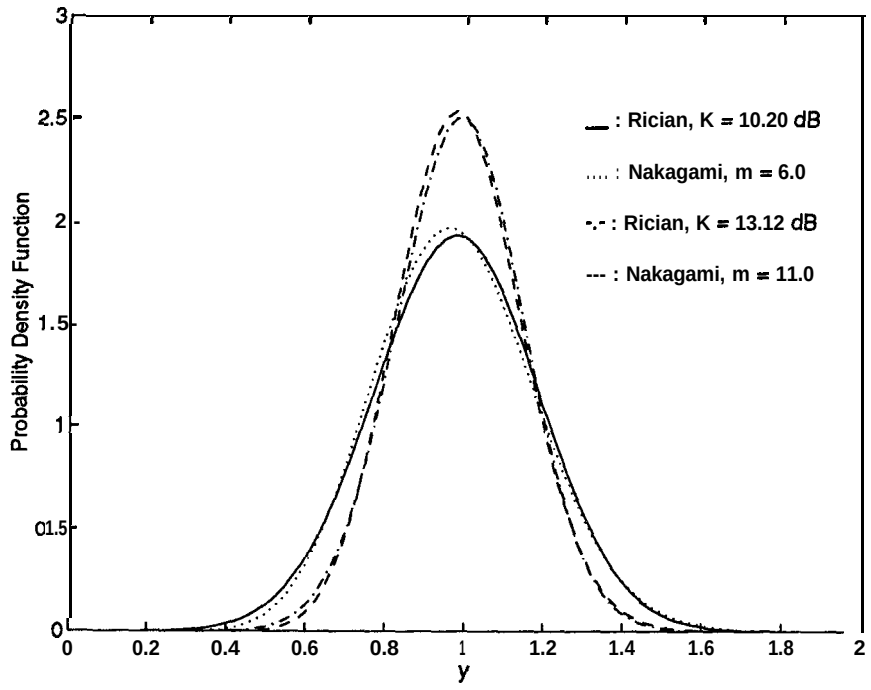

Figure 7.6: Comparison of Nakagami Distribution with its Related Rician Peer

where ,(a, b) is an incomplete beta function and $b=1$ for DPSK and $b=1/2$ for BPSK. The incomplete beta function is (defined by 6.6.2 in (Abramowitz et al. 1964))

$$_x(a,b) = \frac{B_x(a,b)}{B(a,b)} \quad ,0 \le x \le 1 \tag{7.45}$$

where $B(a,b)$ is the beta function given by (Abramowitz et al. 1964)

$$B(a,b) = \frac{\Gamma(a)\Gamma(b)}{\Gamma(a+b)} \tag{7.46}$$

and $B_x(a,b)$ is

$$B_x(a,\ b)\ = \int_0^x t^{a-1}(1-t)^{b-1}\,dt \tag{7.47}$$

Therefore, by inserting equations (7.46) and (7.47) into equation (7.45), we can rewrite the incomplete beta function as

$$_x(a,b)\ = \frac{\Gamma(a+b)}{\Gamma(a)\Gamma(b)} \int^x\ t^{a-1}(1\ -\ t)^{b-1}\ dt \tag{7.48}$$

Since b = 1, the conditional BER for DPSK signals, $P_b(\Psi)$, can be further simplified as follows

$$\begin{aligned} P_b(\Psi)_{DPSK} &= \frac{1}{2}\,[\tfrac{m}{m+1/(2\Psi)}](m,1) \\ &= \frac{\Gamma(m+1)}{2\,\Gamma(m)\,\Gamma(1)} \int_0^{\frac{m}{m+1/(2\Psi)}} t^{m-1}dt \\ &= \frac{1}{2}\left[\frac{m}{m+1/(2\Psi)}\right]^m \end{aligned} \tag{7.49}$$

Setting m = 1, i.e., the amplitude of the desired signal γ_{0i} is Rayleigh, the conditional BER of DPSK signals becomes $1/2[\,1+1/(2\Psi)\,]$ whichis the same as the result in (7.39) with K = 0.

For BPSK, b = 1/2, $P_b(\Psi)_{BPSK}$ is

$$P_b(\Psi)_{BPSK} = \frac{\Gamma(m\ +\ 1/2)}{2\Gamma(m)\sqrt{\pi}} \int_0^{\frac{m}{m+1/(2\Psi)}}\ t^{a-1}(1\ -\ t)^{b-1}\ dt \tag{7.50}$$

where $\Gamma(1/2) = \sqrt{\pi}$.

If the fade parameter m is an integer, $P_b(\Psi)_{BPSK}$ can be further simplified using the following property (25.5.7 in (Abramowitz et al. 1964))

$$1 - I_x(a, b) = I_{(1-x)}(b, a) = (1-x)^{a+b-1} \sum_{i=0}^{a-1} \binom{a+b-1}{i} \left(\frac{x}{1-x}\right)^i \tag{7.51}$$

Therefore, $P_b(\Psi)_{BPSK}$ becomes

$$\begin{aligned} P_b(\Psi)_{BPSK} &= \frac{1}{2} I_{\left[\frac{m}{m+1/(2\Psi)}\right]}(m, 1/2) \\ &= \frac{1}{2}\left[1 - I_{\left[\frac{1/(2\Psi)}{m+1/(2\Psi)}\right]}(1/2, m)\right] \\ &= \frac{1}{2}\left\{1 - \left[\frac{1/(2\Psi)}{m+1/(2\Psi)}\right]^{(m-1/2)} \sum_{i=0}^{m-1} \binom{m-1/2}{i} (2m\Psi)^i\right\} \end{aligned} \tag{7.52}$$

where $\binom{m-1/2}{i}$ isdefinedas

$$\binom{m-1/2}{i} = \begin{cases} \frac{(m-1/2)\cdot\ldots\cdot[m-1/2-(i-1)]}{i!} & i \neq 0 \\ 1 & i = 0 \end{cases} \tag{7.53}$$

If m = 1, then $P_b(\Psi)_{BPSK}$ becomes

$$P_b(\Psi)_{BPSK} = \frac{1}{2}\left[1 - \sqrt{\frac{1/(2\Psi)}{1+1/(2\Psi)}}\right] \tag{7.54}$$

which yields the same result as in (7.28).

We summarize the conditional BER, $P_b(\Psi)$, for DS/CDMA systems employing BPSK and DPSK modulation in Rician/Nakagami fading channels as follows.

- Rician Fading

  - BPSK

$$P_b(\Psi) = Q(u, w) - \frac{1}{2}\left(1 + \sqrt{\frac{d}{1+d}}\right) \exp\left[-\frac{K(1+2d)}{2(1+d)}\right] I_0\left[\frac{K}{2(1+d)}\right]$$

where

$$d = \frac{1}{2(K+1)\Psi}$$

$$u = \sqrt{\frac{K\left[1 + 2d - 2\sqrt{d(1+d)}\right]}{2(1+d)}}$$

$$w = \sqrt{\frac{K\left[1 + 2d + 2\sqrt{d(1+d)}\right]}{2(1+d)}}$$

– DPSK

$$P_b(\Psi) = \frac{\Psi}{2\Psi + 1/(K+1)} \exp\left[-\frac{K}{2(K+1)\Psi + 1}\right]$$

- Nakagami Fading

– BPSK

* m is not an integer:

$$P_b(\Psi) = \frac{\Gamma(m + 1/2)}{2\Gamma(m)\sqrt{\pi}} \int_0^{\frac{m}{m+1/(2\Psi)}} t^{a-1}(1-t)^{b-1}\, dt$$

* m is an integer:

$$P_b(\Psi) = \frac{1}{2}\left\{1 - \left[\frac{1/(2\Psi)}{m + 1/(2\Psi)}\right]^{(m-1/2)} \cdot \sum_{i=0}^{m-1}\binom{m-1/2}{i}(2m\Psi)^i\right\}$$

– DPSK

$$P_b(\Psi) = \frac{1}{2}\left[\frac{m}{m + 1/(2\Psi)}\right]^m$$

Knowing the conditional BER, we can evaluate the average BER by averaging over the conditional variance Ψ.

Numerical Evaluation of the BER

In this section, the average BER as a function of the number of active users is evaluated. Unless otherwise noted, we assume that each cell has the same number of active users N, the spreading ratio, η, equals 511, the cell length, D, is 1 km, the Fresnel break point, g, is 200

m, and the propagation exponents, a and b, are both equal to 2. Also, the rectangular chip waveform is employed and log-normal shadowing is assumed with the standard deviation σ being 6 dB. The interference outside the six adjacent cells is not taken into account. Due to the relatively short propagation distance, microcellular systems can operate with very high Signal-to-noise ratios (i.e., $E_b/\mathcal{N}_0$ >> I). Hence, we assume that the AWGN can be ignored compared with the MAI. This implies that microcellular systems are interference-limited.

Figures 7.7 and 7.8 illustrate the average BER of DPSK as a function of N for N_c = 1 (nearest BS) and 2 (nearest two BS's), respectively. The results show that for this range of N, the average BER evaluated by the SGA is less than that evaluated by the IGA. For N_c = 1, the results from the SGA method are very optimistic when the number of active users is small and the Rician factor K is large. Furthermore, the Rician factor K has a great impact on the average BER for N_c = 2, but a little impact on that for N_c = 1. The reason for this phenomenon can be explained as follows. The conditional BER $P_b(\Psi)$ is illustrated in figure 7.9. Applying the theorem proposed in (Dresher 1953), which provides a relation between the moments of a random variable, the average BER for N_c = 1 will be located in the range $[P_{L1}, P_{U1}]$ (Morrow et al. 1989). Hence, P_b^G, which equals P_{L1}, becomes the lower bound of P_b when N_c = 1 if μ_ψ is in the convex portion of $P_b(\Psi)$. For N_c = 2, P_b^G is still a lower bound of P_b, but it is closer to P_b than for N_c = 1. The reason is that the possible[1] deviation of Ψ for N_c = 2 is much less than that for N_c = 1. Thus, P_b^G is a good approximation of P_b for N_c = 2 even when N is small and K is large. This implies that we can directly employ the SGA method to evaluate the average BER with sufficient accuracy.

In order to further investigate the effect of K on the average BER, we illustrate the average BER of DPSK as a function of K in figure 7.10, for N = 35. It can be found that the larger the Rician factor, the smaller the average BER. Although the desired user and the interfering users both have less multipath fading as K becomes large, the Rician factor K has positive effect on the average BER performance. Thus, the system operating in a Rician fading channel can have better performance than that operating in a Rayleigh fading channel. Furthermore, the fact that the macro-selection diversity significantly decreases the

[1] In theory the maximum value of Ψ approaches ∞. However, for each Monte Carlo Integration, we can have finite deviation of Ψ.

BER when K is large implies that we can further employ the microdiversity technique to combat the Rician fading and thus improve the BER performance.

It is interesting to study the effect of σ on the BER performance. We illustrate the average BER as a function of N with parameter σ in figure 7.12 for N_c = 1 and in figure 7.12 for N_c = 2, respectively. For N_c = 1, we find that the average BER increases rapidly when the value of σ becomes large. However, for N_c = 2, the average BER increases slightly with σ. Thus, the macro-selection diversity can effectively reduce the MA1 from other cells when the shadowing is heavy. This observation coincides with the results shown in Tables 7.1 and 7.2.

We illustrate the average BER versus N for BPSK in figures 7.13 and 7.14. In order to compare the average BER of DPSK with that of BPSK, we define the effective signal-to-noise ratio, SNR_{eff}, as

$$SNR_{eff} = \frac{E(\gamma_{0i}^2)}{E(\Psi)} = \frac{1}{\mu_\psi} \tag{7.55}$$

In figure 7.15, we illustrate the average BER of DPSK and BPSK versus the SNR_{eff} for K = 10 dB. When the average BER is equal to 10^{-3} and N_c = 1, the SNR_{eff} of BPSK is approximately 3 dB better than that of DPSK. When the average BER is 10^{-4} and N_c = 2, the SNR_{eff} of BPSK is about 2 dB better than that of DPSK.

In figure 7.16, the BER versus N is depicted for DPSK signals with rectangular, half-sine, and raised cosine chip waveforms, respectively. As expected, the raised-cosine waveform provides the best BER performance because it possesses the least MA1 interference (m_ψ is minimum). For N_c = 1 and $P_e = 10^{-3}$, the system can accommodate 25 users using the raised-cosine waveform, but only 15 users using the rectangular waveform. Therefore, the raised-cosine waveform can significantly increase the user capacity.

It is also interesting to find the effect of the propagation pair (a, b) on the system performance. We illustrate the BER versus N for (a, b) $= (1.5, 1.0), (2, 2)$, and $(2, 3)$ in figure 7.17. In (Pickholtz et al. 1991), field measurements in several urban areas result in different values for a and b.

In the SGA method, we assume that the MA1 is an unconditional Gaussian random variable. Therefore, the second moment information of T is sufficient to find the averaged BER performance. On the other hand, in the IGA method, the MA1 is assumed to be a conditional Gaussian random variable on $\underline{\chi}, \underline{\gamma}, \underline{\Phi}$, and $\underline{S}$. The overall moment information is needed in order to evaluate the averaged BER. From figure 7.7, we find that the SGA method produces optimistic results when N is small for N_c = 1. Hence, we have to find which of the vectors $\underline{\chi}, \underline{\gamma}, \underline{\Phi}$, and $\underline{S}$ plays a dominant role in the BER calculation. In figure 7.18, the BER is plotted versus N for N_c = 1. Besides the IGA and the SGA methods, we also illustrate BER results by using two other approximation methods, namely the IGA-K and the IGA-L methods. In the IGA-K method, the conditional variance is assumed to be function of $\underline{\chi}$ only. Hence, Ψ in (7.18) becomes

$$\Psi_{IGA-K} = \frac{\mathcal{N}_0}{2E_b} + \frac{m_\psi(N_0 - 1)}{\eta} + \frac{m_\psi}{\eta}\sum_{k=1}^{K}\sum_{n=1}^{N_k}\chi_{kn} \qquad (7.56)$$

In the IGA-L method, we assume that the total interference T is a conditional Gaussian random variable conditioned on the shadowing. Thus, Ψ_{IGA-L} is a function of the log-normal components, which can be written as follows

$$\Psi_{IGA-L} = \frac{\mathrm{No}}{2E_b} + \frac{m_\psi(N_0 - 1)}{\eta} + \frac{m_\psi}{\eta}\sum_{k=1}^{K}\sum_{n=1}^{N_k} E\left\{\frac{L_p\left[r_{kn}^{(0)}\right]}{L_p\left[r_{kn}^{(k)}\right]}\right\} 10^{\left(X_{kn}^{(0)} - X_{kn}^{(k)}\right)/10} \qquad (7.57)$$

where $10^{X_{kn}^{j}/10}$ denotes the shadowing along the path between the user kn and the BS j. Figure 7.18 shows that the BER calculated by the IGA-K method is close to that calculated by the IGA method. We conclude that the random vector $\underline{\chi}$ plays a dominant role in the BER calculation. Therefore, we can reduce the computation effort by using the IGA-K method and still preserve the accuracy.

Figures 7.19 and 7.20 show plots of the average BER of DPSK as a function of N in Nakagami fading channels for N_c = 1 and 2, respectively. Comparing the results with those in Rician fading channels shown in figures 7.7 and 7.8, we notice that the SGA method in Nakagami fading channels yields much more optimistic results, when N is small.

Finally, we compare the average BER performance of a system in the Nakagami channel

for m = 6 with that in its Rician peer for K = 10.2 dB in figure 7.21. Without macro-diversity $(N_c = 1)$, the BER performance in the Nakagami channel fits the performance in the corresponding Rician channel. However, optimistic results can be found in the Nakagami fading channel for N_c = 2. Hence, whether or not we can approximate the Rician distribution by its corresponding Nakagami distribution cannot be judged simply by their pdfs. The results in figure 7.21 show that the macro-selection diversity also affects the approximation result.

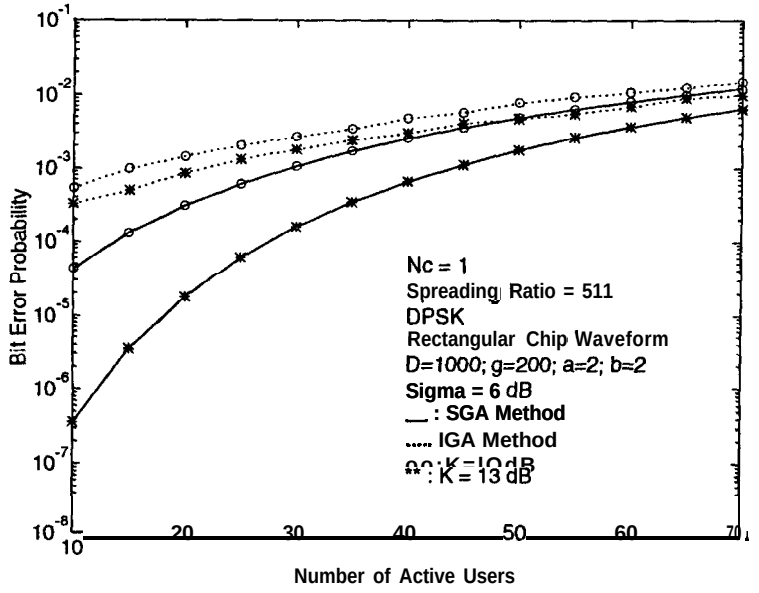

Figure 7.7: BER versus N for DPSK in Rician Fading Channels (IV, = 1)

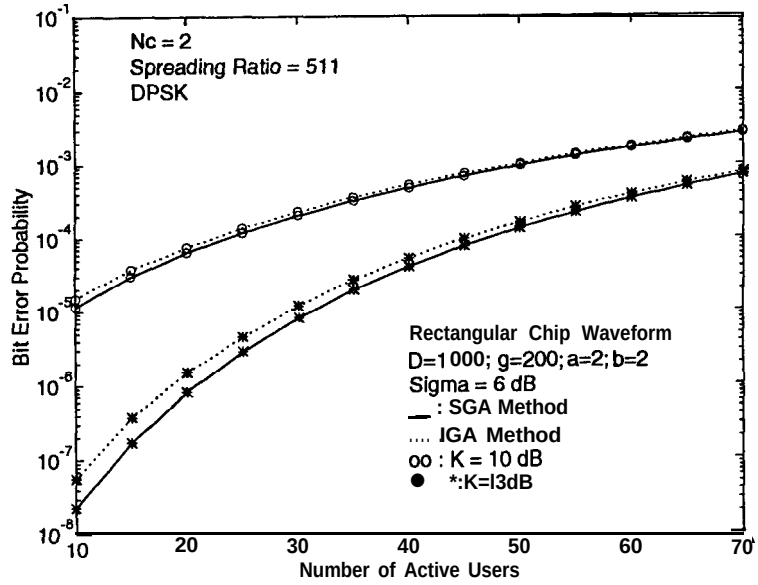

Figure 7.8: BER versus N for DPSK in Rician Fading Channels (N_c = 2)

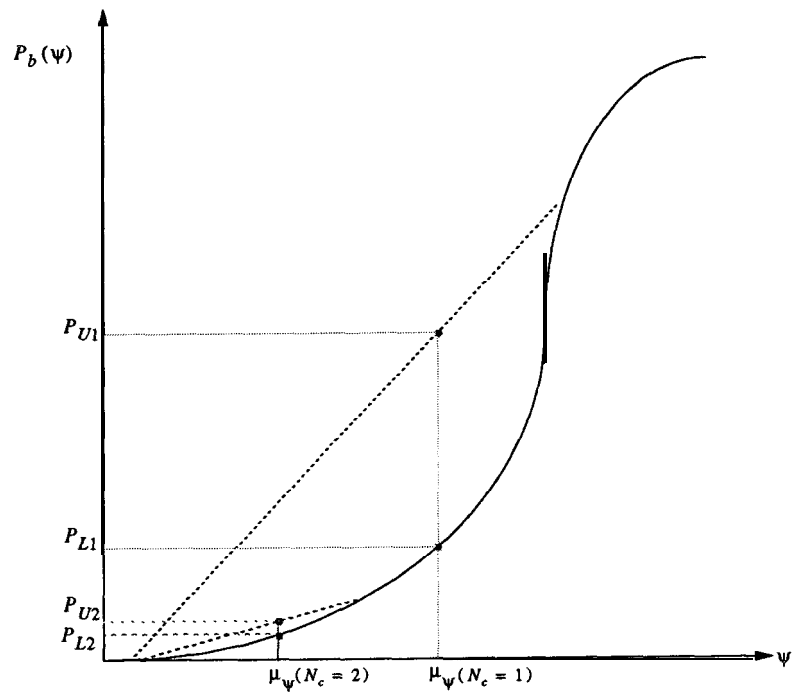

Figure 7.9: $P_b(\Psi)$ versus Ψ. The average BER for N_c = 1 will be in the interval $[P_{L1}, P_{U1}]$; the average BER for N_c = 2 will be in the interval $[P_{L2}, P_{U2}]$.

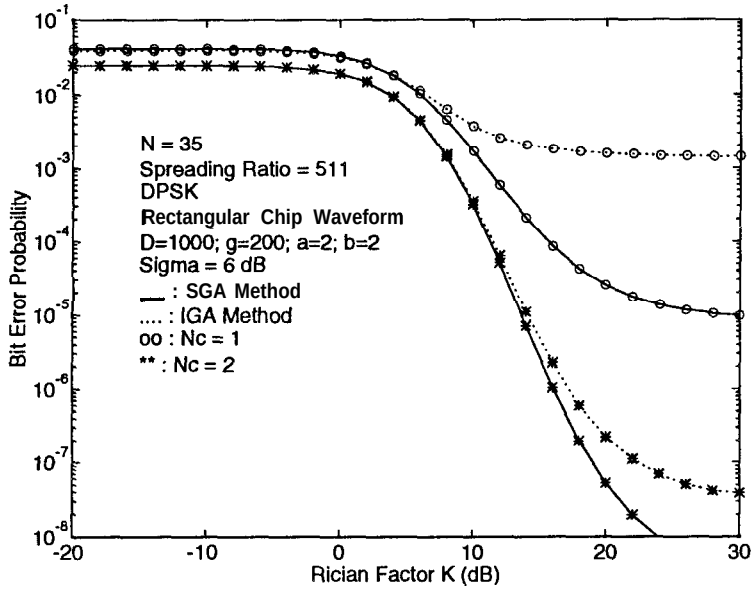

Figure 7.10: BER versus K for DPSK in Rician Fading Channels, for N_c = 1 and N_c = 2

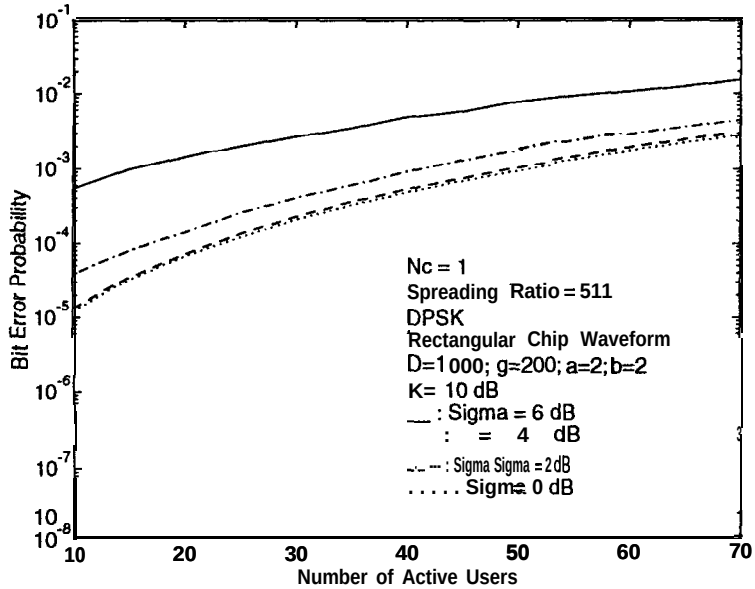

Figure 7.11: BER versus N for DPSK using the IGA Method in Rician Fading Channels, for N_c = 1 and σ = 0, 2, 4, 6 dB

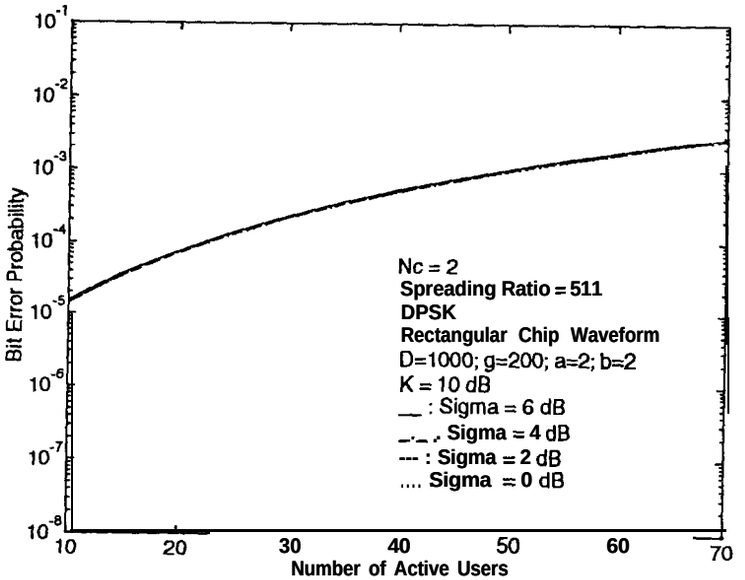

Figure 7.12: BER versus N for DPSK using the IGA Method in Rician Fading Channels, for N_c = 2 and σ= 0, 2, 4, 6 dB

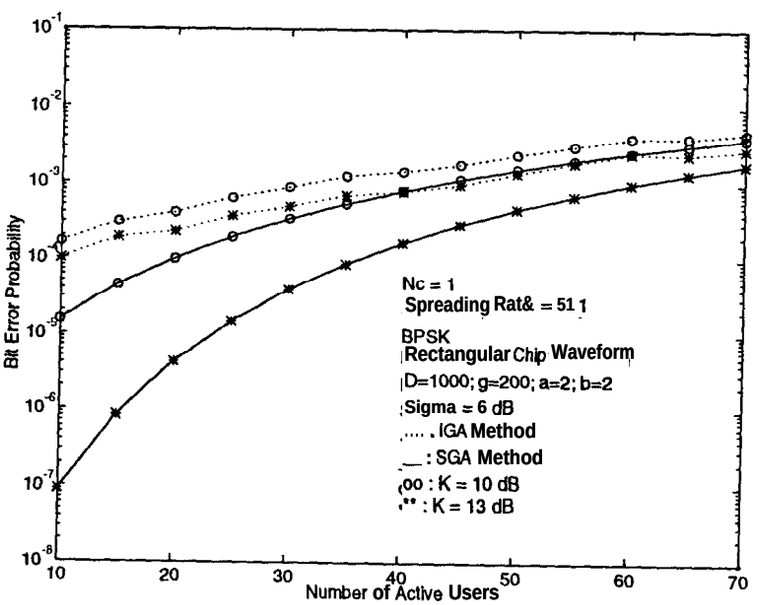

Figure 7.13: BER versus N for BPSK in Rician Fading Channels (N_c = 1)

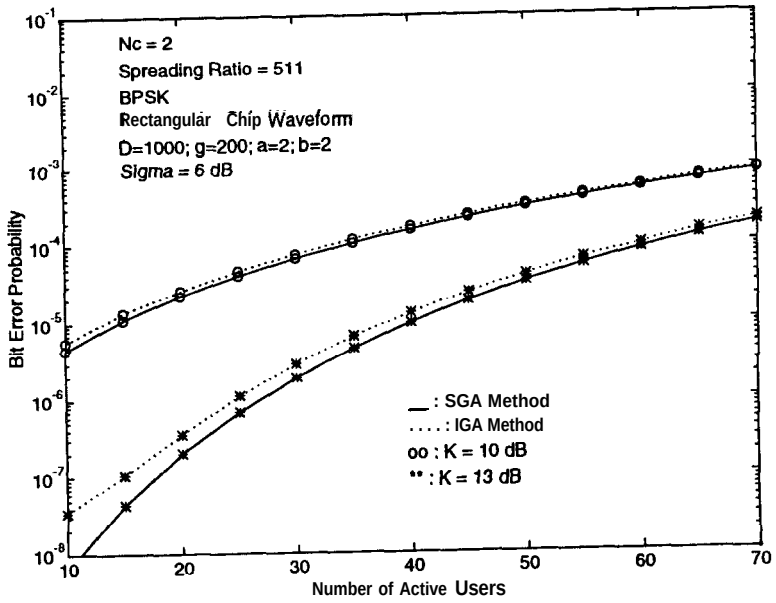

Figure 7.14: BER versus N for BPSK in Rician Fading Channels ($N_c = 2$)

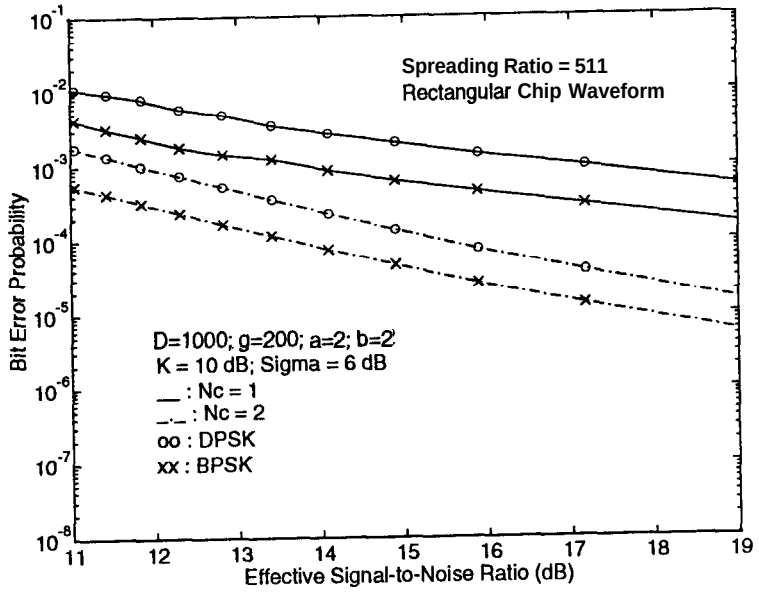

Figure 7.15: BER versus the SNR_{eff} of DPSK and BPSK using the IGA Method in Rician Fading Channels for $N_c = 1$ and $N_c = 2$ with $K = 10$ dB

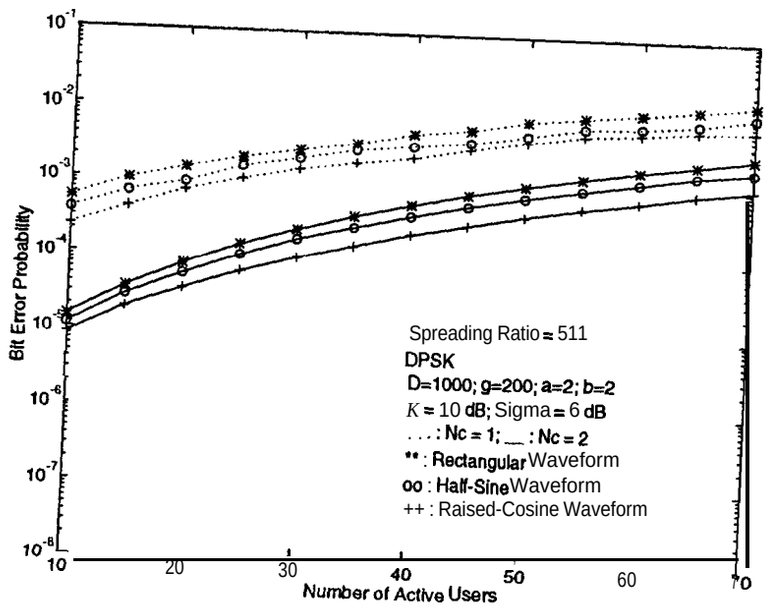

Figure 7.16: BER versus N for DPSK using the IGA Method for Rectangular, Half-Sine, and Raised-Cosine Waveforms with $K = 10$ dB in Rician Fading Channels for $N_c = 1$ and $N_c = 2$.

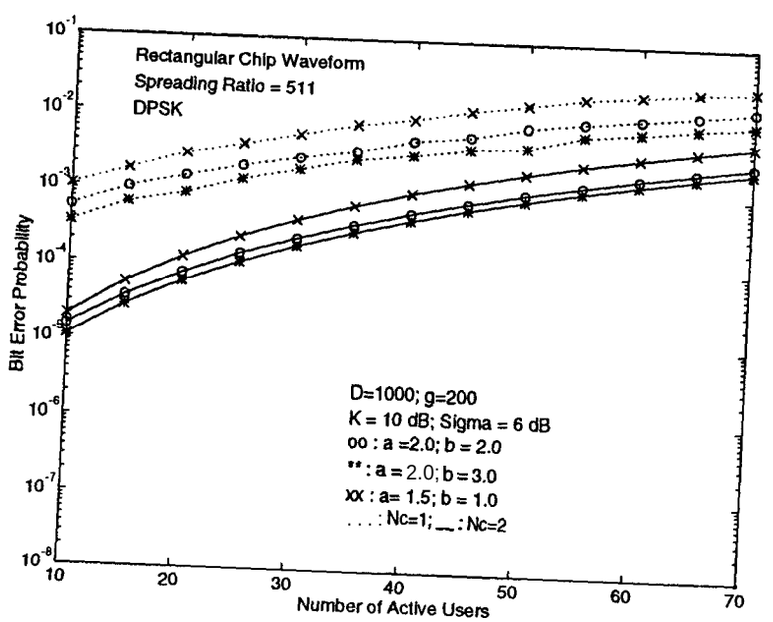

Figure 7.17: BER versus N for DPSK using the IGA Method for Different Propagation Exponents in Rician Fading Channels

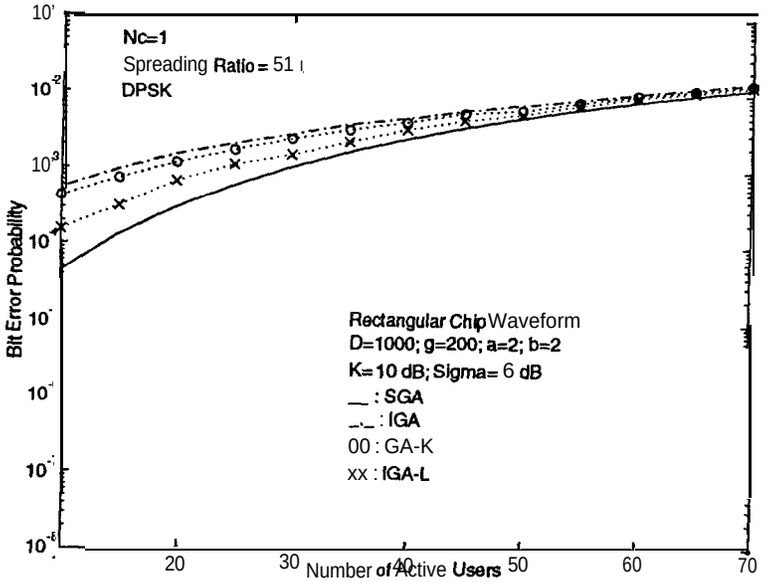

Figure 7.18: BER versus N for DPSK in Rician Fading Channels for $N_c = 1$ with Several Approximation Methods

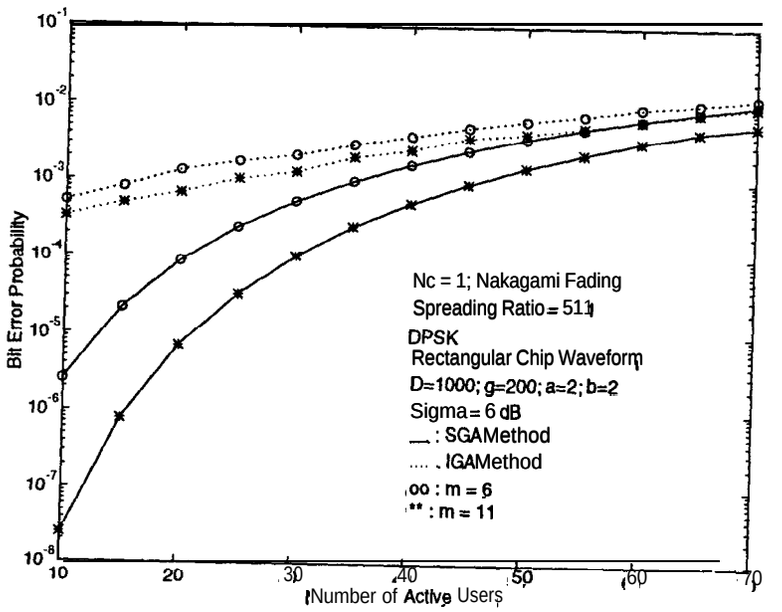

Figure 7.19: BER versus N for DPSK in Nakagami Fading Channels ($N_c = 1$)

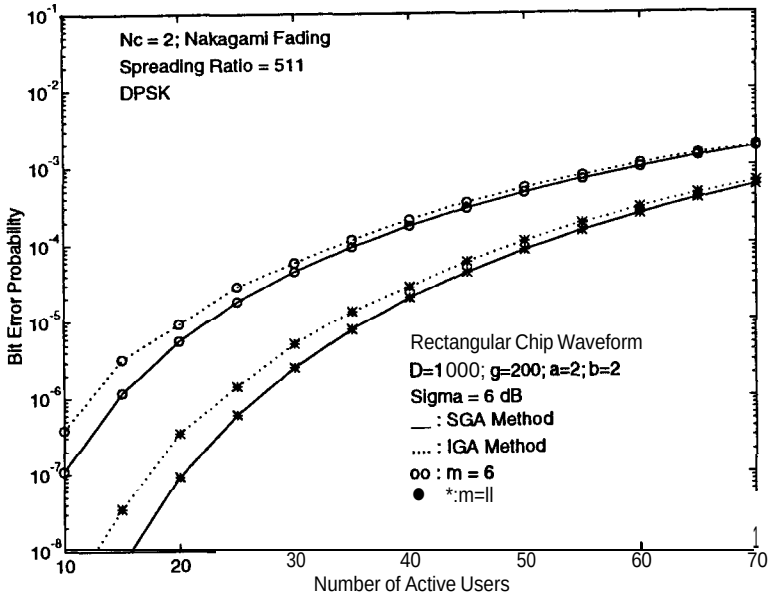

Figure 7.20: BER versus N for DPSK in Nakagami Fading Channels ($N_c = 2$)

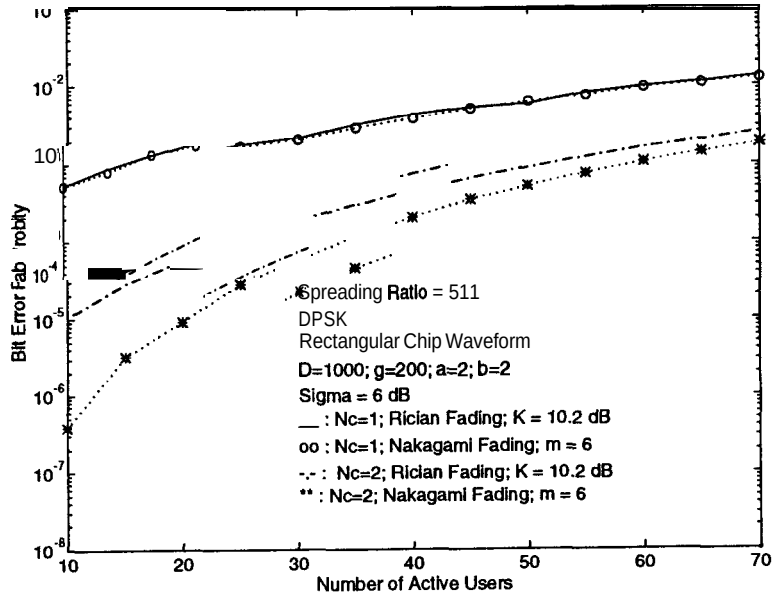

Figure 7.21: Comparisons of the BER Performance in Nakagami Fading Channels with its Related Rician peers

7.2.3 Outage Probability Analysis

Sometimes it is desirable to compute the outage probability, which is defined as the probability that the conditional (or instantaneous) BER exceeds a specific constant P_e. For telecommunications, the outage probability is usually used as the criterion to assess the user capacity (Gilhousen et al. 1991), (Yung 1991).

Outage Probability Analysis in Rician Fading Channels

Based on the above definition, the outage probability for the desired user i can be evaluated by

$$\begin{aligned} P_{out} &= P_r\,[\,\{P_b(\Psi,\gamma_{0i}) > P_e\}\,] \\ &= E_{\Psi}\{E_{\gamma_{0i}}\{U[P_b(\Psi,\gamma_{0i}) - P_e]\,|\,\Psi\}\} \\ &= E_{\Psi}[\,P_{out}(\Psi)\,] \end{aligned} \tag{7.58}$$

Given Ψ, $P_b(\Psi, \gamma_{0i})$ is a monotonically decreasing function of γ_{0i}. Therefore, the event $\{P_b(\Psi,\gamma_{0i}) > P_e\}$ is equivalent to $\{\gamma_{0i} < \Gamma(\Psi, P_e)\}$, where the threshold $\Gamma(\Psi, P_e)$ is a function of Ψ, P_e, and the modulation scheme. From (7.24), the threshold, $\Gamma(\Psi, P_e)$, for BPSK is

$$\Gamma(\Psi, P_e)_{BPSK} = \sqrt{\Psi}\mathbf{Q}^{-1}(P_e) \tag{7.59}$$

where $\mathbf{Q}^{-1}(x)$ denotes the inverse function of $\mathbf{Q}(x)$. Similarly, from (7.39), the threshold, $\Gamma(\Psi, P_e)$, for DPSK is

$$\Gamma(\Psi, P_e)_{DPSK} = \sqrt{2\Psi \ln(1/2P_e)} \tag{7.60}$$

Thus, the conditional outage probability, $P_{out}(\Psi)$, in a Rician fading channel can be found by

$$\begin{aligned} P_{out}(\Psi) &= \int_0^{\Gamma(\Psi,P_e)} f_{\gamma_{0i}}(y)\,dy \\ &= 1 - \int_{\Gamma(\Psi,P_e)}^{\infty} \frac{y}{\sigma_s^2}\exp\left(-\frac{y^2+\alpha^2}{2\sigma_s^2}\right) I_0\left(\frac{\alpha y}{\sigma_s^2}\right) dy \end{aligned}$$

$$= 1 - \mathbf{Q}\left[\left(\frac{\alpha}{\sigma_s}\right), \frac{\Gamma(\Psi, P_e)}{\sigma_s} \right]$$
$$= 1 - \mathbf{Q}\left[\sqrt{2K}, \sqrt{2(K+1)}\,\Gamma(\Psi, P_e) \right] \quad (7.61)$$

If $K = 0$, i.e., no specular component exists, the conditional outage probability in a Rayleigh channel becomes

$$P_{out}(\Psi) = 1 - \exp[\, -\Gamma^2(\Psi,\, P_e)\,] \quad (7.62)$$

As in section 7.2.2, we can apply the Monte Carlo integration method to compute the average outage probability. Meanwhile, the outage probability based on the SGA approach is

$$P_{out}^{G} = P_{out}(\mu_\psi)$$
$$= 1 - \mathbf{Q}\left[\sqrt{2K}, \sqrt{2(K+1)}\,\Gamma(\mu_\psi, P_e) \right] \quad (7.63)$$

Outage Probability Analysis in Nakagami Fading Channels

In this section, we will derive the outage probability for both BPSK and DPSK signals in a Nakagami fading channel. The conditional outage probability $P_{out}(\Psi)$ can be evaluated by the same procedure as the one shown earlier. Thus,

$$P_{out}(\Psi) = P_r\,[\, P_b(\Psi, \gamma_{0i}) > P_e \,]$$
$$= P_r\,[\, \gamma_{0i} < \Gamma(\Psi, P_e) \,]$$
$$= P_r\left[\, \tilde{\gamma}_{0i} < \Gamma^2(\Psi,\, P_e) \,\right] \quad (7.64)$$

where the random variable $\tilde{\gamma}_{0i}$ which is equal to γ_{0i}^2 follows a Gamma distribution with pdf given by

$$f_{\tilde{\gamma}}(y) = \frac{m^m y^{m-1}}{\Gamma(m)} \exp(-my)\, U(y) \quad (7.65)$$

and the threshold, $\Gamma(\Psi,\, P_e)$, is the same as those in (7.59) and (7.60) for BPSK and DPSK modulation schemes, respectively. The reason that we use the variable, $\tilde{\gamma}_{0i}$, instead of γ_{0i} to

compute the conditional outage probability is due to its analytical convenience. Hence, the conditional outage probability, $P_{out}(\Psi)$, can be found by

$$\begin{aligned} P_{out}(\Psi) &= \int_0^{\Gamma^2(\Psi,P_e)} \frac{m^m y^{m-1}}{\Gamma(m)} \exp(-my)\, dy \\ &= \frac{1}{\Gamma(m)} \int_0^{m\Gamma^2(\Psi,P_e)} \exp(-t) t^{m-1}\, dt \\ &= [\, m, \Gamma^2(\Psi, P_e)\,] \end{aligned} \tag{7.66}$$

where (a, x) is an incomplete Gamma function which is defined by 6.5.1 in (Abramowitz et al. 1964) as follows

$$(a, x) = \frac{1}{\Gamma(a)} \int_0^x \exp(-t) t^{a-1}\, \boldsymbol{dt} \tag{7.67}$$

Suppose that the fade parameter, $\boldsymbol{m}$, is an integer. Then, the conditional outage probability $P_{out}(\Psi)$ can be simplified as follows

$$P_{out}(\Psi) = 1 - \exp[\, -m\Gamma^2(\Psi, P_e)\,] \left\{ \sum_{j=0}^{m-1} \frac{[\, m\Gamma^2(\Psi, P_e)\,]^j}{j!} \right\} \tag{7.68}$$

where we have applied the formula (6.5.13 in (Abramowitz et al. 1964))

$$(m, x) = 1 - \exp(-x) \sum_{j=0}^{m-1} \frac{x^j}{j!} \tag{7.69}$$

If $m = 1$, then $P_{out}(\Psi) = 1 - \exp[\, -\Gamma^2(\Psi, P_e)\,]$ which coincides with the result in (7.62).

Finally, the conditional outage probability, $P_{out}(\Psi)$, of systems employing BPSK and DPSK modulation schemes in Rician and Nakagami fading channels are summarized as follows.

- Rician Fading:

$$P_{out}(\Psi) = 1 - \mathbf{Q}\left[\sqrt{2K},\ \sqrt{2(K+1)}\, \Gamma(\Psi,\ P_e) \right]$$

- Nakagami Fading:

  - $\boldsymbol{m}$ is not an integer:

$$P_{out}(\Psi) = \frac{1}{\Gamma(m)} \int_0^{m\Gamma^2(\Psi,P_e)} \exp(-t) t^{m-1}\, \boldsymbol{dt}$$

– m is an integer:

$$P_{out}(\Psi) = 1 - \exp[\,-m\Gamma^2(\Psi, P_e)\,] \left\{ \sum_{j=0}^{m-1} \frac{[\,m\Gamma^2(\Psi, P_e)\,]^j}{j!} \right\}$$

where $\Gamma(\Psi, P_e)$ is equal to $\sqrt{\Psi}\mathbf{Q}^{-1}(P_e)$ for BPSK signals and is equal to $\sqrt{2\Psi \ln(1/2P_e)}$ for DPSK signals.

Numerical Evaluation of the Outage Probability

In this section, the outage probability as a function of the number of active users N is evaluated. Unless otherwise noted, the analytical parameters and assumptions, such as the spreading ratio, the chip waveform, etc, are the same as those used in section 7.2.2.

The outage probability versus N for $N_c = 1$ with $P_e = 10^{-3}$ in a Rician fading channel is shown in figure 7.22 when DPSK modulation is employed. We find that P_{out}^G may become the upper bound of P_{out} when N is large, because the mean value of the conditional variance, μ_ψ, of the total interference is in the concave region of $P_{out}(\,\Psi)$. We can verify this result by applying Jensen's inequality. The outage probability for DPSK as a function of N for $N_c = 2$ in a Rician fading channel is shown in figure 7.23. If we define the system capacity as the maximum number of active users per cell, so that the BER will only exceed 10^{-3} a small fraction of time (e.g., 0.01), the system capacity is 10 for $N_c = 1$ and 40 for $N_c = 2$ with $K = 13$ dB. Figures 7.24 and 7.25 illustrate the outage probability of BPSK for $N_c = 1$ and 2 in a Rician channel. Based on the same criterion, the user capacity becomes 14 for $N_c = 1$ and 54 for $N_C = 2$.

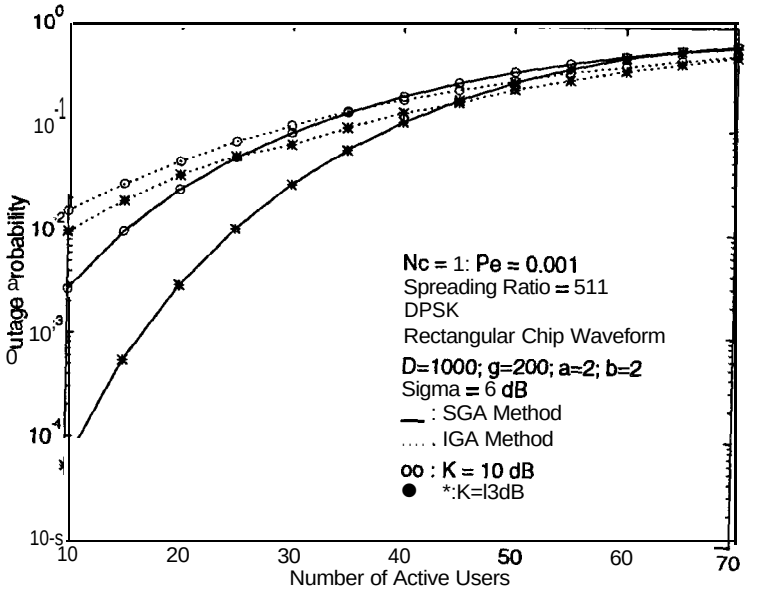

Figure 7.22: Outage Probability versus N for DPSK in a Rician Fading Channel ($N_c = 1$)

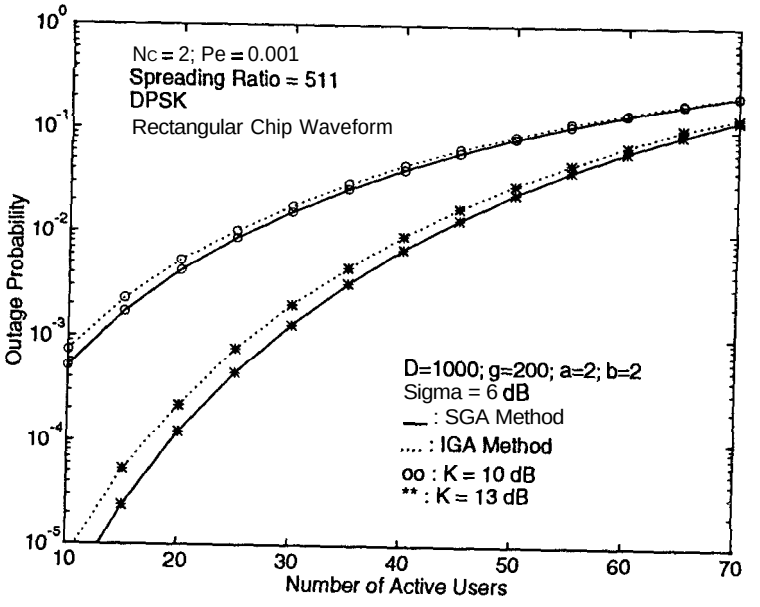

Figure 7.23: Outage Probability versus N for DPSK in a Rician Fading Channel ($N_c = 2$)

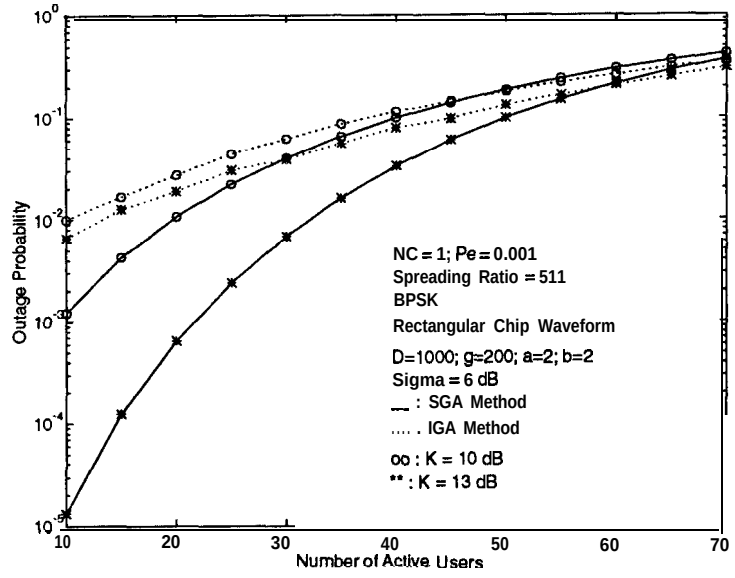

Figure 7.24: Outage Probability versus N for BPSK in a Rician Fading Channel ($N_c = 1$)

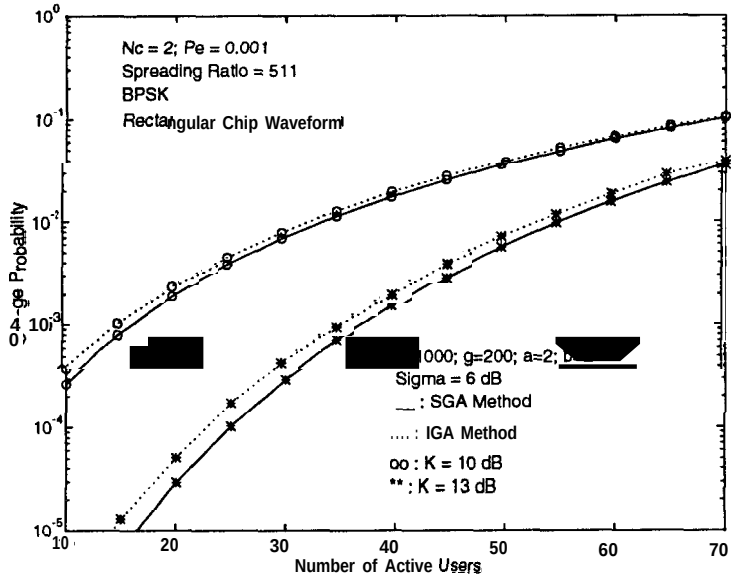

Figure 7.25: Outage Probability versus N for BPSK in a Rician Fading Channel ($N_c = 2$)

7.2.4 Packet Success Rate Analysis

In this section, we will evaluate the packet success rate (PSR) for DS/CDMA systems in a shadowed Rician or Nakagami fading channel. Because of the varying long-term property of the shadowing, we assume that it varies slowly compared to the packet interval. Furthermore, the relative delay $\{\tau_{kn}\}$ between interfering users and the desired user is also assumed to be fixed over the whole packet duration. For the multipath fading, two extreme cases, i.e., slow and fast fading, are considered. The classification of a channel as slow or fast is based on the comparison of the *coherent time*[2] of the channel and the packet duration. When the former is significantly larger then the latter, the channel is classified as slow fading. In slow fading channels, the faded amplitude and phase (i.e., χ_{kn} and Φ_{kn}) of the received signals remain constant throughout the whole packet interval. On the other hand, the faded amplitude and phase vary independently from bit to bit if fast fading is assumed.

PSR Analysis in Slow Fading Channels

We assume that a packet of L bits is transmitted over a memoryless binary communication channel with BER equal to P_b. If the packet has some error correction capabilities and is able to correct t or fewer errors, then, assuming bit-to-bit independence, the PSR becomes

$$P_S = \sum_{l=0}^{t} \binom{L}{l} P_b^l (1-P_b)^{L-l} \triangleq g(P_b; L, t) \quad . \tag{7.70}$$

As mentioned in section 7.2.2, if all the signature sequences are completely random, the spreading ratio is sufficiently large, and the random vectors $\underline{\chi}$, $\underline{\gamma}$, $\underline{\Phi}$, and $\underline{S}$ are fixed, MAI can be accurately modeled by a Gaussian random variable. Furthermore, the BER will be conditional independent from bit to bit within the desired packet (Morrow et al. 1989). Hence, the conditional PSR can be found by using (7.70) and the average PSR can be calculated by averaging over these random vectors.

[2]The coherent time of a channel is usually approximated by the reciprocal of the channel Doppler spread which, in turn, is defined as the width of the power spectrum as a function of the Doppler frequency.

We also assume that the random vectors χ_{kn}, γ_{kn}, Φ_{kn}, and S_{kn} are randomly selected at the beginning of a desired packet and remain constant in the duration of the whole packet. The conditional PSR[3], $P_S(\Psi, \gamma_{0i})$, can be written as follows

$$P_S(\Psi, \gamma_{0i}) = g[\, P_b(\Psi, \gamma_{0i}); L, t\,] \tag{7.71}$$

where the conditional BER (see section 7.2.2), $P_b(\Psi, \gamma_{0i})$, for BPSK and DPSK modulations is $\mathbf{Q}\left(\gamma_{0i}/\sqrt{\Psi}\right)$ and $\frac{1}{2}\exp\left(-\gamma_{0i}^2/2\Psi\right)$, respectively.

By averaging over the faded amplitude of the desired user, γ_{0i}, we can calculate the conditional PSR, $P_S(\Psi)$. For Rician fading, $P_S(\Psi)$ is

$$\begin{aligned} P_S(\Psi) &= E_{\gamma_{0i}}\{\, g[\, P_b(\Psi, \gamma_{0i}); L, t \quad]\ \} \\ &= \int_0^\infty g[\ P_b(\Psi, y); L, t\ ]\, 2(K+1)\, y \exp[-(K+1)y^2 - K] \cdot \\ &\quad I_0\left[\ \sqrt{4K(K+1)}y\ \right] dy \\ &= \int_0^\infty g\quad [\, P_b\left(\Psi, \sqrt{\frac{z}{K+1}}\right); L, t\ \Big]\, I_0\left[\sqrt{4Kz}\ \right] \exp(-z-K)\, dz \end{aligned} \tag{7.72}$$

Given Ψ, the Gaussian Quadrature Rule with Laguerre polynomials can be used to find the numerical results (25.4.45 in (Abramowitz et al. 1964)). Thus, the conditional PSR, $P_S(\Psi)$, as a function of the conditional variance of the total interference, Ψ, becomes

$$P_S(\Psi) = \sum_{j=1}^{N_L} w_j\, g\left[\ P_b\left(\Psi, \sqrt{\frac{x_j}{K+1}}\right); L, t\ \right] \exp(-K)\, I_0\left[\ \sqrt{4Kx_j}\ \right] + R_m \tag{7.73}$$

The weight w_j and the abscissa x_j can be calculated by employing the IMSL scientific program for arbitrary N_L-point integration. The remainder R_m is sufficiently small for N_L in the range of 15 – 20. A similar method can be applied to evaluate the conditional PSR in a Nakagami fading channel which is

$$\begin{aligned} P_S(\Psi) &= \int_0^\infty g[\, P_b(\Psi, y)\,] \frac{2m^m y^{2m-1}}{\Gamma(m)} \exp(-my^2)\, dy \\ &= \frac{1}{\Gamma(m)} \sum_{j=1}^{N_L} w_j\, g\left[\ P_b\left(\Psi, \sqrt{\frac{x_j}{m}}\right); L, t\ \right] x_j^{m-1} + R_m \end{aligned} \tag{7.74}$$

[3]For **DPSK signals, the conditional PSR calculated by using equation (7.71) is just an approximation, because of the dependent nature of the occurrence of errors (they tend to occur in pairs) (Roberts et al. 1980).**

Finally, the unconditional PSR can be found by

$$P_S = E_{\Psi}\{ P_S(\Psi) \} \tag{7.75}$$

and the average packet error rate (PER), P_E, is $(1 - P_S)$.

PSR Analysis in Fast Fading Channels

In the case of fast fading, the channel variations are fast relative to the packet interval. We assume that the random vectors $\underline{\gamma}$ and $\underline{\Phi}$ vary independently from bit to bit. However, the random vectors $\underline{\chi}$ and $\underline{S}$ remain constant throughout the whole packet. Because DPSK signals can be employed only when the phase of the received signals varies slowly at least for two successive bit intervals, we will focus on the BPSK signals in the following discussion.

In order to make the problem tractable, we assume that the total interference $_T$ (defined in (7.13)) can still be approximated by a Gaussian random variable, if the random vectors $\underline{\chi}$ and $\underline{S}$ are fixed. This approximation has been shown to be correct if the number of active users N is large enough. Using the results that the second moment of γ_{ij} is equal to one and $E(\Phi_{ij}^2) = 1/2$, the conditional variance Ψ_{FF} of $_T$ for fast fading can be evaluated by

$$\begin{aligned}
\Psi_{FF} &= \mathbf{Var}\left[{}_T \,|\, \underline{\chi}, \underline{S} \right] \\
&= \frac{\mathcal{N}_0}{2E_b} + \sum_{n=1, n\neq i}^{N_0} \chi_{0n} W_{0n} E\,(\gamma_{0n}^2) E\,[\cos^2(\Phi_{0n})] \\
&\quad + \sum_{k=1}^{K} \sum_{n=1}^{N_k} \chi_{kn} W_{kn} E\,(\gamma_{kn}^2) E\,[\cos^2(\Phi_{kn})] \\
&= \frac{\mathcal{N}_0}{2E_b} + \sum_{n=1, n\neq i}^{N_0} \frac{\chi_{0n} W_{0n}}{2} + \sum_{k=1}^{K} \sum_{n=1}^{N_k} \frac{\chi_{kn} W_{kn}}{2}
\end{aligned} \tag{7.76}$$

Therefore, the conditional PSR, $P_S(\Psi_{FF})$, for fast fading can be evaluated as follows

$$P_S(\Psi_{FF}) = g\left[P_b(\Psi_{FF}); L, t \right] \tag{7.77}$$

where the conditional BER, $P_b(\Psi_{FF})$, is

$$P_b(\Psi_{FF}) = E_{\gamma_{0i}}\left[P_b(\Psi_{FF}, \gamma_{0i}) \right] \tag{7.78}$$

which is equal to (7.26) for Rician fading and is equal to (7.50) for Nakagami fading with Ψ replaced by Ψ_{FF}. Similarly, the unconditional PSR can be found by

$$P_S = E_{\Psi_{FF}}\{ P_S(\Psi_{FF}) \} \tag{7.79}$$

Numerical Evaluation of the PSR

In this section, the packet error rate is evaluated as a function of the number of active users N. The PER results as a function of N for BPSK signals for slow and fast Rician fading are illustrated in figures 7.26 and 7.27, with parameters $L = 100$ bits, $\sigma = 6$ dB, and spreading ratio=511. Both $N_c = 1$ and 2 cases are considered. We also demonstrate the power of error correcting coding for t=1 and 3 bits versus t=0. It can be seen that, without coding, slow fading yields better PER performance than fast fading. This is because the bit errors randomly spread over all packets, for fast fading. Hence, the packet will be decoded incorrectly even though only one bit is in error. In the case of slow fading, errors appear in bursts. Compared to fast fading, there is a certain amount of packets which have a higher PSR. If error control coding is used, the PER is significantly improved for fast fading. For slow fading, error control coding is less effective, because there are less packets with up to t errors that can be corrected. To investigate the effect of σ on the PER performance, we plot the PER versus N with $\sigma = 4$ dB in figure 7.28 for slow fading and in figure 7.29 for fast fading. We can observe that σ has large influence on the PER in fast fading channels, when N_c=1 and error control coding is used.

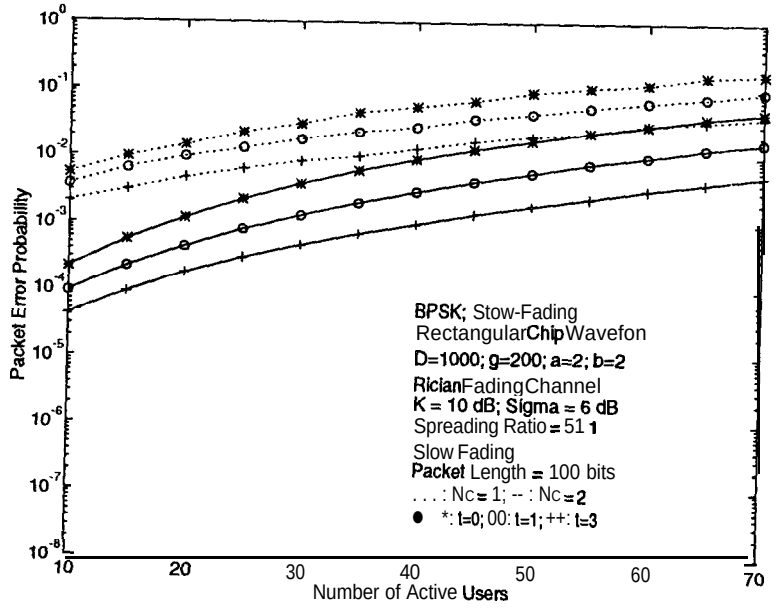

Figure 7.26: Packet Error Probability versus N for BPSK in a Slow Rician Fading Channel, using the IGA Method

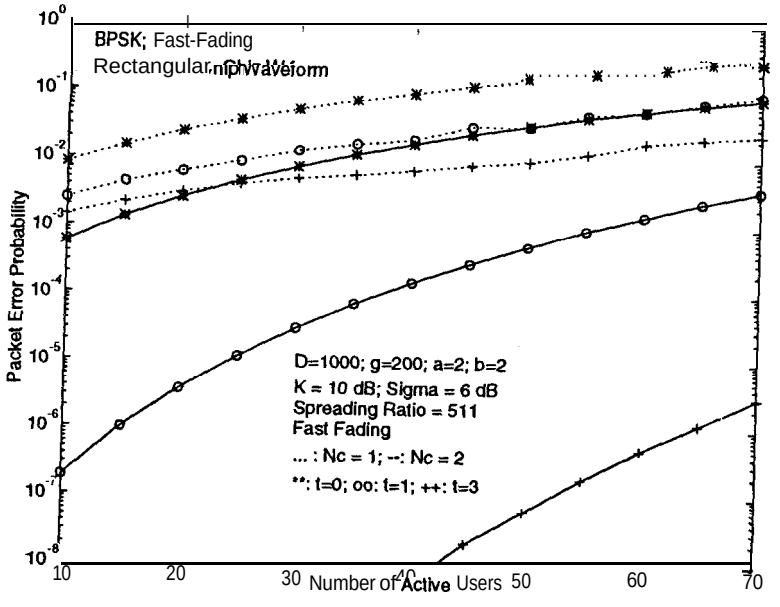

Figure 7.27: Packet Error Probability versus N for BPSK in a Fast Rician Fading Channel, using the IGA Method

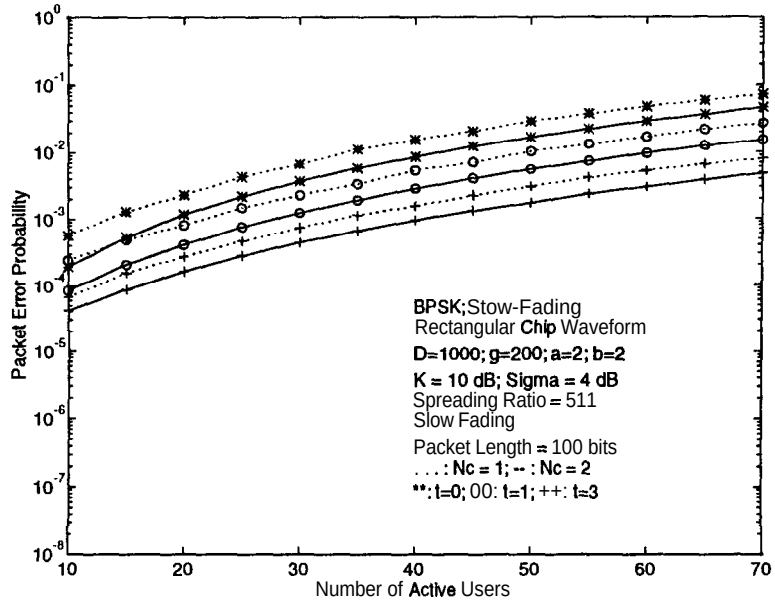

Figure 7.28: Packet Error Probability versus N for BPSK in a Slow Rician Fading Channel, using the IGA Method

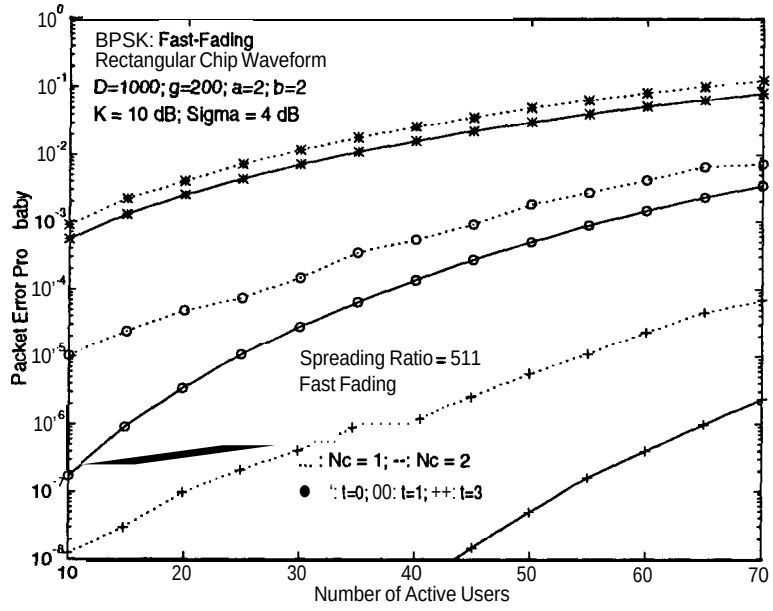

Figure 7.29: Packet Error Probability versus N for BPSK in a Fast Rician Fading Channel, using the IGA Method

7.3 Downlink Performance Analysis

7.3.1 System Model

In this section, we will evaluate the downlink (base station to vehicle) performance of asynchronous DS/CDMA systems in a microcellular environment. The performance measures of interest are the BER and the outage probability. In the downlink, broadcast operation mode is assumed in which several distinct messages or a common message are transmitted simultaneously from a BS to different vehicles. The system and channel models are similar with those described in section 7.2.1. We assume that all signals from the same BS will undergo multipath fading (Rician or Nakagami) with log-normally distributed shadowing. However, the composite signal from each BS is assumed to fade independently. Therefore, the received signal at the desired user $0i$ in the tagged cell, denoted by cell 0, can be expressed as

$$\begin{aligned} r_{0i}(t) &= \sum_{n=1}^{N_0} \sqrt{2P_0 L_p(r_{0i})\, l_0}\, \gamma_0\, a_{0n}(t-\tau_{0n})\, b_{0n}(t-\tau_{0n}) \cos(2\pi f_c t + \Phi_{0n}) \\ &+ \sum_{k=1}^{K} \sum_{n=1}^{N_k} \sqrt{2P_0 L_p(r_{ki})\, l_k}\, \gamma_k a_{kn}(t-\tau_{kn})\, b_{kn}(t-\tau_{kn}) \cos(2\pi f_c t + \Phi_{kn}) \\ &+ n(t) \end{aligned} \tag{7.80}$$

where $L_p(r)$ is the path loss described by the propagation law in (7.2) with r_{ki} the distance between the BS of cell k and the desired user in cell 0; $a_{kn}(t)$ and $b_{kn}(t)$ are the data and the spreading waveforms, respectively, of the n^{th} user in cell k; l_k and γ_k represent the log-normally distributed shadowing and the multipath fading; τ_{kn} and Φ_{kn} are the random delay and phase, respectively. We assume that the spreading codes $(\{a_j^{(kn)}\})$, the information sequences $(\{b_j^{(kn)}\})$, the random delays $(\{\tau_{kn}\})$, the random phases $(\{\Phi_{kn}\})$, the shadowing $(\{l_k\})$, and the multipath fading $(\{\gamma_k\})$ are mutually independent. Furthermore, we also assume that the users are uniformly distributed in cells and the noise $n(t)$ is AWGN with two-sided power spectral density $\mathcal{N}_0/2$.

7.3.2 Bit Error Rate Analysis

BER Analysis in Rician Fading Channels

In this subsection, we will evaluate the BER for an asynchronous DS/CDMA system with Rician fading and log-normally distributed shadowing. We assume that the receiver can perfectly track the phase and the time delay of the desired user. Since only the relative delays and phases between the desired user and the interfering users are important, we can set $\tau_{0i} = \Phi_{0i} = 0$, without loss of generality. The correlator receiver is the same as that in figure 7.2 and the normalized sample signal at the output of the correlator is

$$\begin{aligned}\xi_{0i} &= \frac{1}{\sqrt{2P_0TL_p(r_{0i})}}\int_0^T r_{0i}(t)2a_{0i}(t)\cos(2\pi f_c t)\,dt \\ &= \sqrt{l_0\gamma_0^2}+\sqrt{l_0\gamma_0^2}\left[\sum_{n=1,n\neq i}^{N_0}\cos(\Phi_{on})W_{on}\right] \\ &\quad +\sum_{k=1}^{K}\sqrt{\frac{L_p(r_{ki})}{L_p(r_{0i})}}\sqrt{l_k\gamma_k^2}\left[\sum_{n=1}^{N_k}\cos(\Phi_{kn})W_{kn}\right]+n \end{aligned} \tag{7.81}$$

where $l_k = 10^{X_k/10}$, $k = 0,\ldots,K$, with X_k being a zero-mean Gaussian random variable with variance σ_k^2; γ_k is a normalized Rician distributed random variable with pdf given in *(7.4)*; n is the AWGN with variance $\sigma_{th}^2 = \mathcal{N}_0/[2E_bL_p(r_{0i})]$; and W_{kn} is given in (7.14).

In order to simplify the notation, we define

$$P_k = \frac{L_p(r_{ki})}{L_p(r_{0i})} \text{ and } \mathcal{L}_k = P_k l_k \gamma_k^2$$

where $P_0 = 1$. Therefore, the correlator output, ξ_{0i}, can be expressed as

$$\begin{aligned}\xi_{0i} &= \sqrt{\mathcal{L}_0}+\sqrt{\mathcal{L}_0}\left[\sum_{n=1,n\neq i}^{N_0}\cos(\Phi_{on})W_{on}\right]+\sum_{k=1}^{K}\sqrt{\mathcal{L}_k}\left[\sum_{n=1}^{N_k}\cos(\Phi_{kn})W_{kn}\right]+n \\ &= \sqrt{\mathcal{L}_0}+I_T \end{aligned} \tag{7.82}$$

where the total interference, I_T, consists of the AWGN and the MAI from users in the same cell as well as from those in other cells.

Let us define the random vectors $\underline{\mathcal{L}}$, $\underline{\Phi}$, and $\underline{S}$ as

$$\underline{\mathcal{L}} = (\mathcal{L}_0,\ldots,\mathcal{L}_K)$$

$$\underline{\Phi} = (\Phi_{0,1}, \ldots, \Phi_{0,i-1}, \Phi_{0,i+1}, \ldots, \Phi_{0,N_0}, \Phi_{1,1}, \ldots, \Phi_{K,N_K})$$
$$\underline{S} = (S_{0,1}, \ldots, S_{0,i-1}, S_{0,i+1}, \ldots, S_{0,N_0}, S_{1,1}, \ldots, S_{K,N_K})$$

In order to employ the IGA method for BER calculation, we need to find the conditional variance Ψ of $_T$, which is

$$\begin{aligned}
\Psi &= \mathbf{Var}(_T \mid \underline{\mathcal{L}}, \underline{\Phi}, \underline{S}) \\
&= \sigma_{th}^2 + \mathcal{L}_0 \left\{ \sum_{n=1, n\neq i}^{N_0} \cos^2(\Phi_{0n}) \frac{\eta}{T^2} \left[R_\psi^2(S_{0n}) + \hat{R}_\psi^2(S_{0n}) \right] \right\} \\
&\quad + \sum_{k=1}^{K} \mathcal{L}_k \left\{ \sum_{n=1}^{N_k} \cos^2(\Phi_{kn}) \frac{\eta}{T^2} \left[R_\psi^2(S_{kn}) + \hat{R}_\psi^2(S_{kn}) \right] \right\} \\
&= \sigma_{th}^2 + \mathcal{L}_0 Z_0 + \sum_{k=1}^{K} \mathcal{L}_k Z_k \\
&= \sigma_{th}^2 + \mathcal{L}_0 Z_0 + \Psi_{oth}
\end{aligned} \tag{7.83}$$

where the random variables Z_0, Z_k, $k = 1, \ldots, K$, and the conditional variance of the other-cell interference Ψ_{oth} are given by

$$\begin{aligned}
Z_0 &= \sum_{n=1, n\neq i}^{N_0} \cos^2(\Phi_{0n}) \frac{\eta}{T^2} \left[R_\psi^2(S_{0n}) + \hat{R}_\psi^2(S_{0n}) \right] \\
Z_k &= \sum_{n=1}^{N_k} \cos^2(\Phi_{kn}) \frac{\eta}{T^2} \left[R_\psi^2(S_{kn}) + \hat{R}_\psi^2(S_{kn}) \right] \\
\Psi_{oth} &= \sum_{k=1}^{K} \mathcal{L}_k Z_k
\end{aligned}$$

Note that the term $\mathcal{L}_0 Z_0$ represents the MAI from the tagged cell. Since the shadowing fades in unison for users in the same cell, the faded amplitude of the desired user and the total interference are dependent. This situation is totaly different from that in the uplink.

As mentioned before, given the random vectors $\underline{\mathcal{L}}$, $\underline{\Phi}$, and $\underline{S}$, $_T$ can be accurately modeled a Gaussian random variable (Morrow et al. 1989). Hence, for the system employing BPSK modulation, the conditional BER can be written as

$$P_b(\mathcal{L}_0, Z_0, \Psi_{oth}) = \mathbf{Q}\left(\sqrt{\frac{\mathcal{L}_0}{\sigma_{th}^2 + \mathcal{L}_0 Z_0 + \Psi_{oth}}} \right) \tag{7.84}$$

In the following analysis, we assume that the AWGN can be ignored when compared to the MAI, regardless of the location of the user within the cell. This results from the fact that the microcellular environment is usually interference-limited (Milstein et al. 1992). Hence, the conditional BER can be approximated by

$$P_b(\mathcal{L}_0, Z_0, \Psi_{oth}) = \mathbf{Q}\left(\sqrt{\frac{\mathcal{L}_0}{\mathcal{L}_0 Z_0 + \Psi_{oth}}}\right) \tag{7.85}$$

Therefore, we can evaluate the average BER by

$$P_b = E_{\mathcal{L}_0, Z_0, \Psi_{oth}}[\, P_b(\mathcal{L}_0, Z_0, \Psi_{oth})\,] \tag{7.86}$$

The composite pdf of the log-normal non-central chi-square distribution $\mathcal{L}_0$ is (see Appendix C)

$$\begin{aligned} f_{\mathcal{L}_0}(y) &= \frac{(K+1)}{\sqrt{\pi}} \exp(-K) \int_{-\infty}^{\infty} \exp(-A_0 x) \exp\left[-(K+1) y e^{-A_0 x}\right] \cdot \\ &\quad I_0\left[\sqrt{4K(K+1) y \exp(-A_0 x)}\right] \exp\left(-x^2\right) dx \end{aligned} \tag{7.87}$$

where $A_0 = \sqrt{2}\lambda\sigma_0$ and $\lambda = \ln 10/10$. Let $\sigma_0 = 0$, this pdf becomes a non-central chi-square distribution as described in (C.3). We can use the Gauss-Hermit method (Abramowitz et al. 1964) to find the pdf of $\mathcal{L}_0$.

$$\begin{aligned} f_{\mathcal{L}_0}(y) = \frac{(K+1)}{\sqrt{\pi}} \exp(-K) \sum_{j=1}^{N_{H1}} w_j \exp(-A_0 x_j) \exp\left[-(K+1) y \exp(-A_0 x_j)\right] \cdot \\ I_0\left[\sqrt{4K(K+1) y \exp(-A_0 x_j)}\right] + R_m \end{aligned} \tag{7.88}$$

where w_j and x_j are the weights and the abscissa associated with the Hermit polynomials which can be evaluated using the IMSL program for arbitrary N_{H1}-point integration. The remainder R_m can be reduced, increasing the value of N_{H1}.

Averaging the conditional BER given in (7.86) over $\mathcal{L}_0$, we have

$$\begin{aligned} P_b(Z_0, \Psi_{oth}) &= E_{\mathcal{L}_0}[\, P_b(\mathcal{L}_0, Z_0, \Psi_{oth})\,] \\ &= \frac{(K+1)}{\sqrt{\pi}} \exp(-K) \sum_{j=1}^{N_{H1}} w_j \exp(-A_0 x_j) \cdot \\ &\quad \int_0^{\infty} \mathbf{Q}\left(\sqrt{\frac{y}{y Z_0 + \Psi_{oth}}}\right) \exp\left[-(K+1) y e^{-A_0 x_j}\right] \cdot \\ &\quad I_0\left[\sqrt{4K(K+1) y \exp(-A_0 x_j)}\right] dy \end{aligned} \tag{7.89}$$

Manipulating the above equation by changing the variable and applying the Gauss-Laguerre integration method (Abramowitz et al. 1964), we can approximate $P_b(Z_0, \Psi_{oth})$ by

$$P_b(Z_0, \Psi_{oth}) \approx \frac{\exp(-K)}{\sqrt{\pi}} \sum_{j=1}^{N_{H1}} w_j \left\{ \sum_{k=1}^{N_L} \tilde{w}_k \mathbf{Q} \left[\sqrt{\frac{\left(\frac{\tilde{x}_k}{K+1}\right) \exp(A_0 x_j)}{Z_0 \left(\frac{\tilde{x}_k}{K+1}\right) \exp(A_0 x_j) + \Psi_{oth}}} \right] \cdot I_0\left(\sqrt{4K\tilde{x}_k}\right) \right\} \tag{7.90}$$

Therefore, we can avoid the original two-order integration by a two-layer summation which can substantially reduce the computation complexity and still preserves satisfactory accuracy. Finally, the average BER can be calculating by averaging $P_b(Z_0, \Psi_{oth})$ over the random variables Z_0 and Ψ_{oth}. One practical way is to use the Monte Carlo integration method. That is,

$$P_b = \lim_{M \to \infty} \frac{1}{M} \sum_{j=1}^{M} P_b[(Z_0)_j, (\Psi_{oth})_j] \tag{7.91}$$

We denote this approach as the IGA-MC method. However, with some approximations, we can analytically evaluate the average BER. These approximations are

1. If the number of users N_k is large enough, Z_0 and Z_k can be approximated by their mean value. That is

$$Z_0 \approx C_0 = \boldsymbol{E}(Z_0) = \frac{(N_0 - 1)m_\psi}{\eta}$$

and

$$Z_k \approx C_k = \boldsymbol{E}(Z_k) = \frac{N_k m_\psi}{\eta}$$

The accuracy of this approximation has been validated in figure 7.18 which illustrates that the spatial distribution and the shadowing play the dominant role in the BER calculation.

2. We show in Appendix D that if $\sigma_k \geq 4$ dB and $K \geq 7$ dB then, $\mathcal{L}_k$ can be approximated by a log-normally distributed random variable. In order to maintain accuracy, we still treat the desired signal (i.e., $\mathcal{L}_0$) as a composite log-normal noncentral chi-square.

3. The sum of a finite number of uncorrelated log-normal random variables can be approximated, at least the first order moment, by another log-normal probability distribution (Janos 1970), (Panter 1972). This approximation is in close agreement with the results of the Monte Carlo simulation in the range of 0.1 to 99 percent of the cumulative distribution function (Schwartz et al. 1982). Using the above assumption, Schwartz and Yeh (Schwartz et al. 1982) have developed a recursive procedure for an approximation of the mean and variance of the sum of a number of uncorrelated log-normal random variables. This method has been widely used in the performance analysis of mobile cellular communication systems. We present this method in Appendix E.

Based on the above assumptions, the conditional BER given in (7.90), becomes

$$\begin{aligned} P_b(Z_0,\ \Psi_{oth}) &\approx P_b(\mathcal{L}_I) \\ &= \frac{\exp(-K)}{\sqrt{\pi}} \sum_{j=1}^{N_{H1}} w_j \left\{ \sum_{k=1}^{N_L} \tilde{w}_k \mathbf{Q}\left[\sqrt{\frac{\left(\frac{\tilde{x}_k}{K+1}\right)\exp(A_0 x_j)}{C_0\left(\frac{\tilde{x}_k}{K+1}\right)\exp(A_0 x_j) + \mathcal{L}_I}} \right] \cdot \right. \\ &\quad \left. I_0\left(\sqrt{4K\tilde{x}_k}\right) \right\} \end{aligned} \tag{7.92}$$

which has been simplified to be a function of the conditional other-cell interference power only, denoted as $\mathcal{L}_I$, and given by

$$\mathcal{L}_I = \sum_{k=1}^{K} C_k \mathcal{L}_k \tag{7.93}$$

and $\mathcal{L}_I$ itself can be also approximated by a log-normal distributed random variable which can be expressed as

$$\mathcal{L}_I = 10^{(m_I + X_I)/10} \tag{7.94}$$

where X_I is zero-mean Gaussian with variance σ_I^2. The values of m_I and σ_I^2 can be found by applying the recursive technique described in Appendix E. The pdf of $\mathcal{L}_I$ is

$$f_{\mathcal{L}_I}(y) = \frac{1}{\sqrt{2\pi}\lambda\,\sigma_I\,y} \exp\left[-\frac{(\ln\ y\ -\lambda m_I)^2}{2\lambda^2\sigma_I^2} \right] U(y) \tag{7.95}$$

where $U(y)$ is the unit step function. Finally , we can find the average BER by

$$\begin{aligned} P_b &= E_{\mathcal{L}_I}[\ P_b(\mathcal{L}_I)\ ] \\ &= \int_0^\infty P_b(y) \frac{1}{\sqrt{2\pi}\sigma_I \lambda y} \exp\left[-\frac{(\ln y - \lambda m_I)^2}{2\lambda^2\sigma_I^2} \right] dy \end{aligned}$$

$$= \frac{1}{\sqrt{\pi}} \int_{-\infty}^{\infty} P_b\left(\tilde{m}_I e^{A_I x}\right) \exp\left(-x^2\right)\, dx$$
$$\approx \frac{1}{\sqrt{\pi}} \sum_{i=1}^{N_{H2}} \hat{w}_i P_b\left(\tilde{m}_I e^{A_I \hat{x}_i}\right) \qquad (7.96)$$

where $A_I = \sqrt{2}\lambda\sigma_I$ and $\tilde{m}_I = \exp(\lambda m_I) = 10^{m_I/10}$.

We denote this approximation method as the IGA-AP method. The advantages of this approach are that we can not only avoid the time-consuming Monte Carlo simulation as required in the IGA-MC method, but also we can use a three-fold summation instead of a three-fold integration to find the average BER. The numerical error can be as small as desired by increasing the numbers of N_{H1}, N_{H2}, and N_L.

The above BER expressions depend on where the desired user is located. When the user moves, its area-average BER can be obtained by averaging over the possible locations of its path traversing the cell.

BER Analysis in Nakagami Fading Channels

In a Nakagami fading channel, the pdf of the composite log-normal Gamma random variable $\mathcal{L}_0$ is (see Appendix C)

$$f_{\mathcal{L}_0}(y) = \frac{m^m y^{m-1}}{\Gamma(m)\sqrt{\pi}} \int_{-\infty}^{\infty} \exp(-mA_0 x) \exp\left[-me^{-A_0 x} y\right] \exp\left(-x^2\right)\, dx$$
$$\approx \frac{m^m y^{m-1}}{\Gamma(m)\sqrt{\pi}} \sum_{j=1}^{N_{H1}} w_j \left\{\exp(-mA_0 x_j) \exp\left[-me^{-A_0 x_j} y\right]\right\} \qquad (7.97)$$

Using the same approach as in the previous section and with some manipulations, the conditional BER becomes

$$P_b(Z_0, \Psi_{oth}) \approx \frac{1}{\Gamma(m)\sqrt{\pi}} \sum_{j=1}^{N_{H1}} w_j \left\{ \sum_{k=1}^{N_L} \tilde{w}_k\, \tilde{x}_k^{m-1} \cdot \right.$$
$$\left. \mathrm{Q}\left[\sqrt{\frac{(\tilde{x}_k/m)\exp(A_0 x_j)}{Z_0\,(\tilde{x}_k/m)\exp(A_0 x_j) + \Psi_{oth}}} \right] \right\} \qquad (7.98)$$

Therefore, the average BER calculated by the IGA-MC method is the same as that in (7.91). As in the case of shadowed Rician channels, the distribution of a composite log-normal Gamma in some operation range can be also approximated by another log-normal distribution (Ho et al. 1993). Hence, we can simplify the conditional BER shown in (7.98) to be only a function of the conditional other-cell interference power $\mathcal{L}_I$. Hence, the average BER evaluated by the IGA-AP method is

$$\begin{aligned} P_b &= E_{\mathcal{L}_I}[P_b(\mathcal{L}_I)] \\ &\approx \frac{1}{\sqrt{\pi}} \sum_{i=1}^{N_{H2}} \hat{w}_i P_b\left(\tilde{m}_I e^{A_I \hat{x}_i}\right) \end{aligned} \tag{7.99}$$

where $P_b(\mathcal{L}_I)$ is given by

$$\begin{aligned} P_b(\mathcal{L}_I) = \frac{1}{\Gamma(m)\sqrt{\pi}} \sum_{j=1}^{N_{H1}} w_j \left\{ \sum_{k=1}^{N_L} \tilde{w}_k \tilde{x}_k^{m-1} \cdot \right. \\ \left. \mathbf{Q}\left[\sqrt{\frac{(\tilde{x}_k/m)\exp(A_0 x_j)}{C_0(\tilde{x}_k/m)\exp(A_0 x_j) + \mathcal{L}_I}} \right] \right\} \end{aligned} \tag{7.100}$$

Numerical Evaluation of the BER

We plot BER as a function of the transversal distance between the desired user and the BS in figure 7.30. Both IGA-MC and IGA-AP methods are used. Although we have made three approximations in the IGA-AP method, its results are very close to those generated by the IGA-MC method. Furthermore, as expected, the worst BER occurs when the desired user is at the boundary between two cells. This is because of the propagation path loss, the desired user in the interior of a given cell experiences a power advantage in the reception of the signal transmitted from its own BS relative to signals transmitted from other BS' in neighboring cells. However, when the user is at the boundary between two cells, this advantage disappears. In (Milstein et al. 1992), the worst BER is used to assess the user capacity. In figure 7.31, we illustrate the worst and the area-averaged BER as a function of N for σ= 4 and 6 dB, respectively. For σ = 4 dB, if a BER of 10^{-3} is required, the system can support about *5 0* users by using the area-averaged BER as the criterion. However, only 13 users can be accommodated based on the worst BER criterion. This is due to the "graceful

degradation" feature of the spread-spectrum technique. Therefore, the worst BER criterion may yield a very pessimistic assessment to the user capacity.

It is also interesting to examine the effect of the Rician factor K on the area averaged BER performance. Figure 7.32 shows the area averaged BER as a function of K for $N = 35$. For larger values of σ, the area averaged BER is less sensitive to the variations of K.

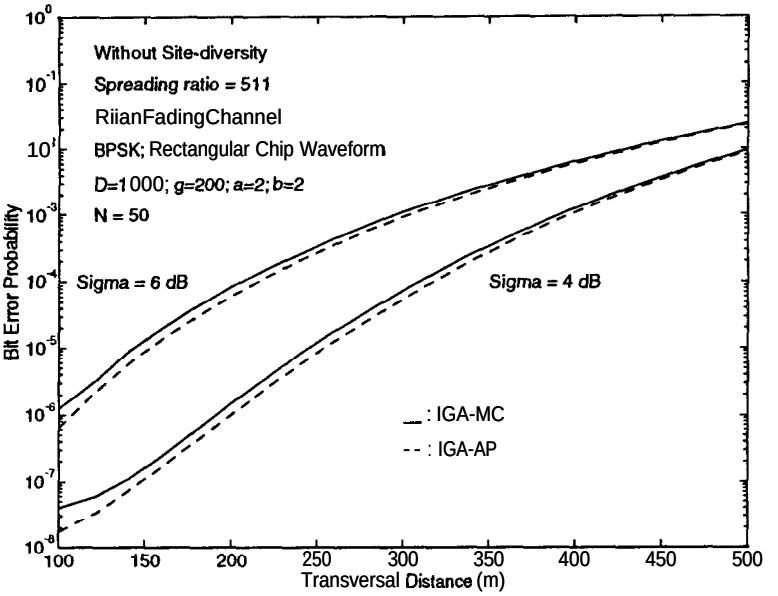

Figure 7.30: BER versus Transverse Distance for $N_c = 1$ in Rician Fading Channels

7.3.3 Outage Probability Analysis

As defined in section 7.2.3, the outage probability is the probability that the instantaneous BER exceeds a specific constant P_e. In order to facilitate the computation, we make the same assumptions as in subsection 7.3.2. These assumptions are: (1) the AWGN can be ignored, *(2)* $Z_k, k = 0 \ldots K$ are approximated by their mean value, (3) the composite log-normal non-central chi-square can be approximated by another log-normal distribution, (4) the sum

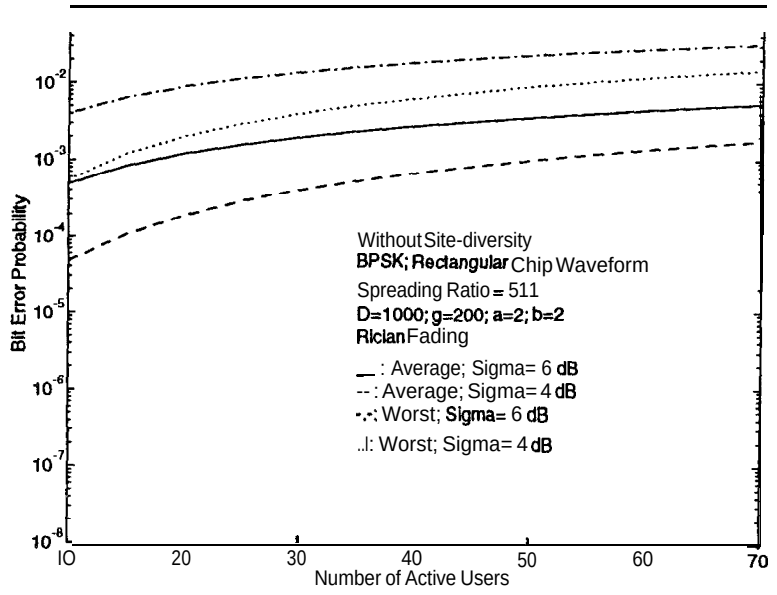

Figure 7.31: Average and Worst BER versus N for $N_c = 1$ in Rician Fading Channels

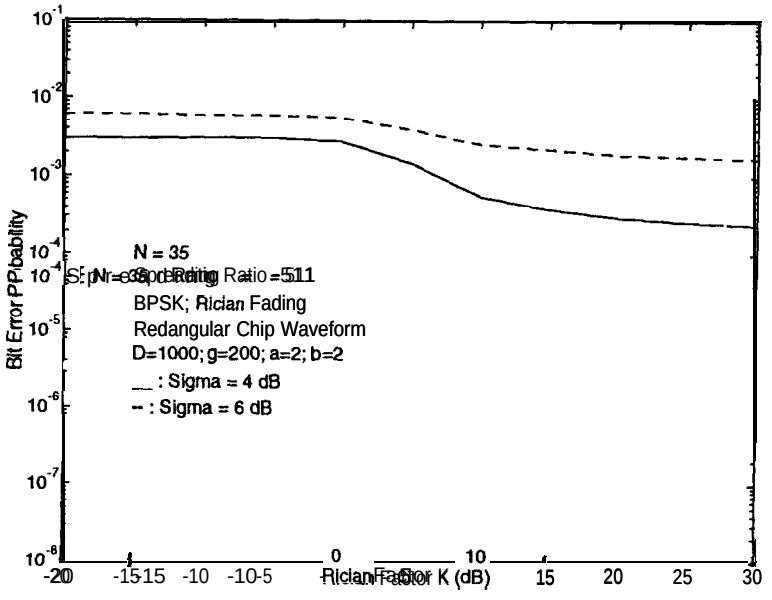

Figure 7.32: Average and Worst BER versus K for $N_c = 1$ in Rician Fading Channels

of a finite number of log-normal random variables can be approximated by another log-normal distribution. Thus, the outage probability for DS/CDMA systems in the downlink is

$$\begin{aligned} P_{out} &= P_r\left(P_b(\mathcal{L}_0,\mathcal{L}_I) > P_e\right) \\ &= P_r\left\{ \mathbf{Q}\left(\sqrt{\frac{\mathcal{L}_0}{C_0\mathcal{L}_0+\mathcal{L}_I}}\right) > P_e \right\} \\ &= P_r\left\{ \frac{\mathcal{L}_0}{C_0\mathcal{L}_0+\mathcal{L}_I} < \left[\mathbf{Q}^{-1}(P_e)\right]^2 \right\} \\ &= P_r\left\{(\Gamma_0 - C_0)\mathcal{L}_0 < \mathcal{L}_I\right\} \end{aligned} \tag{7.101}$$

where $\mathbf{Q}^{-1}(x)$ is the inverse function of the complementary error function and $\Gamma_0 = 1/[\mathbf{Q}^{-1}(P_e)]^2$. Because both $\mathcal{L}_0$ and $\mathcal{L}_I$ are positive, the outage probability can be written as

$$P_{out} = \begin{cases} P_r\{\ \mathcal{L}_0 < \mathcal{L}_I/(\Gamma_0 - C_0)\ \} & , \ \Gamma_0 \geq C_0 \\ 1 & , \ \Gamma_0 < C_0 \end{cases} \tag{7.102}$$

Since $C_0 = (N_{max}-1)m_\psi/\eta$ and C_0 has to be less than Γ_0 so that the outage probability is less than one, given P_e, there will be an inherent user capacity, denoted by N_{max}, such that $C_0 = (N_{max}-1)m_\psi/\eta \leq \Gamma_0$. Therefore, N_{max} is given by

$$N_{max} = \left\lfloor \frac{\eta\Gamma_0}{m_\psi} + 1 \right\rfloor \tag{7.103}$$

where $\lfloor x \rfloor$ is the largest integer which is less than x.

Alternatively, if N_0, η, and m_ψ are determined, we have a lower bound of P_e, denoted by $P_{e,min}$, which is

$$P_{e,min} = \mathbf{Q}^{-1}\left[\sqrt{\frac{\eta}{(N_0-1)m_\psi}}\right] \tag{7.104}$$

Actually, $P_{e,min}$ is the BER without considering the other-cell interference. If the desired P_e is less than $P_{e,min}$, then the outage probability will be one. Next, we will derive the outage probability in the case where the number of users is less than N_{max}. Based on the property that a log-normal random variable divided by another log-normal random variable is still log-normal, we can find the outage probability as

$$P_{out} = P_r\left\{ Lo = l_0\tilde{\gamma}_0 < \frac{\mathcal{L}_I}{\Gamma_0 - C_0} \right\}$$

$$
\begin{aligned}
&= E_{\tilde{\gamma}_0}\left\{ P_r\left[\frac{\mathcal{L}_I}{l_0} > (\Gamma_0 - C_0)\tilde{\gamma}_0 \mid \tilde{\gamma}_0 \right] \right\} \\
&= E_{\tilde{\gamma}_0}\left\{ P_r\left[10^{\frac{m_I + X_I - X_0}{10}} > (\Gamma_0 - C_0)\tilde{\gamma}_0 \mid \tilde{\gamma}_0 \right] \right\} \\
&= E_{\tilde{\gamma}_0}\left\{ P_r\left[X_I - X_0 > \frac{\ln(\Gamma_0 - C_0) + \ln\tilde{\gamma}_0}{\lambda} - m_I \; I \; \tilde{\gamma}_0 \right] \right\} \\
&= E_{\tilde{\gamma}_0}\left\{ \mathbf{Q}\left[\frac{\ln(\Gamma_0 - C_0) + \ln\tilde{\gamma}_0 - \lambda m_I}{\lambda\sqrt{\sigma_0^2 + \sigma_I^2}} \right] \right\}
\end{aligned}
\tag{7.105}
$$

where $\tilde{\gamma}_0 = \gamma_0^2$, $\mathcal{L}_I = 10^{\frac{m_I + X_I}{10}}$ and $l_0 = 10^{X_0/10}$, respectively.

The above expression for the outage probability is the same for Rician and Nakagami fading. For the former, $\tilde{\gamma}_0$ is a non-central chi-square distributed random variable with pdf as in (7.4), whereas for the latter, $\tilde{\gamma}_0$ follows a gamma distribution with pdf as in (C.7). Similarly, the area averaged outage probability can be obtained by averaging over the possible locations when the user travels in the cell.

Figure 7.33 plots the area-averaged outage probability versus N in a Rician fading channel with parameters $P_e = 10^{-3}$, K=10 and 13 dB, and σ=4 and 6 dB, respectively. From figure 7.24 , if the outage probability of 0.01 is required for $K = 10$ dB and σ =6 dB, 10 users can be supported in the uplink, but less than 10 can be accommodated in the downlink. This is because we do not employ power control in the downlink. Furthermore, the area averaged outage probability degrades slower in the downlink than that in the uplink, when N is large.

7.3.4 Effects of the Macro-Diversity on the Downlink Performance

Recall that we have defined the relative other-cell interference f_I in the uplink to assess the effectiveness of the macro-diversity. In that part, we reached the conclusion that $N_c = 2$

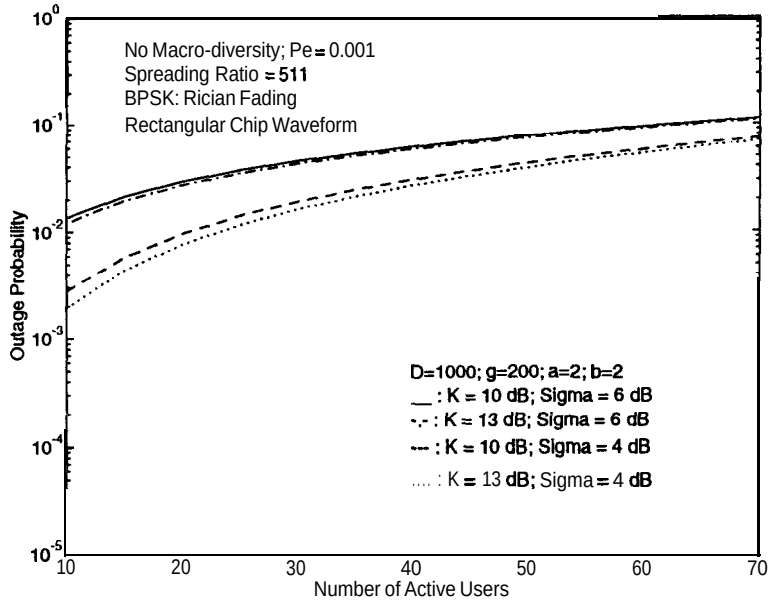

Figure 7.33: Area-averaged Outage Probability versus N for $N_c = 1$ in Rician Fading Channels, using the IGA-MC Method

(i.e., stronger-of-two-nearest-BS processing) is adequate not only to combat the shadowing, but also to keep the system complexity low. Based on this measure (i.e., f_I), it is very simple to examine the impact of the macro-diversity on suppressing the other-cell interference.

In this subsection, we will define a similar measure to assess the influence of the macro-diversity on the system performance in the downlink. There are many kinds of macro-diversity techniques in the literature. Here, we are interested in the macro-selection diversity method, where the vehicle has access to more than one BS and can select the BS with the best downlink transmission path. It is impossible for the vehicle to access all BS'. In this analysis, we assume that the vehicle can only access the nearest N_c BS'.

Without using the macro-diversity, it is straightforward to define the relative interference from the BS' of other cells as

$$\begin{aligned} D_I &= E\left\{\frac{\sum_{k=1}^{K} L_p(r_{ki})\ l_k}{L_p(r_{0i}) l_0}\right\} \\ &= E\left\{\frac{\sum_{k=1}^{K} P_k\ l_k}{l_0}\right\} \end{aligned} \tag{7.106}$$

where we assume that the multipath will not affect the average power level and only K adjacent cells are considered. D_I can be interpreted as the average ratio of other-cell interference to the desired signal power.

For systems employing macro-selection diversity, D_I should be modified as follows

$$\begin{aligned} D_I &= E\left\{\frac{\sum_{k=1}^{N_c-1} W_k + \sum_{k=N_c}^{K} \alpha_k}{W_0}\right\} \\ &= E\left\{\frac{\sum_{k=1}^{N_c-1} W_k}{W_0}\right\} + E\left\{\frac{\sum_{k=N_c}^{K} \alpha_k}{W_0}\right\} \\ &= D_{I1} + D_{I2} \end{aligned} \tag{7.107}$$

where $\alpha_k = P_k l_k$ and $\{W_k\}$ is a set of ordered random variables such that $W_0 \geq W_1 \geq \ldots \geq W_{N_c-1}$ and $W_0 = \max\{\alpha_0, \ldots, \alpha_{N_c-1}\}$.

The expressions for D_{I1} and D_{I2} are derived in Appendix F as a function of the user's location. Figure 7.34 shows D_I versus the transversal distance between the user and the BS. We assume that the standard deviation (STD) of the log-normal component is the same for each BS. We notice that a significant improvement in D_I is obtained by using $N_c = 2$ instead of $N_c = 1$, but little improvement is obtained when we go from $N_c = 2$ to 3. The same conclusion has been reached in the uplink analysis. Furthermore, the relative other-cell interference, D_I, becomes insensitive to the user's location in the cell when the macro-selection diversity is used. This will dramatically decrease the required dynamic range of the power control function.

7.4 Conclusions and Future Work

7.4.1 Conclusions

In this chapter, we studied the performance of an asynchronous multi-cell DS/CDMA system for uplink and downlink transmissions in microcells.

In the uplink, the performance measures of interest include the bit error rate, the outage probability, and the packet success rate. We evaluated the system performance under sha-

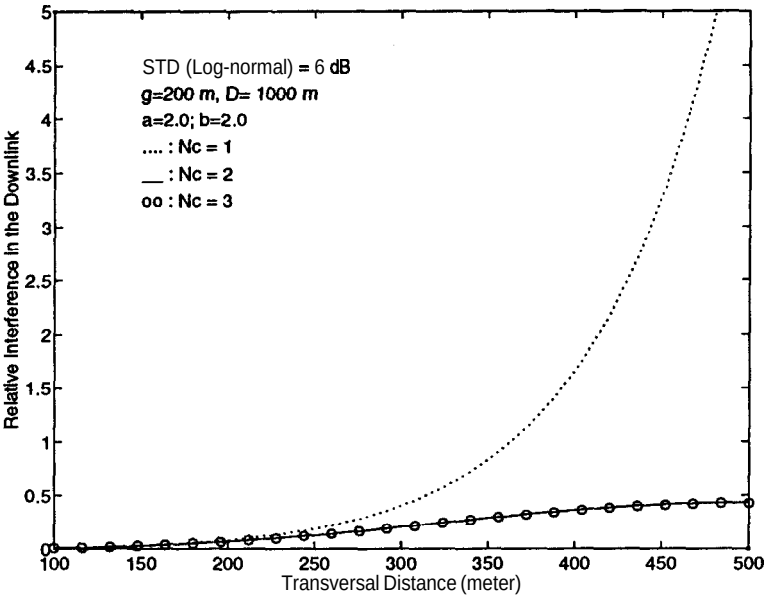

Figure 7.34: Relative Other-cell Interference, D_I, versus the Transversal Distance

dowed Rician/Nakagami fading in the presence of other-cell interference. Both the BPSK and DPSK modulation schemes are considered. The conclusions for the uplink are summarized as follows.

- When the number of active users in the system is small, the commonly used SGA (Standard Gaussian Approximation) method may yield very optimistic results compared with those obtained by the IGA (Improved Gaussian Approximation) method. This is because the user distribution and the shadowing (i.e., the vector $\underline{\chi}$) play a dominant role in the performance evaluation and utilization of their second moment information only, is not sufficient.

- Macro-selection diversity with $N_c = 2$, where the user is power controlled by one of the two nearest BS' with less attenuation, can effectively combat the shadowing and thus, suppress the other-cell interference.

- The Rician factor has a large influence on the performance for $N_c = 2$, but only little for $N_c = 1$.

- We can utilize better chip waveforms in order to improve the user capacity.

- Whether or not we can replace the Rician distribution by its relative Nakagami distribution, for analytical convenience, cannot be simply judged by their probability density functions. The analytical results in this chapter indicate that the macro-selection diversity also affects the approximation results.

- Without error control coding, slow fading yields better system performance than fast fading. If error control coding is used and the fading is not too heavy, the packet error rate is significantly improved for fast fading. However, the error control coding is less effective for slow fading.

In the downlink, we evaluated the BER and the outage probability. We also define a performance measure in order to investigate the effect of the macro-selection diversity on suppressing the other-cell interference. The properties of a composite log-normal Rician distribution were also studied. The conclusions for the downlink are summarized as follows.

- The composite log-normal noncentral chi-square distribution can be approximated by another log-normal distribution in some operation range. This approximation can significantly reduce the computation complexity.

- The macro-selection diversity can effectively suppress the other-cell interference. Furthermore, if it is used, the other-cell interference is rather insensitive to the user's location within the cell.

- User capacity assessed by the worst BER criterion may yield very pessimistic results.

7.4.2 Future Work

The plan for the second year of this research effort includes the following tasks:

- Study of the performance of narrow-band systems (taking into account the co-channel interference), using the analytical model introduced in this chapter.

- Investigation of the effect of the spatial (multipath) diversity inherent in the spread-spectrum technique on systems operating in frequency-selective channels.
- Evaluation of the system performance, using frequency-hopping (FH) or the FH/DS hybrid signaling.
- Investigation of an appropriate power control scheme for short-range data communications in DS/CDMA systems.

Chapter 8

Conclusions and Future Work

8.1 Conclusions

In this chapter we summarize the conclusions that we have reached so far in the first year of this project. We have devised a general analytical procedure for the design and evaluation of a packet radio communication system for IVHS. We examined the options and the constraints that the designer of a communication system faces, as well as the effects of the physical environment, the vehicular traffic, and the information flow requirements of the IVHS applications on the evaluation modules. Packet radio systems have the unique characteristic that the Physical and the Data Link layers are strongly interconnected. Thus, in order to optimize the overall system, we must jointly optimize the two layers, rather than design, analyze, and optimize each layer independently from the other.

During the last year, we have thoroughly examined the ATMIS **a n d** AVCS services in order to extract the communication needs of an integrated ATMIS/AVCS system. Furthermore, we assessed the information flow requirements associated with the various communication needs, and we suggested a new possible way for determination of a vehicle's location based on magnetic strips mounted on the roadway.

We have concluded that uplink (vehicle to base station) and vehicle-to-vehicle communications require the exchange of short messages (64 - 100 bits) for both ATMIS and AVCS

transactions. The message size for the downlink (base station to vehicle) however, depends on the application. AVCS services require transmission of short messages, whereas ATMIS services such as traveler advisory and information (including the transmission of digitized maps) require the transmission of long messages which can be broken up into several packets, each containing, say 512 bits. All the necessary parameters for the calculation of the integrated system's communication requirements have been identified. However, no numbers for the data rate were presented, because the values of the most parameters of interest are still unknown.

In order to coordinate the accessing of the channel by a large number of users, we have studied three classes of multiple access schemes, namely fixed assignment, random access, and reservation schemes. The identification of the communication needs for each of the three links in PR-IVHS (Packet Radio IVHS) and careful analysis of these schemes have shown that random access and reservation schemes are the possible candidates for the uplink, whereas fixed assignment and reservation schemes seem to be the best candidates for the downlink. For the vehicle-to-vehicle link, random access schemes are suitable for random inter-platoon communications, and hybrid schemes (reservation plus random access) are more appropriate for intra-platoon communications, where both random and periodic data traffic exist.

We have analyzed the performance of the three most feasible multiple access protocols in each of the three communication links, for a single cell. Two different performance measures were used for the performance evaluation of the protocols. The throughput was used for non-real-time communications, whereas the deadline failure probability was used for real-time communications (e.g., intra-platoon communications). The simulations for the performance evaluation were carried under certain assumptions about the conditional capture probability, the distribution of the number of active transmissions, the transmission probability, the number of slots or frames in a deadline period, and the spreading ratio.

Our goal for the second year of this project is to design a single protocol that can accommodate all the communication needs of the integrated ATMIS/AVCS data traffic. Two possible candidates are the SR-ALOHA (a hybrid scheme of Slotted-ALOHA and Reservation-ALOHA) and the Spread Spectrum Slotted-ALOHA protocols, with Direct-Sequence

modulation. The most important design parameter for SR-ALOHA is the ratio of the number of slots for periodic data traffic to the number of slots for random data traffic, whereas the most important design parameter for SS/S-ALOHA is the spreading ratio. The optimal design parameters should be able to maximize the throughput for random data traffic and maintain the deadline failure probability below a certain threshold at the same time. The optimization of these design parameters will be the focus of our future efforts.

The greater part of our conclusions come from the performance analysis of an asynchronous multi-cell Direct-Sequence Code Division Multiple-Access (DS/CDMA) system for both uplink and downlink communications in a microcellular environment. For the uplink, we calculated the bit error rate, the outage probability, and the packet success rate for two modulation schemes. The performance measures were evaluated under the assumption of random signature sequences and shadowed Rician/Nakagami fading in the presence of other-cell interference. We used both the SGA (Standard Gaussian Approximation) and the IGA (Improved Gaussian Approximation) methods, with the former yielding more optimistic results than the latter. Macro-selection diversity was found to reduce the other-cell interference, even in the presence of heavy shadowing. We found that the Rician factor affects greatly the system performance, when there are two control base stations, but, it does not have a great impact when there is only one base station. Bandwidth increase can be avoided by utilizing better chip waveforms. Furthermore, slow fading yields better system performance than fast fading in the absense of error control coding, whereas by using coding (always assuming that the fading is not catastrophic) the packet error rate is significantly improved in the case of fast fading. However, coding is less effective for slow fading.

For the downlink, we calculated the bit error rate and the outage probability without employing macro-diversity. We also identified a performance measure that can be used for the study of the macro-selection diversity effect on the suppression of other-cell interference. Finally, we found that the user capacity assessed by the worst BER criterion yields very pessimistic results.

8.2 Future work

The research plan for the second year of this project includes the following tasks:

- Survey of on-going IVHS and IVHS-related projects in USA, Europe, and Japan
- Study of packet radio architectures for ATMIS transactions in an urban environment
- Detailed analysis and simulation of multiple access protocols for the integrated ATMIS/AVCS system, taking into account the physical layer parameters
- Performance analysis of narrowband ALOHA with capture for microcellular systems
- Initiate performance analysis of a FH-SS system
- Comparison between the Spread Spectrum and narrowband systems
- Overall analysis and simulation of the proposed communication system
- Detailed system design and iterations
- Final design recommmendations

Appendix A

MA1 Distribution Analysis

The correlator output ξ_{0i} in equation (7.13) can be written as follows

$$\begin{aligned}\xi_{0i} &= \frac{1}{\sqrt{2P_0T}}\int_0^T r_{0i}(t)2a_{0i}(t)\cos(2\pi f_c t)\,\boldsymbol{dt} \\ &= \gamma_{0i}b_0^{(0i)} + \frac{1}{T}\sum_{n=1,n\neq i}^{N_0}\sqrt{\chi_{0n}}\gamma_{0n}\cos(\Phi_{0n})B_{0n,0i}(\underline{b}_{0n},\tau_{0n}) \\ &\quad +\frac{1}{T}\sum_{k=1}^{K}\sum_{n=1}^{N_k}\sqrt{\chi_{kn}}\gamma_{kn}\cos(\Phi_{kn})B_{kn,0i}(\underline{b}_{kn},\tau_{kn}) + n^*\end{aligned} \tag{A.1}$$

where n^* is a zero-mean Gaussian r.v. with variance $\mathcal{N}_0/(2P_0T) = \mathcal{N}_0/2E_b$ and $B_{kn,0i}(\underline{b}_{kn},\tau_{kn})$ is given by

$$\begin{aligned}B_{kn,0i}(\underline{b}_{kn},\tau_{kn}) &= \int_0^T a_{kn}(t-\tau_{kn})b_{kn}(t-\tau_{kn})a_{0i}(t)dt \\ &= b_{-1}^{(kn)}\int_0^{\tau_{kn}} a_k(t-\tau_{kn})a_{0i}(t)dt \\ &\quad +b_0^{(kn)}\int_{\tau_{kn}}^T a_{kn}(t-\tau_{kn})a_{0i}(t)dt \\ &= b_{-1}^{(kn)}R_{kn,0i}(\tau_{kn}) + b_0^{(kn)}\hat{R}_{kn,0i}(\tau_{kn}) \quad ,\end{aligned} \tag{A.2}$$

where $\underline{b}_{kn} = (b_{-1}^{(kn)}, b_0^{(kn)})$ and the continuous partial cross-correlation functions $R_{kn,0i}(\tau)$ and $\hat{R}_{kn,0i}(\tau)$ are given by

$$R_{kn,0i}(\tau) = \sum_{j=0}^{l-1} a_{j-l}^{(kn)}a_j^{(0i)}\hat{R}_\psi(\tau - lT_c) + \sum_{j=0}^{l} a_{j-l-1}^{(kn)}a_j^{(0i)}R_\psi(\tau - lT_c) \quad , \tag{A.3}$$

and

$$\hat{R}_{kn,0i}(\tau) = \sum_{j=l}^{\eta-1} a_{j-l}^{(kn)} a_j^{(0i)} \hat{R}_\psi(\tau - lT_c) + \sum_{j=l+1}^{\eta-1} a_{j-l-1}^{(kn)} a_j^{(0i)} R_\psi(\tau - lT_c) \quad , \tag{A.4}$$

where $\hat{R}_\psi(\tau) = \int_\tau^{T_c} \psi(t)\psi(t-\tau)\ \boldsymbol{d}\ \boldsymbol{t}$ and $R_\psi(\tau) = \hat{R}_\psi(T_c - \tau)$, and $l = \lfloor \tau/T_c \rfloor$, and $\lfloor x \rfloor$ is the largest integer not greater than x. Therefore, l is uniformly distributed over $\{0, \ldots, \eta - 1\}$. If we let $S_k = \tau_k - lT_c$, then S_k is uniformly distributed over $[0, T_c]$.

Because the signature sequence is random, the time delay τ_{kn} is needed to be known only to the nearest chip (i.e., we can let $l = 0$), and the value of $B_{kn,0i}$ is independent of $\underline{b}_{kn}$ (Georgiopoulos 1990). Therefore, the continuous partial cross-correlation functions $R_{kn,0i}(S)$ and $\hat{R}_{kn,0i}(S)$ becomes

$$R_{kn,0i}(S) = a_{-1}^{(kn)} a_0^{(0i)} R_\psi(S) \quad , \tag{A.5}$$

and

$$\hat{R}_{kn,0i}(S) = \sum_{j=0}^{\eta-1} a_j^{(kn)} a_j^{(0i)} \hat{R}_\psi(S) + \sum_{j=1}^{\eta-1} a_{j-1}^{(kn)} a_j^{(0i)} R_\psi(S) \, . \tag{A.6}$$

Substituting $R_{kn,0i}(S)$ and $\hat{R}_{kn,0i}(S)$ into equation (A.2), $B_{kn,0i}(S)$ becomes

$$\begin{aligned} B_{kn,0i}(S) \;=\; & a_{-1}^{(kn)} a_0^{(0i)} R_\psi(S) \;+\; a_{\eta-1}^{(kn)} a_{\eta-1}^{(0i)} \hat{R}_\psi(S) \\ & + \sum_{j=0}^{\eta-2} a_j^{(kn)} [a_j^{(0i)} \hat{R}_\psi(S) + a_{j+1}^{(0i)} R_\psi(S)] \quad . \end{aligned} \tag{A.7}$$

If we condition on the reference sequence $a_j^{(0i)} = \hat{a}_j^{(0i)}$ for $j \in \{0, 1, \cdots, \eta - 1\}$ and use the fact that $(\hat{a}_j^{(0i)})^2 = 1$, $B_{kn,0i}(S)$ becomes

$$\begin{aligned} B_{kn,0i}(S) \;=\; & a_{-1}^{(kn)} \hat{a}_0^{(0i)} R_\psi(S) + a_{\eta-1}^{(kn)} \hat{a}_{\eta-1}^{(0i)} \hat{R}_\psi(S) \\ & + \sum_{j=0}^{\eta-2} a_j^{(kn)} \hat{a}_j^{(0i)} \left[\hat{R}_\psi(S) + \hat{a}_j^{(0i)} \hat{a}_{j+1}^{(0i)} R_\psi(S) \right] \quad . \end{aligned} \tag{A.8}$$

Further simplification is possible by noting that $\hat{a}_j \hat{a}_{j+1} = \pm 1$. Let the sets α and β be defined as

$$\alpha = \{ j : \hat{a}_j^{(0i)} \hat{a}_{j+1}^{(0i)} = +1 \} \, , \tag{A.9}$$

and

$$\beta = \{ j : \hat{a}_j^{(0i)} \hat{a}_{j+1}^{(0i)} = -1 \} \, , \tag{A.10}$$

for $j \in \{0, 1, \ldots, (\eta - 2)\}$.

After rearranging the terms, $B_{kn,0i}(S)$ becomes

$$B_{kn,0i}(S) = P_{kn} R_\psi(S) + Q_{kn} \hat{R}_\psi(S) + X_{kn} f_\psi(S) + Y_{kn} g_\psi(S) \quad , \tag{A.11}$$

where $P_{kn} = a_{-1}^{(kn)} \hat{a}_0^{(0i)}$ and $Q_{kn} = a_{\eta-1}^{(kn)} \hat{a}_{\eta-1}^{(0i)}$ are equally likely ± 1 r.v.'s, X_{kn} is

$$X_{kn} = \sum_{j \in \alpha} a_j^{(kn)} \hat{a}_j^{(0i)} \quad , \tag{A.12}$$

and Y_{kn} is

$$Y_{kn} = \sum_{j \in \beta} a_j^{(kn)} \hat{a}_j^{(0i)} \quad , \tag{A.13}$$

and $f_\psi(S) = \hat{R}_\psi(S) + R_\psi(S)$, $g_\psi(S) = \hat{R}_\psi(S) - R_\psi(S)$.

Suppose now that A and B are the cardinalities of α and β, respectively. Then X_{kn} and Y_{kn} are the sum of unbiased Bernoulli trials given by

$$P_{X_{kn}}(j) = \binom{A}{\frac{j+A}{2}} 2^{-A} \, , \; j \in \{-A, \; -A + 2, \ldots, A - 2, A\} \, , \tag{A.14}$$

and

$$P_{Y_{kn}}(j) = \binom{B}{\frac{j+B}{2}} 2^{-B} \, , \quad j \in \{-B, -B+2, \ldots, B-2, B\} \; . \tag{A.15}$$

From the definitions of α and β, it is obvious that $A + B = \eta - 1$. Also, $A - B = C$, where $C = C_{0i,0i}(1)$ is the aperiodic auto–correlation of the signature sequence of user $0i$ with offset by one chip. Therefore, $A = (\eta - 1 + C)/2$ and $B = (\eta - 1 - C)/2$. Note that if any two of the four quantities A, B, C, and η are known, the other two can be found. The r.v. C is given by

$$C = \sum_{j=0}^{\eta-2} a_j^{(0i)} a_{j+1}^{(0i)} \quad , \tag{A.16}$$

which is the sum of $\eta - 1$ unbiased Bernoulli r.v.'s, so that the density of C is given by

$$P_C(j) = \binom{\eta - 1}{\frac{j+\eta-1}{2}} 2^{1-\eta} \quad , \quad j \in \{1 - \eta, 3 - \eta, \ldots, \eta - 3, \eta - 1\} \; . \tag{A.17}$$

Since the random variables P_{kn}, Q_{kn}, X_{kn}, and Y_{kn} are composed of disjoint set of symmetric Bernoulli trials for a particular desired signature sequence, they are conditionally

independent given $\boldsymbol{B}$ (or C). Because of the symmetry of the distribution of the $\boldsymbol{n}^*$, and $\sqrt{\chi_{kn}}\gamma_{kn}B_{kn,0i}(S_{kn})\cos\Phi_{kn}$, the conditional BER given $b_0^{(0i)}$ does not depend on the value of $b_0^{(0i)}$,so we take it to be +1. Combining equation (A.1) and (A.11), ξ_{0i} can be expressed in the simplified form

$$\begin{aligned}\xi_{0i} &= \gamma_{0i} + \sum_{n=1,n\neq i}^{N_0} \sqrt{\chi_{0n}}\gamma_{0n}\cos(\Phi_{0n})W_{0n} \\ &\quad + \sum_{k=1}^{K}\sum_{n=1}^{N_k} \sqrt{\chi_{kn}}\gamma_{kn}\cos(\Phi_{kn})W_{kn} + n^* \end{aligned} \tag{A.18}$$

where W_{ij} is given by

$$W_{ij} = \frac{1}{T}[\, P_{ij}R_\psi(S_{ij}) + Q_{ij}\hat{R}_\psi(S_{ij}) + X_{ij}f_\psi(S_{ij}) + Y_{ij}g_\psi(S_{ij})\,] \tag{A.19}$$

Morrow and Lehnert (Morrow et al. 1989) invoke the central limit theorem to show that if the relative delays and phases between the desired and interfering users are fixed for a DS/CDMA system in an AWGN channel, and if a particular autocorrelation property of the desired signature sequence (i.e., the value of C or $\boldsymbol{B}$ for the desired user) is also fixed, then the MAI can be accurately modeled as a Gaussian r.v. when all interfering signature sequences are randomly generated. By using a characteristic function approach (Morrow et al. 1989) however, they also showed that the MAI converges in distribution to a Gaussian r.v. for desired signature sequences that are completely random, provided once again that the relative delays and phases between the desired and interfering signals are fixed. This important result is also discussed in (Georgiopoulos 1990). We can interpret this result as follows: when $\eta \to \infty$, the coefficient of variation of $\boldsymbol{B}$ goes to zero. This suggests that the mean of $\boldsymbol{B}$, $(\eta-1)/2$, can be used and conditioning is unnecessary. The question remains as to the effect of not conditioning on $\boldsymbol{B}$ and using only its mean for small η when the coefficient of variation of $\boldsymbol{B}$ is not small. Simpson (Simpson 1992)showed that the difference of BER and PER between conditioning on $\boldsymbol{B}$ and not conditioning on $\boldsymbol{B}$ is negligible even for $\eta = 7$. Therefore, we can just set $\boldsymbol{B} = (\eta-1)/2$ which willsignificantly simplify the computation. The above results can be easily extended to the systems in a fading channel. That is, if the random variables $\{\chi_{ij}\}$, $\{\gamma_{ij}\}$, $\{\tau_{ij}\}$, and $\{\Phi_{ij}\}$ are fixed and the signature sequences are completely random, the MAI can be accurately modeled as a Gaussian random variable.

Appendix B

Derivation of M_χ

From equation (7.33), M_χ is

$$M_\chi = \sum_{n=1, n\neq i}^{N_0} E(\chi_{0n}) + \sum_{k=1}^{K}\sum_{n=1}^{N_k} E(\chi_{kn}) \tag{B.1}$$

Note that χ_{kn} is a function of the mobile location in the cell. Its expected value can be evaluated by

$$\begin{aligned} E(\chi_{kn}) &= \int_{C_k} E\left\{\min_{j\in\mathcal{S}_c}\left[\frac{PL_{kn}^{(0)}}{PL_{kn}^{(j)}}\right]\right\}\rho\, dA \\ &= \int_{C_k} E\left\{\min_{j\in\mathcal{S}_c}\left[\frac{L_p(r_0)10^{X_0/10}}{L_p(r_j)10^{X_j/10}}\right]\right\}\rho\, dA \\ &= \int_{C_k} I_k\,\rho\, dA \end{aligned} \tag{B.2}$$

where ρ is the spatial density of the user. We have assumed that the user position is uniformly distributed within the cell. For example, if there are five lanes in each direction of a highway and the diameter of the cell is D, then ρ equals $1/10D$. The distance between the knth user and the BS j is r_j and the corresponding power fluctuation is X_j. X_i and X_j, $i \neq j$, are assumed to be independent. This obviously results from the fact that the propagation condition from the user to different BS' will be independent. We have dropped the subindex $k\ n$ in r_j and X_j to make the notation simple.

We can define the relative mean path loss as follows

$$R_j = \frac{L_p(r_0)}{L_p(r_j)}, \quad M_j = 10\log_{10} R_j$$

The expected value of χ_{kn} will be computed separately depending on whether the BS 0 is one of the N_c nearest BS' of the kn^{th} user or not.

Case I: $0 \notin \mathcal{S}_c$

We can apply the total probability formula in order to evaluate I_k as follows:

$$\begin{aligned} I_k &= E\left[\min_{j\in\mathcal{S}_c} R_j\ 10^{-\frac{X_j - X_0}{10}}\right] \\ &= \sum_{j\in\mathcal{S}_c} R_j\ E\left(10^{\frac{X_0}{10}}\right) E\left[10^{-\frac{X_j}{10}} \mid R_j 10^{-\frac{X_j - X_0}{10}} < R_i 10^{-\frac{X_i - X_0}{10}},\ \forall i \neq j\right] P_r(A_j) \\ &= \sum_{j\in\mathcal{S}_c} R_j\, E\left(10^{\frac{X_0}{10}}\right)\ E\left[10^{-\frac{X_j}{10}} \mid X_i < X_j + M_i - M_j\right] P_r(A_j) \\ &= \sum_{j\in\mathcal{S}_c} R_j\ E\left(10^{\frac{X_0}{10}}\right)\left\{\int_{-\infty}^{\infty} 10^{-\frac{X_j}{10}} f_{X_j}(x_j)\, dx_j \cdot \right. \\ &\qquad \left. \left[\prod_{i\neq j, i\in\mathcal{S}_c} F_{X_i}(x_j + M_i - M_j)\right]\right\} \end{aligned} \tag{B.3}$$

where A_j is the event $\{ R_j 10^{-\frac{X_j - X_0}{10}} < R_i 10^{-\frac{X_i - X_0}{10}}, \forall i \neq j \}$, and $f_{X_j}(x_j)$ and $F_{X_j}(x_j)$ are the pdf and cumulative density function of r.v. X_j, respectively.

Case II: $0 \in \mathcal{S}_c$

In this case, the N_c nearest BS' include the BS 0. We can use the same procedure as above, but now one of the N_c BS' has index $j = 0$. Hence, I_k is

$$I_k = E\left[\min\left(1, \ldots, R_{N_u} 10^{-\frac{X_{N_u} - X_0}{10}}\right)\right] \tag{B.4}$$

where $N_u = \max_{j\in\mathcal{S}_c} j$.

We can first condition on each of $R_j 10^{-\frac{X_j - X_0}{10}}$ being less than 1 if they are to be the minimum, while they are all greater than 1, then 1 is the minimum. Hence, I_k is Equation

(B.4) can be derived as follows

$$
\begin{aligned}
I_k &= \sum_{j\in\mathcal{S}_c, j\neq 0} R_j E\left[10^{-\frac{X_j-X_0}{10}} \mid \hat{A}_j\right] P_r(\hat{A}_j) \\
&\quad +1\cdot P_r\left(R_j 10^{-\frac{X_j-X_0}{10}} > 1, \forall j \neq 0,\ j\in\mathcal{S}_c\right) \\
&= \sum_{j\in\mathcal{S}_c, j\neq 0} R_j E\left[10^{-\frac{X_j-X_0}{10}} \mid X_0 < X_j - M_j,\right. \\
&\quad \left. X_i < X_j + M_i - M_j, \forall i\neq j\right] P_r(\hat{A}_j) \\
&\quad +P_r(X_j < X_0 + M_j,\ \forall j\in\mathcal{S}_c,\ j\neq 0) \\
&= \sum_{j\in\mathcal{S}_c, j\neq 0} R_j \int_{-\infty}^{\infty} 10^{-\frac{x_j}{10}} f_{X_j}(x_j)\,dx_j \left[\int_{-\infty}^{x_j-M_j} 10^{\frac{x_0}{10}} f_{X_0}(x_0)dx_0\right]\cdot \\
&\quad \left[\prod_{i\in\mathcal{S}_c, i\neq j, i\neq 0} F_{X_j}(x_j+M_i-M_j)\right] \\
&\quad + \int_{-\infty}^{\infty} f_{X_0}(x_0)\,dx_0 \left[\prod_{j\in\mathcal{S}_c, j\neq 0} F_{X_j}(x_0+M_j)\right]
\end{aligned}
\tag{B.5}
$$

where $\hat{A}_j$ is the event $\left\{R_j 10^{-\frac{X_j-X_0}{10}} < R_i 10^{-\frac{X_i-X_0}{10}},\ \forall i \neq j \text{ and } R_j 10^{\frac{X_j-X_0}{10}} < 1\right\}$

If X_j's are all-zero mean Gaussian random variables with equal variance σ^2, I_k for the case $\{0 \notin \mathcal{S}_c\}$ is

$$
\begin{aligned}
I_k &= \sum_{j\in\mathcal{S}_c} R_j \exp(\lambda^2\sigma^2) \int_{-\infty}^{\infty} \frac{1}{\sqrt{2\pi}} \exp\left(-\frac{z^2}{2}\right) dz \cdot \\
&\quad \left\{\prod_{i\in\mathcal{S}_c, i\neq j} \left[1-\mathbf{Q}\left(z+\frac{M_i-M_j}{\sigma}-\lambda\sigma\right)\right]\right\}
\end{aligned}
\tag{B.6}
$$

where $\lambda = \log(10)/10$, and I_k for the case of $\{0\in\mathcal{S}_c\}$ is

$$
\begin{aligned}
I_k &= \sum_{j\in\mathcal{S}_c, j\neq 0} R_j \exp(\lambda^2\sigma^2) \int_{-\infty}^{\infty} \frac{1}{\sqrt{2\pi}} \exp\left(-\frac{z^2}{2}\right) dz \cdot \\
&\quad \left[1-\mathbf{Q}\left(z-\frac{M_j}{\sigma}-2\lambda\sigma\right)\right]\cdot \\
&\quad \left\{\prod_{i\in\mathcal{S}_c, i\neq j, i\neq 0} \left[1-\mathbf{Q}\left(z+\frac{M_i-M_j}{\sigma}-\lambda\sigma\right)\right]\right\} \\
&\quad + \int_{-\infty}^{\infty} \frac{1}{\sqrt{2\pi}} \exp\left(-\frac{z^2}{2}\right) dz \left\{\prod_{j\in\mathcal{S}_c, j\neq 0} \left[1-\mathbf{Q}\left(z+\frac{M_j}{\sigma}\right)\right]\right\}
\end{aligned}
\tag{B.7}
$$

Appendix C

Probability Density Function of a log-normal noncentral Chi-square/Gamma Distribution

As defined in section 7.3.2, the log-normal noncentral chi-square $\mathcal{L}_k$ is given by

$$\mathcal{L}_k = P_k l_k \gamma_k^2 = \varsigma_k \tilde{\gamma}_k \tag{C.1}$$

where $\varsigma_k = P_k\, l_k$ has a log-normal distribution with pdf

$$f_{\varsigma_k}(y) = \frac{1}{\sqrt{2\pi}\lambda\sigma_k y} \exp\left[-\frac{(\ln \mathbf{Y} - \lambda m_k)^2}{2\lambda^2\sigma_k^2} \right]_I U(y) \tag{C.2}$$

where $m_k = 10\log_{10}(P_k)$ and γ_k follows a normalized Rician or Nakagami distribution.

Case I: γ_k is normalized Rician

If γ_k is normalized Rician, then $\tilde{\gamma}_k$ will be non-central chi-square with pdf as follows

$$f_{\tilde{\gamma}_k}(y) = (K+1)e^{-(K+1)y-K}\, I_0\left(\sqrt{4K(K+1)y}\right) U(y) \tag{C.3}$$

We can write the conditional pdf $f_{\mathcal{L}_k}(y|\varsigma_k)$ as

$$\begin{aligned} f_{\mathcal{L}_k}(y|\varsigma_k) &= f_{\tilde{\gamma}_k}(y/\varsigma_k)/\varsigma_k \\ &= \frac{(K+1)}{\varsigma_k} \exp\left(-\frac{(K+1)y}{\varsigma_k} - K \right) \cdot \\ &\quad I_0\left(\sqrt{4K(K+1)y/\varsigma_k}\right) U(y) \end{aligned} \tag{C.4}$$

Therefore, the pdf of $\mathcal{L}_k$ can be found by averaging the conditional pdf $f_{\mathcal{L}_k}(y|\varsigma_k)$ over ς_k.

$$\begin{aligned} f_{\mathcal{L}_k}(y) &= \int_0^\infty f_{\mathcal{L}_k}(y|u)\, f_{\varsigma_k}(u)\, du \\ &= \int_0^\infty \frac{(K+1)}{u} \exp\left(-\frac{(K+1)y}{u} - K \right) I_0\left(\sqrt{4K(K+1)y/u} \right) \cdot \\ &\quad \frac{1}{\sqrt{2\pi}\lambda\sigma_k\, u} \exp\left[-\frac{(\ln u - \lambda m_k)^2}{2\lambda^2\sigma_k^2} \right] du \end{aligned} \tag{C.5}$$

Let $A_k = \sqrt{2}\lambda\sigma_k$ and $x = (\ln u - \lambda m_k)/A_k$. Then, the pdf of $\mathcal{L}_k$ becomes

$$\begin{aligned} f_{\mathcal{L}_k}(y) &= \frac{(K+1)}{\sqrt{\pi}} \exp(-K) \int_{-\infty}^{\infty} \exp\left[-(A_k x + \lambda m_k) \right] \cdot \\ &\quad \exp\left[-(K+1)y\, e^{-(A_k x + \lambda m_k)} \right] \exp\left(-x^2 \right) \cdot \\ &\quad I_0\left(\sqrt{4K(K+1)y \exp\left[-(A_k x + \lambda m_k) \right]} \right) dx \end{aligned} \tag{C.6}$$

Case II: γ_k is normalized Nakagami

If γ_k is normalized Nakagami, then $\tilde{\gamma}_k = \gamma_k^2$ is a Gamma function with pdf

$$f_{\tilde{\gamma}_k}(y) = \frac{m^m\, y^{m-1}}{\Gamma(m)} \exp(-my)\, U(y) \tag{C.7}$$

Hence, the conditional pdf $f_{\mathcal{L}_k}(y|\varsigma_k)$ yields

$$\begin{aligned} f_{\mathcal{L}_k}(y|\varsigma_k) &= f_{\tilde{\gamma}_k}(y/\varsigma_k)/\varsigma_k \\ &= \frac{(m/\varsigma_k)^m\ y^{m-1}}{\Gamma(m)} \exp\left(-my/\varsigma_k \right) U(y) \end{aligned} \tag{C.8}$$

Integrating the conditional pdf $f_{\mathcal{L}_k}(y|\varsigma_k)$ over ς_k, we can find the pdf of the log-normal Gamma $\mathcal{L}_k$

$$\begin{aligned} f_{\mathcal{L}_k}(y) &= \int_0^\infty f_{\mathcal{L}_k}(y|u)\, f_{\varsigma_k}(u)\, du \\ &= \frac{m^m\, y^{m-1}}{\Gamma(m)\sqrt{\pi}} \int_{-\infty}^{\infty} \exp\left[-m\,(A_k x + \lambda m_k) \right] \cdot \\ &\quad \exp\left[-my\, e^{-(A_k x + \lambda m_k)} \right] \exp\left(-x^2 \right) d\, x \end{aligned} \tag{C.9}$$

Appendix D

Approximation of the log-normal noncentral Chi-square distribution by another log-normal distribution

The composite log-normal noncentral chi-square distribution, as described by (C.6), is rather complicated and not easy to handle mathematically. It would be very useful to have an approximation. Muammar and Gupta (Muammar et al. 1982) suggested that, under certain conditions, the composite log-normal Rayleigh can be approximated by a log-normal distribution. This is very convenient since a log-normal distribution can be specified completely in terms of two parameters, the mean and the standard deviation (in dB).

In this appendix, we will investigate under what conditions a log-normal noncentral chi-square distributed random variable can be approximated by a log-normal distribution. As defined in section 7.3.2, the log-normal noncentral chi-square distributed random variable, $\mathcal{L}_k$, is

$$\mathcal{L}_k = P_k \, l_k \, \tilde{\gamma}_k \tag{D.1}$$

whose pdf is described by equation (C.6) in appendix C.

We can express (D.1) in dB units by writing

$$10\log_{10} \mathcal{L}_k = 10\log_{10} P_k + 10\log_{10} l_k + 10\log_{10} \tilde{\gamma}_k \tag{D.2}$$

i.e.

$$\mathcal{L}_{k(dB)} = m_k + X_k + \tilde{\gamma}_{k(dB)} \tag{D.3}$$

If $\mathcal{L}_k$ can be approximated by a log-normal, $\mathcal{L}_{k(dB)}$ will be a Gaussian random variable. We assume that the mean and the standard deviation of $\mathcal{L}_{k(dB)}$ are μ_k and s_k, respectively. Because X_k is a zero mean Gaussian with standard variation σ_k, and X_k and $\tilde{\gamma}_{k(dB)}$ are independent, we can write μ_k and s_k as (Parsons 1992):

$$\begin{aligned} \mu_k &= m_k + E\left[\tilde{\gamma}_{k(dB)}\right] \\ s_k &= \sqrt{\sigma_k^2 + \text{var}\left[\tilde{\gamma}_{k(dB)}\right]} \end{aligned} \tag{D.4}$$

Table D.1 contains $E\left[\tilde{\gamma}_{k(dB)}\right]$ and $\textbf{Var}\left[\tilde{\gamma}_{k(dB)}\right]$ as a function of K. The larger the value K, the smaller the values of $E\left[\tilde{\gamma}_{k(dB)}\right]$ and $\textbf{Var}\left[\tilde{\gamma}_{k(dB)}\right]$. This implies that the approximation of a log-normal Rician by another log-normal is better for large values of K.

K (dB)	$E\left[\tilde{\gamma}_{k(dB)}\right]$	$\textbf{Var}\left[\tilde{\gamma}_{k(dB)}\right]$
$-\infty$	-2.5068	31.0254
4	-1.3489	16.2869
7	-0.7852	8.4503
10	-0.4319	3.9943
13	-0.2124	1.9416

Table D.1: $E\left[\tilde{\gamma}_{k(dB)}\right]$ and $\textbf{Var}\left[\tilde{\gamma}_{k(dB)}\right]$ as a function of K

In ***figure*** D.1, we compare the CDF of a log-normal noncentral chi-square distribution with the CDF of its log-normal approximation with K=7 dB for several values of σ. It can be found that the approximation of a log-normal noncentral chi-square distribution by another log-normal is appropriate when $K \geq 7$ dB and $\sigma \geq 4$ dB.

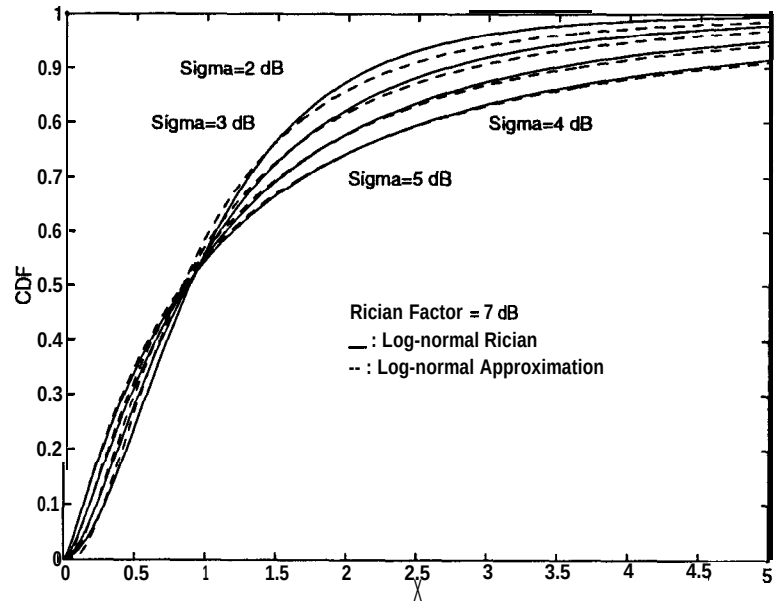

Figure D.1: CDF of the composite log-normal noncentral Chi-square and its log-normal approximation, for $K = 7$ dB

Appendix E

Statistical Analysis of the sum of multiple log-normal components

Suppose that we want to find the approximated mean and variance of the variable Z which is the logarithm of the sum of K log-normally distributed variables of the form $10^{Z_k/10}$. Z_k has a normal distribution with mean m_{Z_k} and variance σ_{Z_k}. Thus, Z can be written as follows

$$Z = 10\log_{10}\left(\sum_{k=1}^{K} 10^{Z_k/10}\right) \tag{E.1}$$

The recursive method suggested by Schwartz and Yeh (Schwartz et al. 1982) and manipulated, making some simplifications, by Safak (Safak 1993) can be summarized as follows

1. Let $Y_k = \lambda Z_k$, where $\lambda = \ln 10/10$. Then, $m_{Y_k} = \lambda m_{Z_k}$ and $\sigma_{Y_k} = \sigma_{Z_k}$.

2. Let $S_1 = Y_1$. Then, $m_{S_1} = m_{Y_1}$ and $\sigma_{S_1} = \sigma_{Y_1}$.

3. $W_k = Y_k - S_{k-1}$, $k \geq 2$.
   i.e., $m_{W_k} = m_{Y_k} - m_{S_{k-1}}$ and $\sigma^2_{W_k} = \sigma^2_{Y_k} + \sigma^2_{S_{k-1}}$

4. $m_{S_k} = m_{S_{k-1}} + G_1(\sigma_{W_k}, m_{W_k})$
   $\sigma^2_{S_k} = \sigma^2_{S_{k-1}} - G_1^2(\sigma_{W_k}, m_{W_k}) + G_2(\sigma_{W_k}, m_{W_k}) - 2\left(\frac{\sigma_{S_{k-1}}}{\sigma_{W_k}}\right)^2 G_3(\sigma_{W_k}, m_{W_k})$

5. If $k \neq K$, *go* to ***Step 3.***

6. $m_Z = m_{S_K}/\lambda$ and $\sigma_Z = \sigma_{S_K}/\lambda$

The functions G_1, G_2, and G_3 are

$$G_1(\sigma, m) = m\Phi\left(\frac{m}{\sigma}\right) + \frac{\sigma}{\sqrt{2\pi}}\exp\left(-\frac{m^2}{2\sigma^2}\right) + \sum_{k=1}^{\infty} C_k[\,F(\sigma, m, k) + F(\sigma, -m, k)\,] \tag{E.2}$$

$$G_2(\sigma, m) = \left(m^2 + \sigma\right)\Phi\left(\frac{m}{\sigma}\right) + (m + \ln 4)\frac{\sigma}{\sqrt{2\pi}}\exp\left(-\frac{m^2}{2\sigma^2}\right) + 2\sum_{k=1}^{\infty} C_k\left(m - k\sigma^2\right)F(\sigma, m, k) + \sum_{k=2}^{\infty} B_{k-1}[\,F(\sigma, m, k) + F(\sigma, -m, k)\,] \tag{E.3}$$

$$G_3(\sigma, m) = \sigma^2 \sum_{k=0}^{\infty} (-1)^k[\,F(\sigma, m, k) + F(\sigma, -m, k+1)\,] \tag{E.4}$$

where

$$F(\sigma, m, k) = \exp\left(-km + \frac{k^2\sigma^2}{2}\right)\Phi\left(\frac{m - k\sigma^2}{\sigma}\right) \tag{E.5}$$

$$\Phi(x) = 1 - \mathbf{Q}(x) \tag{E.6}$$

$$C_k = \frac{(-1)^{k+1}}{k} \tag{E.7}$$

$$B_k = \frac{2(-1)^{k+1}}{k+1}\sum_{j=1}^{k}\frac{1}{j} \tag{E.8}$$

Appendix F

Relative other-cell Interference D_I in the Downlink

Derivation of D_{I1}

In order to evaluate D_{I1}, one direct way is to derive the pdf of the ordered statistics $\{W_k\}$ and find the numerical results. The pdf of an ordered statistics can be found by applying the method described in (Papoulis 1991). However, this approach is rather difficult. We will introduce an evaluation method such that we will not need to find the pdf of $\{ W_k\}$.

In section 7.3.4, we defined D_{I1} as

$$D_{I1} = E\left\{ \frac{\sum_{k=1}^{N_c-1} W_k}{W_0} \right\} \tag{F.1}$$

By using the concept of total probability, D_{I1} can be evaluated by

$$\begin{aligned} D_{I1} &= \sum_{j=0}^{N_c-1} \left\{ \sum_{k\in\mathcal{S}_c, k\neq j} E\left[\frac{\alpha_k}{\alpha_j} | \alpha_j = \max\{\alpha_i\},\ \ i \in \mathcal{S}_c \right] \cdot Pr(A_j) \right\} \\ &= \sum_{j=0}^{N_c-1} \left\{ \sum_{k\in\mathcal{S}_c, k\neq j} E\left[10^{\frac{m_k-m_j}{10}} 10^{\frac{X_k-X_j}{10}} \mid X_i \leq X_j + m_j - m_i, \right.\right. \\ &\qquad \left.\left. \forall i \in \mathcal{S}_c,\ i \neq j \ \right] \cdot Pr(A_j) \ \} \end{aligned} \tag{F.2}$$

where $\alpha_i = 10^{(m_i+X_i)/10}$ and X_i is zero-mean Gaussian with variance σ_i^2, $m_i = 10\log_{10}(P_i)$, event $A_j = \{\ \alpha_j = \max\{\alpha_i\},\ \ i \in \mathcal{S}_c\ \}$, and $\mathcal{S}_c$ is the set of the nearest N_c BS for the desired user.

We define R_{kj} as

$$R_{kj} = 10^{(m_k - m_j)/10} = P_k/P_j = \left(\frac{r_{ki}}{r_{kj}}\right)^{-a} \left(\frac{1 + r_{ki}/g}{1 + r_{kj}/g}\right)^{-b} \tag{F.3}$$

which is just the ratio of path loss from the BS' k and j to the desired user. Since the random variables X_k and X_j are independent if $k \neq j$, D_{I1} becomes

$$\begin{aligned} D_{I1} &= \sum_{j=O}^{N_c-1} \sum_{k \in \mathcal{S}_c, k \neq j} R_{kj} \int_{-\infty}^{\infty} 10^{-x_j/10} f_{X_j}(x_j)\, dx_j \cdot \\ &\quad \left[\int_{-\infty}^{x_j + m_j - m_k} 10^{x_k/10} f_{X_k}(x_k)\, dx_k\right] \left\{\prod_{i \in \mathcal{S}_c, i \neq k,j} F_{X_i}(x_j + m_j - m_i)\right\} \\ &= \sum_{j=1}^{N_c-1} \sum_{k \in \mathcal{S}_c, k \neq j} R_{kj} \int_{-\infty}^{\infty} e^{-\lambda x_j} \frac{1}{\sqrt{2\pi}\sigma_j} \exp\left(-\frac{x_j^2}{2\sigma_j^2}\right) dx_j \cdot \\ &\quad \left\{\int_{-\infty}^{x_j + m_j - m_k} e^{\lambda x_k} \frac{1}{\sqrt{2\pi}\sigma_k} \exp\left(-\frac{x_k^2}{2\sigma_k^2}\right) dx_k\right\} \cdot \\ &\quad \left\{\prod_{i \in \mathcal{S}_c, i \neq k,j} \left[1 - \mathbf{Q}\left(\frac{x_j + m_j - m_i}{\sigma_i}\right)\right]\right\} \end{aligned} \tag{F.4}$$

It is straightforward to find that

$$\begin{aligned} &\int_{-\infty}^{x_j + m_j - m_k} e^{\lambda x_k} \frac{1}{\sqrt{2\pi}\sigma_k} \exp\left(-\frac{x_k^2}{2\sigma_k^2}\right) dx_k \\ &= \exp\left(\frac{\lambda^2 \sigma_k^2}{2}\right) \left[1 - \mathbf{Q}\left(\frac{x_j + m_j - m_k}{\sigma_k} - \lambda\sigma_k\right)\right] \end{aligned} \tag{F.5}$$

Then, D_{I1} can be written as follows

$$\begin{aligned} D_{I1} &= \sum_{j=O}^{N_c-1} \sum_{k \in \mathcal{S}_c, k \neq j} R_{kj} \exp\left[\frac{\lambda^2\left(\sigma_k^2 + \sigma_j^2\right)}{2} \int_{-\infty}^{\infty} \frac{1}{\sqrt{2\pi}} \exp\left(-\frac{z^2}{2}\right) dz\right] \cdot \\ &\quad \left[1 - \mathbf{Q}\left(\frac{\sigma_j z - \lambda\sigma_j^2 + m_j - m_k}{\sigma_k} - \lambda\sigma\right)\right] \cdot \\ &\quad \left\{\prod_{i \in \mathcal{S}_c, i \neq k\, j} \left[1 - \mathbf{Q}\left(\frac{\sigma_j z - \lambda\sigma_j^2 + m_j - m_i}{\sigma_i}\right)\right]\right\} \end{aligned} \tag{F.6}$$

In the case that $\sigma_k^2 = \sigma^2$, $\forall k \in \mathcal{S}_c$, D_{I1} becomes

$$D_{I1} = \sum_{j=0}^{N_c-1} \sum_{k \in \mathcal{S}_c, k \neq j} R_{kj} \exp\left(\lambda^2\sigma^2\right) \int_{-\infty}^{\infty} \frac{1}{\sqrt{2\pi}} \exp\left(-\frac{z^2}{2}\right) dz \cdot$$

$$\left[1-\mathbf{Q}\left(z+\frac{m_j-m_k}{\sigma}-2\lambda\sigma\right)\right]\cdot$$
$$\left\{\prod_{i\in\mathcal{S}_c,i\neq k,j}\left[1-\mathbf{Q}\left(z+\frac{m_j-m_i}{\sigma}-\lambda\sigma\right)\right]\right\} \tag{F.7}$$

Derivation of D_{I2}

$$D_{I2} = E\left(\sum_{k=N_c}^{K}\alpha_k\right)E\left(\frac{1}{W_0}\right) = E\left(\mathcal{L}_R\right)E\left(\frac{1}{W_0}\right) \tag{F.8}$$

where $\mathcal{L}_R = \sum_{k=N_c}^{K}\alpha_k$, which can be approximated by a log-normally distributed random variable and its statistics can be found by applying the recursive method described in appendix E. Therefore, $E\left(\mathcal{L}_R\right)$ is

$$E\left(\mathcal{L}_R\right) = E\left(10^{\frac{m_R+X_R}{10}}\right) = \exp\left(\lambda m_R+\frac{\lambda^2\sigma_R^2}{2}\right) \tag{F.9}$$

Following the same method used in the derivation of D_{I1}, we can find $E\left(1/W_0\right)$ which is

$$\begin{aligned}
E\left(\frac{1}{W_0}\right) &= \sum_{j=0}^{N_c-1}E\left[10^{-\alpha_j}\,|\,\alpha_j=\max\{\alpha_i\},\ \forall i\in\mathcal{S}_c\right]\cdot P_r(A_j)\\
&= \sum_{j=0}^{N_c-1}E\left[10^{-\frac{m_j+X_j}{10}}\,|\,X_i\neq X_j+m_j-m_i,\ \forall i\in\mathcal{S}_c,\ i\neq j\right]P_r(A_j)\\
&= \sum_{j=1}^{N_c-1}\exp(-\lambda m_j)\int_{-\infty}^{\infty}\exp(-\lambda x_j)\,f_{X_j}(x_j)\,dx_j\cdot\\
&\quad\left[\prod_{i\in\mathcal{S}_c,,i\neq j}F_{X_i}(x_j+m_j-m_i)\right]\\
&= \sum_{j=0}^{N_c-1}\exp(-\lambda m_j)\exp\left(\frac{\lambda^2\sigma_j^2}{2}\right)\int_{-\infty}^{\infty}\frac{1}{\sqrt{2\pi}}\exp\left(-\frac{z^2}{2}\right)dz\cdot\\
&\quad\left\{\prod_{i\in\mathcal{S}_c,i\neq j}\left[1-\mathbf{Q}\left(\frac{\sigma_j z-\lambda\sigma_j^2+m_j-m_i}{\sigma_i}\right)\right]\right\}
\end{aligned} \tag{F.10}$$

Multiplying the above two terms, we get

$$\begin{aligned}
D_{I2} &= \left[\exp\left(\lambda m_R+\frac{\lambda^2\sigma_R^2}{2}\right)\right]\sum_{j=0}^{N_c-1}\left[\exp\left(-\lambda m_j+\frac{\lambda^2\sigma_j^2}{2}\right)\right]\cdot\\
&\quad\int_{-\infty}^{\infty}\frac{1}{\sqrt{2\pi}}e^{-\frac{z^2}{2}}dz\left\{\prod_{i\in\mathcal{S}_c,i\neq j}\left[1-\mathbf{Q}\left(\frac{\sigma_j z-\lambda\sigma_j^2+m_j-m_i}{\sigma_i}\right)\right]\right\}
\end{aligned} \tag{F.11}$$

If $\sigma_k^2 = \sigma^2 \; \forall k$, then D_{I2} becomes

$$D_{I2} = \left[\exp\left(\lambda m_R + \frac{\lambda^2\sigma_R^2}{2}\right)\right] \sum_{j=0}^{N_c-1} \left[\exp\left(-\lambda m_j + \frac{\lambda^2\sigma^2}{2}\right)\right] \cdot \left\{ \prod_{i\in\mathcal{S}_c, i\neq j} \left[1 - \mathbf{Q}\left(z + \frac{m_j - m_i}{\sigma} - \lambda\sigma\right)\right] \right\} \tag{F.12}$$

Special Cases: $N_c = 1$, $N_c = 2$, and $\sigma_k = \sigma$

1. $N_c = 1$

$$D_I = E\left(\frac{\sum_{k=1}^{K}\alpha_k}{\alpha_0}\right) = E\left(\frac{\mathcal{L}_R}{\alpha_0}\right) = E\left(\mathcal{L}_F\right) = \exp\left(\lambda m_F + \frac{\lambda^2\sigma_F^2}{2}\right) \tag{F.13}$$

where $m_F = (m_R - m_0)$ and $\sigma_F^2 = (\sigma_R^2 + \sigma_0^2)$.

2. $N_c = 2$

$$D_{I1} = \sum_{j=0}^{1} R_{1-j,j} \exp\left(\lambda^2\sigma^2\right) \int_{-\infty}^{\infty} \frac{1}{\sqrt{2\pi}} \exp(-z^2/2)\, dz \cdot \left[1 - \mathbf{Q}\left(z + \frac{m_j - \text{7721-j}}{\sigma} - 2\lambda\sigma\right)\right]$$

$$= \sum_{j=0}^{1} R_{1-j,j} \exp\left(\lambda^2\sigma^2\right)[\;\; 1 - \mathbf{Q}\left(\frac{m_j - m_{1-j}}{\sqrt{2}\sigma} - \sqrt{2}\lambda\sigma\right)\Bigg] \tag{F.14}$$

and

$$D_{I2} = \left[\exp\left(\lambda m_R + \frac{\lambda^2\sigma_R^2}{2}\right)\right] \sum_{j=0}^{1} \left[\left(-\lambda m_j + \frac{\lambda^2\sigma^2}{2}\right)\right] \cdot \left[1 - \mathbf{Q}\left(\frac{m_j - m_{1-j}}{\sqrt{2}\sigma} - \frac{\lambda\sigma}{\sqrt{2}}\right)\right] \tag{F.15}$$

Note that the above expressions for D_{I1} and D_{I2} depend on the user's location in the cell. The area-averaged D_I can be evaluated by averaging over the possible locations of the user traversing the cell.

References

Abramowitz, M., and I. Stegun. 1964. ***Handbook of Mathematical Functions.*** NBS Applied Math. Series, Number 55. Washington, DC: U.S. Government Printing Office.

Abramson, N. 1970. The Aloha system – Another alternative for computer communications. Proc. Fall Joint Comput. Conf., APIPS Conf., p. 37.

Abramson, *N.* (Ed.)1993. ***Multiple Access Communications.*** IEEE Press.

Abu-Dayya, A., and N. Beaulier. 1991. Outage probabilities of cellular mobile systems with multiple Nakagami interfers. ***IEEE Trans. on Vehicular Technology,*** Vol. VT-40, pp. *757-768.*

Beaulieu, N., and A. Abu-Dayya. 1991. Analysis of equal gain diversity on Nakagami fading channels. ***IEEE Trans.on Commun.,*** Vol. COM-39, pp. 225-234.

Bhargava, V.K. 1983. Forward error correction schemes for digital communications. ***I E E E Communications Magazine,*** Vol. 21, pp. 11-19.

Biyari, K. 1990. Binary communications over random channels. Ph.D. dissertation, University of Southern California.

Bultitude, R., and G. Bedal. 1989. Propagation characteristics on microcellular urban mobile radio channels at 910 MHz. ***IEEE Journal on Selected Areas in Commun.,*** Vol. SAC-7, pp. 31-39.

Capetanakis, J.I. 1979. The multiple access broadcast channel: Protocol and capacity considerations. *IEEE Trans. Info. Theory,* IT-25, pp. 505-515.

Chang, K.S. et al. 1993. Automated highway system experiments in the PATH program. *IVHS Journal,* Vol.1(1), pp. 63-87.

Chua, K.C. 1992. A variant of the CSMA protocol suitable for a mobile radio LAN. IEEE GLOBECOM '92, pp. 1354-1358.

Cook, C.E., and H.S. Marsh. 1983. An introduction to spread spectrum. *IEEE Communications Magazine,* Vol. 21, pp. 8-16.

Cooper, G.R., and C.D. McGillem. 1986. ***Modern Communications and Spread Spectrum.*** 1st edition. McGraw-Hill.

Cox, D. 1992. Wireless network access for personal communications. ***IEEE Communications Magazine,*** Vol. 30, pp. 96-115.

Crepeau, P. 1992. Uncoded and coded performance of MFSK and DPSK in Nakagami fading channels. ***IEEE Trans. on*** *Commun.,* Vol. COM-40, pp. 487-493.

Crowther, W. et al. 1973. A system for broadcast communication: Reservation-ALOHA. Proc. sixth Hawaii Int. Conf. Sys. Sci., pp. 371-374.

Dixon, R.C. 1976. ***Spread Spectrum Systems.*** 1st edition. New York: John Wiley & Sons.

Dresher, M. 1953. Moment spaces and inequalities. *Duke* ***Math. J.,*** Vol. 20, pp. 261-271.

Garrison, G. 1975. A power spectral density analysis for digital FM. ***IEEE Trans. on Commun.,*** pp. 1228-1243.

Gejji, R. 1992. Channel efficiency in digital cellular communication systems. Proceedings of the 42nd IEEE Vehicular Technology Conference, pp. 1005-1007.

Georgiopoulos, M. 1990. Packet error probabilities in direct-sequence spread-spectrum radio

networks. ***IEEE Trans. on Commun.,*** Vol. COM-38, pp. 1599-1606.

Geraniotis, E., and B. Ghaffari. 1991. Performance of binary and quaternary direct-sequence spread-spectrum multiple-access systems with random signature sequences. ***IEEE Trans. on Commun.,*** Vol. COM-39, pp. 713-724.

Gilhousen, K., I. Jacobs, R. Padovani, A. Viterbi, L. Weaver, and C. Wheatley I. 1991. On the capacity of a cellular CDMA system. ***IEEE Trans. on Vehicular Technology,*** Vol. VT-40, pp. 303-312.

Goodman, D. J. et al. 1989. Packet reservation multiple access for local wireless communications. ***IEEE Trans. Comm.,*** COM-37, No. 8, pp. 885-890.

Goodman, D. J., and A. Saleh. 1987. The near/far effect in local ALOHA radio communications. ***IEEE Trans. Veh. Techn.,*** Vol. 36, No. 1., pp. 19-27.

Harley, P. 1989. Short distance attenuation measurements at 900 MHz and 1.8 GHz using low antenna heights for microcells. ***IEEE Journal on Selected Areas in Commun.,*** Vol. SAC-7, pp. 5-11.

Hitchcock, A. 1993. ***Message Volumes for Two Examples of Automated*** *Freeway.* University of California, Berkeley: Institute of Transportation Studies, California PATH Program. UCB-ITS-PRR-93-1.

Ho, M., and G. Stuber. 1993. Co-channel interference of microcellular systems on shadowed Nakagami fading channels. Proceedings of the 43st IEEE Vehicular Technology Conference, pp. 568-571.

Hubner, D., K. Jakobs, and F. Reichert. 1991. Taking advantage of the disadvantage: interference detection for improved decentral radio channel access. Proceedings of IEEE Veh. Techn. Conference, pp. 374-379.

Ioannou, P., and C.C. Chien. 1993. Autonomous intelligent cruise control. ***I E E E Transuctions on Vehicular Technology,*** Vol. 42, No. 4.

Janos, W. 1970. Tail of the distribution of sums of log-normal variates. ***IEEE Trans. on Information Theory,*** Vol. IT-16, pp. 299-302.

Jurgen, R. K. 1991. Smart cars and highways go global. ***IEEE Spectrum,*** Vol. 28, pp. 26-36.

Kavehrad, M., and B. Ramamurthi. 1987. Direct-sequence spread spectrum with DPSK modulation and diversity for indoor wireless communications. ***IEEE Trans. on Commun.,*** Vol. COM-35, pp. 224-236.

Klein, L. A. et al. 1993. IVHS architecture development. ***IVHS Journal,*** Vol. 1(1), pp. 35-43.

Kleinrock, L., and F. A. Tobagi. 1975. Packet switching in radio channels: Part I – CSMA modes and their throughput-delay characteristics. ***IEEE Trans. Comm.,*** COM-23, pp. 1400-1416.

Kumar, P. V. 1991. Error-correcting codes. In ***Space Communication and Nuclear Scintillation*** , edited by N. Mohanty. New York: Van Nostrand Reinhold.

Lee, W. C. 1986. ***Mobile Communications Design Fundamentals,*** Indianapolis, IN: Howard W. Sams.

Lee, W. 1989. Spectrum efficiency in cellular. ***IEEE Trans. on Vehicular Technology,*** Vol. VT-38, pp. 69-75.

Lehnert, J., and M.B. Pursley. 1987. Error probability for binary DS spread-spectrum communications with random signature sequences. ***IEEE Trans. on Commun.,*** Vol. COM-35, pp. 87-98.

Lin, S., and D. J. Costello, Jr. 1983. ***Error Control Coding: Fundamentals and Applications*** Englewood Cliffs, N.J.: Prentice Hall.

Lindsey, W. 1964. Error probabilities for Rician fading multichannel reception of binary and N-ary signals. ***IEEE Trans. on Information Theory,*** Vol. IT-10, pp. 339-350.

Linnartz, J.-P. 1992. Slotted ALOHA land-mobile radio networks with site diversity. IEE Proceedings-I, Vol. 139, No. 1.

Linnartz, J-P, and J. Walrand. 1993. ***Spectrum Needs for IVHS.*** Working Paper. University of California, Berkeley. UCB-ITS-PWP-93-13.

Mann, A., and J. Ruckert. 1988. A new concurrent slot assignment protocol for traffic information exchange. Proc. of the 38th Veh. Techn. Conf., pp. 503-508.

Marcum, J., and P. Swerling. 1960. Studies of target detection by pulsed radar. ***IRE Trans. on Information Theory,*** Vol. IT-6, pp. 59-144.

Metcalfe, R.M., and D.R. Boggs. 1976. Ethernet: Distributed packet switching for local computer networks. Comm. ACM, pp. 395-404.

Milstein, L., T. Rappaport, and R. Barghouti. 1992. Performance evaluation for cellular CDMA. ***IEEE Journal on Selected Areas in Commvn.,*** Vol. SAC-10, pp. 680-689.

Misser, H., and R. Prasad. 1992. Bit error probability of microcellular spread-spectrum multiple-access system in a shadowed Rician channel. Proceedings of the 42nd IEEE Vehicular Technology Conference, pp. 439-442.

Morrow, R.K., J.S. Lehnert. 1989. Bit-to-bit error dependence in slotted DS/SSMA packet systems with random signature sequences. ***IEEE Trans. on Commun.,*** Vol. COM-37, pp. 1052–1061.

Morrow, R.K., J.S. Lehnert. 1992. Packet throughput in slotted ALOHA DS/SSMA radio systems with random signature sequences. ***IEEE Trans. on Commun.,*** Vol. COM-40, pp. 1223-1230.

Mosely, J., and P.A. Humblet. 1985. A class of efficient contention resolution algorithms for multiple access channels. ***IEEE Trans.*** *Comm.,* COM-33, pp. 145-151.

Muammar, R., and S. Gupta. 1982. Cochannel interference in high capacity mobile radio

systems. ***IEEE Trans. on Commun.,*** Vol. COM-30, pp. 1973-1978.

Murota, K., and K. Hirade. 1981. GMSK modulation for digital radio telephony. ***I E E E Trans. on Commun.,*** Vol. COM-29, pp. 1044-1050.

Nakagami, M. 1960. The m-distribution —a general formula of intensity distribution of fading. In ***Statistical Methods in Radio Wave Propagation,*** edited by W.C. Hoffman. New York: Pergamon.

Oetting, J. 1979. A comparison of modulation techniques for digital radio. ***IEEE Trans. on Commun.,*** Vol. COM-27, pp. 1752-1762.

Okayed, H., Y. Naganas, and Y. Garish. 1978. Analysis of framed ALOHA channel in satellite packet switching networks. Proc. Fourth In. Comfy. Compte. Common., pp. 617-622.

Panter, P. 1972. *Communication* ***Systems Design: Line-of-Sight and Troposcutter. New*** York: McGraw Hill.

Papoulis, A. 1991. ***Probability, Random Variables, and Stochastic Processes.*** Third Edition. McGraw-Hill.

Parsons, J. 1992. ***The Mobile Radio Propagation Channel.*** New York: John Wiley & Sons.

Pasupathy, S. 1979. Minimum shift keying: a spectrally efficient modulation. ***I E E E Commun. Magazine,*** Vol. 17, pp. 14-22.

Pickholtz, R., L. Milstein, and D. Schilling. 1991. Spread spectrum for mobile communications. ***IEEE Trans. on*** *Vehicular* ***Technology,*** Vol. VT-40, pp. 313-322.

Polydoros, A., and J. Silvester. 1987. Slotted random access spread-spectrum networks: An analytic framework. ***IEEE J. SAC,*** Vol. SAC-5, No. 6.

Polydoros, A., K. Dessouky, J. M. Pereira(Ed.), C. M. Sun, K. C. Lee, and T. D. Pa-

pavassiliou.1993. ***Vehicle to Roadside Communications Study.*** Communication Sciences Institute, University of Southern California. California PATH Research Report. UCB-ITS-PRR-93-4.

Press, W., B. Flannery, S. Teukolsky, and W. Vetterling. 1989. ***Numerical Recipes.*** Cambridge University Press.

Proakis, J. 1989. ***Digital Communications.*** 2nd Edition. McGraw-Hill.

Pronios, N.B., and A. Polydoros. 1990. Utilization optimization of CDMA systems. Proceedings of the 1990 Bilkent International Conference, Ankara, Turkey, pp. 560-566.

Pursley, M.B. 1987. The role of spread spectrum in packet radio networks. Proceedings IEEE, Vol. 75, No. 1, pp. 116-134.

Rivest, R.L. 1987. Network control by Bayesian broadcast. ***IEEE Trans. Infom. Theory,*** IT-33, pp. 323-328.

Roberts, L.G. 1975. Aloha packet system with and without slots and capture. ***Comput. Commun. Rev.,*** Vol. 5, pp. 28-42.

Sachs, S., and P. Varaiya. 1993. ***A Communication System for the*** Control ***of Automated Vehicles.*** University of California, Berkeley: Institute of Transportation Studies, California PATH Program. UCB-ITS-PRR-93-5.

Safak, A. 1993. Statistical analysis of the power sum of multiple correlated log-normal components. ***IEEE Trans. on Vehicular Technology,*** Vol. VT-42, pp. 58-61.

Schilling, D.L., et al. 1991. Spread spectrum for commercial communications. ***IEEE Communications Magazine,*** Vol. 29, pp. 66-79.

Scholtz, R.A. 1982. The origins of spread spectrum communications. ***IEEE Trans. Commun.,*** Vol. COM-30, pp. 822-854.

Schulte, F.C. 1983. Dynamic frame length ALOHA. ***IEEE Trans. Common.,*** Vol. COM-31, no. 4, pp. 565-568.

Schwartz, S., and Y. Yeh. 1982. On the distribution function and moments of power sums with log-normal components. BSTJ, Vol. 61, pp. 1441-1462.

Shaft, P. 1974. On the relationship between scintillation index and Rician fading. ***I E E E Trans. on Commun.,*** Vol. COM-22, pp. 731-733.

Shladover, S.E. 1993a. Draft Glossary of AVCS Terminology.

Shladover, S.E. 1993b. On the path to automated highways and AVCS. ***IVHS Review,*** pp. 95-110.

Simpson, F.D. 1992. Direct sequence CDMA performance analysis methodologies. Ph.D. dissertation. Rutgers University.

Sklar, B. 1988. ***Digital Communications — Fundamental and Applications.*** Prentice-Hall.

Streisand, S.L., and J. Walrand. 1992. ***A Communication Architecture for IVHS.*** University of California, Berkeley: Institute of Transportation Studies, California PATH Program. UCB-ITS-PRR-92-10.

Tabbane, S., and P. Godlewski. 1992. Performance evaluation of the R-BTMA protocol in a distributed mobile radio network context. ***IEEE Trans. Veh. Techn.,*** Vol. 41, No. 1, pp. 24-34.

Taub, H., and D.L. Schilling. 1986. ***Principles of Communication Systems.*** 2nd Edition. McGraw-Hill.

Tobagi, F.A. 1982. Carrier ***s e n s e*** multiple access with message-based priority functions. ***IEEE Trans. Comm.,*** Vol. 30, No. 1, pp. 185-200.

Tobagi, F.A., and L. Kleinrock. 1975. Packet switching in radio channels: Part II – The

hidden terminal problem in CSMA and busy-tone solution. ***IEEE Truns Comm.*** COM-23, pp.1417-1433.

Transportation Research Board (TRB). 1993a. Communicating with vehicles. ***Circular,*** Number 411.

Transportation Research Board (TRB). 1993b. Spectrum needs for IVHS applications. To be appear in Circular.

Turin, G. 1984. The effects of multipath and fading on the performance of DS CDMA system. ***IEEE Trans. on Vehicular Technology,*** Vol VT-33, pp.213-219.

Varaiya, P., and S.E. Shladover. 1991. ***Sketch of an IVHS System Architecture,*** University of California, Berkeley: Institute of Transportation Studies, California PATH Program. UCB-ITS-PRR-91-3.

Viterbi, A.J. 1991. Wireless Digital Communication: A View Based on Three Lessons Learned. ***IEEE Communications Magazine,*** Vol. 29, pp. 33-36.

Viterbi, A.M., and A.J. Viterbi. 1993. Erlang capacity of a power controlled CDMA system. ***IEEE Journal on Selected Areas in Commun.,*** Vol. SAC-11, pp. 892-899.

Viterbi, A.J., A.M. Viterbi and E. Zehavi. 1994. Other-cell interference in cellular power-controlled CDMA. ***IEEE Trans. on Commun.,*** Vol. COM-42, pp. 1501-1504.

Webb, W. 1992. Modulation methods for PCNs. ***I E E E*** *Commun. Magazine,* Vol. 30, pp. 90-95.

Westerlies, J.E., A. Overmodest, and L.A. Michaels. 1989. An exact analysis and performance evaluation of framed ALOHA with capture. ***IEEE Trams. Common.,*** Vol. COM-37, No. 2, pp. 125-137.

Wilson, N.D. et al. 1993. Packet CDMA versus dynamic TDMA for multiple access in an integrated voice/data PCN. ***J. SAC,*** Vol. 11, No. 6, pp. 870-884.

Wojnar, A. 1986. Unknown bounds on performance in Nakagami channels. ***IEEE Trans. on Commun.,*** Vol. COM-34, pp. 22-24.

Xia, H., et al. 1992. Radio propagation measurements and modeling for line-of-sight micro-cellular systems. Proceedings of the 42nd IEEE Vehicular Technology Conference, pp. 349-354.

Yung, W. 1991. DS/CDMA cellular systems in Rayleigh fading and log-normal shadowing channel. ICC'91, pp. 28.2.1-6.

Zhang, K., and K. Pahlavan. 1992. Relation between transmission and throughput of slotted ALOHA local packet radio networks. ***IEEE Trans. Comm.,*** Vol. 40, No. 3, pp. 577-583.

Zhu, W., T. Hellmich, and B. Walke. 1991. DCAP, a decentral channel access protocol: performance analysis. Proceedings of IEEE Veh. Techn. Conference, pp. 463-468.